EFFECT OF SPATIAL VARIABILITY OF RAINFALL

ON MODELING HYDROLOGIC/WATER

QUALITY PROCESSES

By

INDRAJEET CHAUBEY

Bachelor of Technology
University of Allahabad
Allahabad, India
1990

Master of Science
University of Arkansas
Fayetteville, Arkansas, U.S.A.
1994

Submitted to the Faculty of the
Graduate College of the
Oklahoma State University
in partial fulfilment of
the requirements for
The degree of
DOCTOR OF PHILOSOPHY
December, 1997

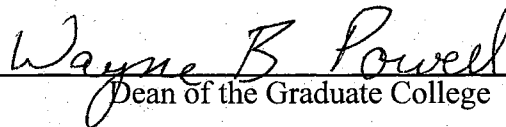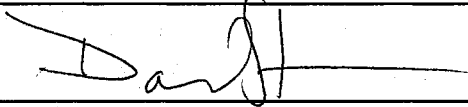EFFECT OF SPATIAL VARIABILITY OF RAINFALL

ON MODELING HYDROLOGIC/WATER

QUALITY PROCESSES

Thesis Approved:

_____
Thesis Advisor

_____

_____

_____
Dean of the Graduate College

ACKNOWLEDGMENTS

A scientific endeavor of this nature requires cooperation and encouragements of many individuals. Very little, if any, of this work would have been possible without the commitment made in good faith, trust and encouragement by a very special group of people associated with me. These are the people who helped me personally and professionally.

I wish to express my deepest appreciation to Dr. C.T. Haan, my major advisor, who gave me an opportunity to work with him. It was a dream coming true for me. I feel extremely fortunate to have working with him for the last three years. His passion for the knowledge, great insight into the subject matter, and a friendly and charming personality has taught me lessons that will go a long way in shaping up my personal and professional career. Without his scientific expertise, timely encouragements, and financial assistance, completion of this dissertation could have never been possible.

I owe a great deal to my other committee members Drs. Ron Elliott, Dan Storm, and Nick Basta for their invaluable suggestions and encouragements throughout the course of this research.

This research could have been very difficult to complete without the timely availability of data needed. I am grateful to Drs. J.D. Garbrecht and P.J. Starks for giving permission to use the data from the Little Washita basin and the Micronet. Sincere thanks are extended to Mark Morrissey and Mark Safer of the National Severe Storms Laboratory

complete this degree. This accomplishment could have been very difficult without their love and support.

Last but not the least, I owe a great deal of my success to my wife Shraddha. Her patience, love and support made this difficult task very enjoyable. She spent endless nights alone at home when I was working on this research. She always encouraged me to thrive for the best. Without her love, support and encouragement, working on this research could have been very difficult and boring.

I would like to dedicate this dissertation to my father - my personal hero. I wish he was with me to enjoy this important moment of my life. He taught me to believe in myself. Without his power of dreams, I could have never traveled from Jawahi Diyar to Stillwater and got all the success on the way to this long journey.

TABLE OF CONTENTS

vii

LIST OF TABLES

LIST OF FIGURES

LIST OF SYMBOLS

AE	Arithmetic error
AGNPS	Agricultural Non Point Source Pollution model
a_k	kth polynomial coefficient
CF	Radar rainfall calibration factor
CN	Curve Number
cov	Covariance
C.V.	Coefficient of variation
D	Raindrop diameter
dD	Incremental value of D
d_{oj}	Distance between points o and j
DPA	Digital Precipitation Array
EARTHR	Radius of the earth (km)
HRAP	Hydrologic Rainfall Analysis Project
H/WQ	Hydrology/water quality
$\underline{I}$	Vector of erroneous inputs to a H/WQ model
$\underline{I}^*$	Vector of true inputs to a H/WQ model
K	USLE K factor, Mg/(rainfall energy intensity unit)

$\underline{P}$	Vector of erroneous parameters
$\underline{P}*$	Vector of true parameters
p	Rainfall depth
R	Rainfall rate (mm/h)
RE	Relative error
Rg	Gauge measured rainfall (inches)
Rrc	uncalibrated radar rainfall (inches)
RER	Radar estimated rainfall
S	Retention parameter
SE	Standard error
V_t	Drop terminal velocity of a drop
WSR-88D	Weather Surveillance Radar-88 Doppler
w_j	Weight at sampling point j used in rainfall interpolation
x_j, y_j	Coordinates of a point j in two dimensional space
XLAT	Latitude (degrees)
XLON	Longitude (degrees)
ZMESH	Grid length at 60^0 latitude (4.7625 km) in HRAP coordinate
z	Radar reflectivity (mm^6/m^3)
Z	Grid length in HRAP coordinate system (km)
$\varphi_k(x_0, y_0)$	kth monomial in terms of x_0, y_0
β_{kj}	Element of the inverse of the n x n matrix with elements $\varphi_k(x_0, y_0)$
σ^2	Variance

CHAPTER 1

INTRODUCTION

1.1 Statement of the Problem

Pollution of surface and ground water systems from agricultural activities has been reported to be a serious problem. One of the most convenient ways to study the impact of various agricultural activities on surface and ground water quality is the use of hydrology/water quality (H/WQ) models. During the last decade many models, such as AGNPS (Young et al., 1987), ANSWERS (Beasley et al., 1980), CREAMS/GLEAMS (Knisel, 1980), EPIC (Williams et al., 1984), WEPP (Lane et al., 1989), SWAT (Arnold et al., 1993), and SIMPLE (Sabbagh et al., 1995) have been developed for use in making environmental decisions on rural watersheds. These models require input parameters to describe specific situations. The actual processes occurring in the field are more complex and variable than can currently be represented even in the most sophisticated models. Algorithms included in a model that are designed to represent a particular process are forced to represent processes that are not included in the model precisely because there is no other representation of these processes in the model (Haan et al., 1995).

Rainfall is a key input variable used in all H/WQ models. It activates flow and mass transport in hydrological systems. Modeling of hydrological processes in which the rainfall is the driving force has generated considerable interest with respect to possibilities of solving

increasing environmental problems. However, most of the hydrological calculation methods used in practical applications are still based on assumptions and simplifications from the early history of hydrology (Berndtsson and Niemczynowicz, 1988). For example, it is no longer practical to maintain the assumption that rainfall is spatially homogeneous across a watershed area. Thus, one of the ways to improve the accuracy of calculated runoff and runoff driven pollutant transport is to take spatial and dynamic properties of rainfall into consideration.

The sensitivity of model outputs to the changes in input parameters has been of great interest to both model developers and model users. One parameter that has received little attention in modeling is the temporal and spatial distribution of rainfall. The storm rainfall is usually represented by an average precipitation uniformly distributed throughout the watershed, even though the storm events that cause the greatest movement of sediment and nutrients are rarely uniform (Young et al., 1992). This spatial variability in rainfall input may introduce significant errors in model parameters and subsequently in the model outputs.

1.2 Objectives

The overall goal of this research was to study the variability induced in H/WQ model parameters and model outputs solely due to the spatial variability in the rainfall. This will help isolate the variability in the model parameters/outputs caused by a spatially variable rainfall which is otherwise thought to be uniform and is usually assumed not to contribute towards the model parameter/output uncertainty. The specific objectives of this research are:

2

1. To combine rain gauge and radar data to capture spatial variability of rainfall.

2. To estimate parameter uncertainty in H/WQ models solely due to the spatial variability of rainfall.

3. To study the impact of spatial variability of rainfall on model outputs, i.e. runoff, sediment and nutrient losses.

Research Hypothesis. Rainfall input as required by most H/WQ models is spatially variable and introduces significant uncertainty in modeling H/WQ processes.

1.3 Scope of the Study

This research was conducted using data from the Little Washita basin, a tributary of the Washita River in Southwest Oklahoma. Two subwatersheds known as Cyril and Cement watersheds were delineated and used in this study. Rainfall spatial variability was captured using data from Micronet stations and NEXRAD radar data. Further details are given in Chapter 4.

Most H/WQ models that use rainfall as an input, assume spatial homogeneity of rainfall across the watershed. The results obtained in this study can be used as a guideline to estimate the errors in the model parameters/outputs induced by the rainfall spatial variability. Very few studies have been conducted in the past to assess the effect of rainfall spatial variability on model outputs. Most of these studies concentrated on hydrologic components of the model such as runoff volume, peak runoff rate and time to peak. No

study has been conducted to estimate the uncertainty in the model parameters induced by rainfall spatial variability. All of these studies were limited by the smaller size of the watersheds, and a small number of raingauges available to capture the rainfall spatial variability. This study was conducted on two watersheds. The rainfall spatial variability was captured using a dense network of raingauges and radar data. The following steps were taken to accomplish the objectives of this study:

1. Rainfall spatial variability was captured using Micronet raingauges and radar. Radar data were calibrated using the Micronet data.

2. AGNPS model was modified to input a grid-based rainfall and energy intensity.

3. AGNPS was calibrated using true rainfall pattern and runoff data. Calibrated parameters and the true rainfall pattern were used to obtain the 'observed' model outputs.

4. Model parameter uncertainty solely due to rainfall spatial variability was obtained by estimating the model parameters using observed outputs and rainfall observed at each gauge location assuming the spatial homogeneity of rainfall.

5. Model output uncertainty resulting solely from the spatial variation in rainfall was estimated by running the model using calibrated parameters and rainfall observed at each gauge location, one at a time, assuming that the rainfall was spatially homogeneous across the watershed.

1.4 Significance of the Study

Historically, in the application of H/WQ models, rainfall has been assumed to be a uniform process and it is assumed not to contribute to parameter uncertainty. Consequently, a single rainfall depth is input in the models. Several studies have shown that rainfall is spatially variable and it may cause a variability in the model outputs. Rudra et al. (1993) observed that: "failure to take these variations into account during calibration could lead to highly distorted estimates of model parameters; and failure to consider the detailed variations during model application could lead to serious inaccuracies in predicted results".

In recent years, a rapid increase in both the number and size of various kinds of pollutant releases and the spread of pollutants has been observed. In pace with the increasing environmental problems the need for accurate hydrological estimation methods is also increasing. For the identification and estimation of pollution management technologies, it is very important to calculate pollutant release and pollutant transport with accurate temporal and spatial resolution. Since rainfall is a driving force behind many kinds of pollutant release and subsequent transport and spread mechanisms, an accurate description of temporal and spatial rainfall variability should be used for these calculations (Berndtsson and Niemczynowicz, 1988). O'Connell and Todini (1996) stressed that the use of radar and dense raingauge data should be the type of experiment needed to gain a better understanding of the hydrological importance of spatial variability in rainfall.

With the advent of modern precipitation measurement techniques it is now possible to measure spatial variability of rainfall easily and more accurately. Spatial variability of rainfall was captured by the use of raingauge and radar measured rainfall. This spatially

5

variable rainfall was applied to AGricultural Non-Point Source Pollution (AGNPS) model. The results of this study give an insight about parameter uncertainty that was caused solely by the spatial variability of rainfall. Also, it gives information about how much variability in the model output can result when rainfall is assumed uniform. The results of this study can be applied to other H/WQ models that use rainfall as an input.

CHAPTER 2

REVIEW OF LITERATURE

Haan (1989) has mentioned that in any modeling effort there are at least three types of uncertainty involved - parameter uncertainty, model uncertainty, and uncertainty in the true state of nature. Parameter uncertainty reflects incomplete models, incomplete information and inadequate parameter estimation techniques. Parameter uncertainty arises because parameters are random variables and one can never be sure of the proper value of the parameters. Uncertainty in the model parameters results from the approximate nature of the model containing the parameters. Model uncertainty arises because any model is a simplification of processes occurring in the nature and it does not represent the true system. Because many simplifying assumptions are made while modeling hydrologic processes on a watershed scale, algorithms included in the model do not represent all the processes that are actually occurring on a watershed. Uncertainty in the true state of nature refers to the variability in space and time of meteorologic factors such as rainfall, temperature, solar radiation, stream flow, etc. This work is mainly focused on the parameter uncertainty and the uncertainty due to the true state of nature.

Traditionally, the distribution of rainfall depth has been assumed to be homogenous and consequently very few attempts have been made to model the spatial variability of rainfall. As rainfall is measured conventionally at a finite (and sometimes sparse) set of

points, the resulting estimate of average rainfall in space is subject to error (1) because the spatial variability of rainfall has been averaged out and (2) because the accuracy of the resulting average will depend on the density of the raingauge network (Shah et al., 1996). When a particular process such as rainfall variability is not modeled or is incompletely modeled, other components of the model are forced to compensate for this model shortcoming. Consequently, physically-based parameters may lose their strict physical interpretation. These parameters then reflect processes they were not originally intended to represent.

2.1 Spatially Distributed Rainfall Models

In seeking to characterize the behavior of rainfall in time and in space, Rhenals-Fegueredo et al. (1974) have classified various stochastic modeling approaches as follows:

(1). Point Rainfall Models: These models are based on observations of rainfall from a single raingauge taken over a relevant time interval (e.g., hourly, daily) and thus characterize a time series of rainfall at a single point.

(2). Multivariate Rainfall Models: In these models the correlation structure of the historical point rainfalls for the relevant time is preserved by considering several raingauges simultaneously. When using such models for Monte Carlo simulations, rainfall depths can only be generated at the given gauge locations.

(3). Multidimensional Rainfall Field Models: Such models seek to characterize the statistical structure of the rainfall at any point in the area of interest, and not just the locations of the raingauges. These type of models can be used to assess the impact of spatial

variability in rainfall on watershed response, as they can be used to simulate a fully distributed true rainfall input to a distributed model to obtain a corresponding true response.

The concept of simulating a spatial rainfall distribution is not new. Amorocho and Brandstetter (1967), Grayman and Eagleson (1969), and Cole and Sheriff (1972) were among the pioneers in presenting the mathematical descriptions of rainfall distribution in space. Mejia and Rodriguez-Iturbe (1974) developed an 'areal-multidimensional' rainfall model that uses stochastic concepts for simulating storm total rainfall depth at any point. Later, Bras and Rodriguez-Iturbe (1976) expanded this work to develop a 'non-stationary time-varying multidimensional' rainfall generator.

Felgate and Read (1975) adopted the correlation analysis technique developed by Briggs et al. (1950) to qualitatively describe the structure of stationary rainstorms. They assumed that spatial properties of rainfall patterns could be described by a two-dimensional Lagrangian spatial correlation function. Amorocho and Wu (1977) developed a modeling framework to generate precipitation sequences for any sampling time interval and at any ground location in the path of a storm. Their model uses a randomization process to produce clusters of short duration rain cells within a storm band.

In 1978, Eagleson presented a rainfall model that described the changes in storm intensity through time as a Poisson process. Such storms have random and independent total depths. Later, he developed a rainfall model to simulate spatial storm properties (Eagleson, 1984). He modeled the occurrence of wetted rainstorm area within a catchment as a Poisson process in which each storm was composed of stationary, non-overlapping, independent random cell clusters whose centers were Poisson-distributed in space and whose areas were

9

fractals. He used this model to estimate spatial properties of tropical air mass thunderstorms on six tropical catchments in Sudan.

Rodriguez-Iturbe, Gupta, Waldez and Waymire published several articles on concepts in modeling temporal and spatial occurrences of storms (Waymire and Gupta, 1981a, 1981b; Waymire et al., 1984; Rodriguez-Iturbe et al., 1984; Valdes and Rodriguez-Iturbe, 1985; Waymire, 1985). Like Eagleson (1984), they also described storm occurrences as a Poisson process. In their approach, the storm is composed of rain cells that are Poisson-distributed in space. The number of rain cells for a storm is a random variable. Rain intensity for a cell is assumed to follow a decay function that is spatially symmetric around the center of the cell where the maximum intensity occurs. Rodriguez-Iturbe et al. (1987) offered detailed description of several decay functions, and studied their characteristics.

Meadows et al. (1994) used rainfall records to develop a dimensionless rainfall distribution pattern. They found the rainfall distribution pattern to be unimodal and elliptical which can be described by a second degree polynomial equation with two independent variables. The relationship between a spatially variable rainfall and watershed performance was examined by performing storm water simulations using this spatially variant pattern and comparing the results to those generated using a uniform rainfall depth. Based on this comparison the authors illustrated that by using a spatially uniform rainfall depth over the watershed, runoff peaks and volumes were generally overestimated. This rainfall distribution pattern can be applied as a forensic tool to only those watersheds which have sufficient information (historical data) to establish the spatial scale.

10

Loukas and Quick (1996) analyzed 175 storms in a mountainous watershed in the southwestern British Columbia. The precipitation was found to increase up to the mid-distance of the watershed, and then decreased and/or leveled off or increased with the elevation again, depending on the type of event. The average storm intensity at the mid-distance, on average, was found to be 90% larger than the average storm intensity at zero elevation.

2.2 Radar Measurement of Rainfall

A rain gauge is the most direct and accurate way to measure the rainfall at a point where the gauge is located. The watershed physiographic factors, especially topography and the local topography surrounding the gauge strongly affect the gauge measured precipitation. Hovind (1965) showed that a deficiency of up to 70% was possible on the windward side and an excess of up to 100% was possible on the lee slope as compared to the measurements taken at a summit. Also, rain gauges only measure rainfall at a point. There is usually little interest in point rainfall measurements except to determine the relative accuracies of various gauges.

Because there may be large errors in the rain depth at any one gauge representing the areal average, hydrologists have resorted to a network of rain gauges and to radar to improve areal average rainfall estimates. There is no doubt that a sufficiently dense network of gauges can measure rainfall better than a radar. In fact, gauge measurements are accepted as the standard against which other measurement techniques are compared. However,

operational raingauge networks are usually too sparse to capture the spatial variability of rainfall.

Although the accuracy of the radar measured rainfall is highly suspect, radar has the decided advantage of being able to remotely survey large areas and to make millions of measurements in minutes. Radars (e.g., dual polarization or Doppler) capable of measuring more than one parameter (e.g., vertical and horizontal reflectivities or spectrum of terminal velocities) in each resolution volume offer improved estimates of critically important parameters of the drop size distributions so that high-resolution measurements of spatial distribution of rainfall can be made (Doviak and Zrnic, 1984). In the U.S., a network of more than 120 highly sophisticated and state of the art the Next Generation Weather Radar System (NEXRAD) is expected to provide high-quality, high-resolution precipitation data that meet a wide range of hydrometeorological applications. The first NEXRAD unit began operating in 1991 near Oklahoma City, OK. The NEXRAD systems are termed as WSR-88D (Weather Surveillance Radar-88 Doppler). The basic principles of radar meteorology are well described in textbooks such as Battan (1973), Doviak and Zrnic (1984) and Atlas (1990). Only a brief review of the principles of rainfall measurement by a radar will be given here as more detailed discussion is available in these textbooks.

Although indirect, radar estimates of rainfall are continuous in space and provide information on the spatial variability of rainfall. Radar transmits a radio energy and measures the returned energy after reflection and scattering by raindrops, hailstones or snowflakes. Rainfall rate R is estimated from the measurement of the returned energy (radar reflectivity), Z. Unfortunately, there is no universal relationship connecting these two

parameters, although it is a common experience that larger rainfall rates produce more intense echoes (Doviak and Zrnic, 1984). Rainfall rate is dependent on drop size distribution. A real drop size distribution requires an indefinite number of parameters to characterize it, and thus the radar-determined value of Z alone can not provide a unique measurement of R. Due to the uncertain Z-R relationship, miscalibration of electronic components and many other factors, radar rainfall is estimated to have both systematic and random errors of 100% or more (Wilson and Brandes, 1979). Even with the modern radar technology (WSR-88D), Smith et al. (1996), and Pereira and Crawford (1995) reported that radar underestimated rainfall at all ranges. The underestimation of the rainfall by radar was found to be range dependent and the underestimation was most severe for far and close ranges.

The radar reflectivity factor (Z in units of mm^6/m^3) is proportional to the summation of the sixth power of particle diameters in a unit volume illuminated by the radar beam and is defined as

$$Z = \Sigma_i N_i D_i^6 = \int_0^\infty N(D)D^6 dD \qquad (2.1)$$

where N_i is number of drops per unit volume of air with diameter D_i and N(D) is the number of drops with diameters between D and D+dD in a unit volume of air. The desired parameter, rainfall rate (R), is related to D through the following equation assuming that there is no vertical air motion present.

$$R = \frac{\pi}{6} \int_0^\infty N(D)D^3 V_t(D) dD \qquad (2.2)$$

where $V_t(D)$ is the drop terminal velocity of a drop of diameter D that is approximated, in units of cm/s, by $V_t = 1400\ D^{1/2}$ (Wilson and Brandes, 1979).

Measurement of drop size distribution around the globe has been made under different climate conditions. Battan (1973) lists more than 69 different R-Z relations. In general a R-Z relation is described using the empirical relationship,

$$Z\ =\ aR^{\ b} \tag{2.3}$$

where a and b are constants. For stratiform rains the relation $Z = 200\ R^{1.6}$ was given by Marshall et al. (1955) and is known as the Marshall-Palmer formula, with R in mm/hr and Z in $mm^6\ m^{-3}$.

It is quite difficult to calibrate radars to within a decibel, and there could be a systematic bias in the radar measured reflectivity. Some of these errors can be compensated by choosing an appropriate R-Z relation. According to Cain and Smith (1976), the relation $Z = 1.55R^{1.88}$ removes any pervasive bias in the radar estimated rainfall (RER) in North Dakota, whereas in Miami, Florida, Woodley et al. (1975) reported that the relation $Z = 300R^{1.4}$ worked better. Filho (1996) used the same relationship in North-Central Oklahoma as suggested by Woodley et al. (1975). In a recent study using data from Tulsa and Twin Lakes, Oklahoma, Smith et al. (1996) suggested the parameter values to be a=0.017 and b=0.714 for the Oklahoma conditions.

Liu and Krajewski (1996) compared advection methods and a space-time kriging interpolation method to calculate hourly accumulation of radar-rainfall. The space-time evolution of rainfall fields was generated from a stochastic model. The generated fields were

sampled following typical radar scanning strategies. Based on the statistical results and a visual analysis of the graphical images, the authors suggested to use an interpolation scheme for radar observations even when storm velocity was not high. The space-time kriging method was found to provide the smallest mean error. The advection method gave the smallest standard error when advection velocity was high. The kriging method provided the best results for a low wind velocity.

Wilson and Brandes (1979) have discussed the factors that produce errors in radar rainfall measurement. These sources can be categorized as:

1. errors in estimating radar reflectivity factor;

2. variations in the Z-R relation; and

3. gauge and radar sampling differences.

Brandes (1975) has suggested a technique whereby gauges can be used to adjust the RER. Atlas et al. (1984) suggested that improvements in the accuracy of radar rainfall measurements can be achieved by measuring radar parameters in addition to reflectivity to overcome the ambiguity in drop size distribution. Goddard and Cherry (1984) suggested measurements of path-integrated microwave attenuation and also dual polarization methods to improve accuracy.

Smith et al. (1996) analyzed more than one year of data from two WSR-88D radars located in Oklahoma to characterize the systematic biases in the hourly precipitation accumulation estimates. The authors analyzed the biases in three contexts: (1) biases that arise from the range dependent sampling of the radar, (2) systematic differences between radar rainfall estimates when two radars are observing the same area, and (3) systematic

15

differences between radar and gauge measured rainfall values. A significant underestimation of rainfall was observed to occur within a 40 km range of the radar due to bias in reflectivity observations at the higher elevation angles used for rainfall estimation close to the radar. Bright band and anomalous propagation lead to systematic overestimation of rainfall at intermediate ranges. Beyond 150 km in spring-summer and beyond 100 km in winter-fall, underestimation of precipitation was pronounced due to incomplete beam filling and overshooting of precipitation. Radar-radar intercomparison analyses indicated that radar calibration was a significant problem at some sites.

2.3 Comparisons of Rain Gauge Data With Radar Scanned Data

Numerous articles have been published over the years comparing accuracy of radar scanned rainfall against rain gauge measured rainfall. There has been considerable debate in recent years about accuracy of different rainfall measurement techniques and whether measurement techniques based upon remote sensing technology, using radar and/or satellite systems, can replace or complement rain gauge measurements. Several researchers have suggested that radar estimated rainfall (RER) when calibrated with rain gauges can give a rainfall estimate with the point accuracy of gauges and the spatial resolution and coverage of a radar.

Wilson and Brandes (1979) compared the radar and gauge measurements for 14 Oklahoma storms observed by the NSSL WSR-57 radar. The average ratio of gauge and radar measured depth varied from 0.41 (radar overestimate) to 2.41 (radar underestimate). The average difference between radar and gauge point measurements for all 14 storms was

found to be 63%. But by removing the mean storm bias, the average difference was reduced to 24%. Much of the radar error results were attributed to storm-to-storm differences in the Z-R relationship caused by microphysical and kinematic processes that affect the drop-size distribution and drop-fall speeds. The authors suggested that the combined radar-gauge estimates were usually better than the gauge only for gauge densities < 1 per 300-400 km^2, whereas, radar-gauge estimates were no longer better than the gauge-only estimates when the density increased to about 1 per 250-300 km^2.

Legates and Willmott (1990) found that the mean standard error for a particular network and rain field was a function of the number of gauges in the network, the raining fraction of the area and the ratio of the standard deviation to the mean of the non-zero portion of the rain field. The authors found that the raingauge errors were directly proportional to total precipitation and amount to nearly 11% of the global catch.

Collier (1986) compared the bias and random errors in rainfall measured by a telemetering gauge network alone, and from a radar calibrated by using data from only a few gauges. He suggested that a very dense gauge network was needed to measure point rainfall very accurately. However, a less dense gauge network with a radar system calibrated using the data from a few of the telemetering gauges was capable of producing measurements which had the same or better accuracy as a sparse gauge network over a large area. The calibrated radar estimates were more accurate within 75 km of the radar site than those using the telemetric raingauge network alone. Based on the comparison of WSR-88D and Oklahoma Mesonet data, Pereira and Crawford (1995) concluded that the statistical

17

integration of radar estimates and Mesonet measurements produced a more accurate final analysis than using either of the two parameter fields alone.

Bellon and Austin (1984) analyzed a total of 37 weather sequences which passed over the City of Montreal, Canada, and found that the radar measured accumulations had an inherent error of the order of 25%, 0.5 hr forecasts had an error of 50% and 3 hr forecasts had an error of about 60%. The authors found that the introduction of the radar calibration factor did not improve forecasts much. In the studies of Wilson (1970) and Brandes (1975), the gauge-radar mean rainfall estimates were more accurate than the estimates obtained using only gauges for large area (29,0000 km^2), low gauge density (no more than one gauge per 700 km^2), and long duration rainfall events. Brandes (1975) showed that radar-measured rainfall corrected by gauge data improved the accuracy from 24% for measurements by gauge alone to 14% for combined radar-gauge measurements with a gauge density of one gauge per 1600 km^2. He suggested that evaporation below the radar beam, wind velocity fluctuations, and sampling were factors contributing to large spatial variations among calibration factors.

Although considerable research has been done to compare the accuracy of raingauge and radar measured rainfall, very limited information is available which compares the measurement of NEXRAD with rain gauges. The research conducted by the National Severe Storms Laboratory in Norman, Oklahoma, has been mostly based on a point comparison in the accuracy of rainfall between NEXRAD and selected rain gauges in central Oklahoma (NSSL, 1992). Also no information is available in terms of examining the relationship between the spatial distribution of runoff and spatial structure of rainfall at the pixel level.

Spatial distribution of runoff within a watershed is extremely important for flood prediction and water resource management, as well as basin planning.

Ma (1993) applied NEXRAD rainfall data, rain gauge network precipitation data, and designed-storm data to compare spatial variation in rainfall depths. The rain gauge network and NEXRAD were found to give a different center of storm. Also, the raingauge measurements over predicted the rainfall in some parts of the watershed and under predicted in other parts as compared to the NEXRAD measured rainfall. Approximately half of the total pixels in the watershed were found to have different runoff values between NEXRAD data and rain gauge network data. The difference between NEXRAD data and the design uniform storm data was found to be less than the difference between NEXRAD and rain gauge data. The author concluded that the spatial distribution of surface runoff was strongly affected by the spatial pattern of precipitation.

Smith et al. (1996) used raingauges and the NEXRAD system of WSR-88D radar located in Twin Lakes and Tulsa, Oklahoma to characterize biases of radar-estimated rainfall compared to the actual rainfall. The intercomparisons were based on WSR-88D hourly rainfall accumulation products and hourly raingauge data. The authors concluded that radar underestimated rainfall at most sites. Underestimation was most severe at far range and close range, but at most sites, underestimation occurred at all ranges. The raingauge observations were found to be 48% larger than WSR-88D rainfall estimates in the range 0-40 km, 18% in the range 40-160 km, and 40% in the range greater than 160 km for the warm season. For the cold season the corresponding values were found to be 30%, 14%, and 100%. However, accurate delineation of the no-rain area was found to be a particular strength of the radar

estimates. For sites within 200 km of the radar location, radar accumulations were found to be zero for more than 98% of the zero raingauge accumulations. Analyses of spatial coverage of heavy rainfall was also found to be a fundamental advantage of radar over raingauge networks for rainfall estimates.

2.4 Effects of Spatial Variability of Rainfall on H/WQ Model Outputs

Although it is acknowledged that, in general, catchments have an integrating or smoothing effect on rainfall both in time and in space, the complex relationship between the degree of spatial variability of rainfall, catchment characteristics (topography, channel network, soils, etc.), antecedent soil moisture conditions and catchment response is poorly understood (Shah et al., 1996). A very few studies have been conducted to investigate the significance of spatial variability of rainfall in H/WQ processes. Dawdy and Bergman (1969) studied the effect of rainfall variability on stream flow simulation in a small basin in Southern California. They concluded that predicting peak discharge based on a single rain gage observation resulted in a standard error on the magnitude of 20%. Similarly, Troutman (1983) suggested that spatial variability of precipitation inflates mean squared errors of prediction in precipitation-runoff modeling. One component of these larger errors was observed to be bias which often takes the form of overprediction for large events and underprediction for small events. He examined this problem assuming stochastic structure for the spatial behavior of rainfall together with a form of the Green-Ampt infiltration equation for prediction of storm runoff volume. In similar studies, Wilson et al. (1979) and other researchers (Beven and Hornberger, 1982; Seliga et al., 1992; Corradini and Singh,

1985; Krajewski et al., 1991; Obled et al., 1994) have concluded that storm runoff hydrographs are sensitive to the spatial distribution and accuracy of the precipitation inputs.

Young et al. (1992) attempted to assess the impact of spatial variability of rainfall on model performance by getting a first approximation of the deviations of runoff volume and sediment load caused by varying the spatial distribution of rainfall input to AGNPS. They generated event rainfall amounts by distributing a known volume of water by a bivariate normal distribution function. The parameters of the distribution were adjusted for the purpose of centering the peak over different locations on the watershed and to adjust the spread of the distribution. The authors found that in one case total N loss was four times more and the total P and sediment yield were five times greater than the estimates obtained from an average uniform rainfall. In a similar study, Luzio and Lenzi (1995) applied AGNPS to a watershed in northern Italy. The authors applied spatially variable rainfall input using the spline method of interpolation. Rainfall erosion index and sediment yield were increased by more than 20% and total N and total P loads were increased by more than 17% when spatially variable rainfall was used. The authors speculated that coupling of radar data to model input data would significantly improve model results.

Shah et al. (1996a) investigated the relationship between the spatial variability of rainfall and catchment response by conducting experiments with a stochastic rainfall field model and a physically distributed Systeme Hydrologique Europeen (SHE) model. They used Turning Bands Method (TBM) incorporating a fractionally differenced line process to generate Gaussian random fields with a specified space-time correlation structure to develop the rainfall field model. A transformation was then applied to the Gaussian field to

reproduce the non-stationary temporal structure and skewed marginal distribution of observed rainfall and this transformed field was then propagated in space with the required velocity. Comparisons of the means, variances, skewness, cross- and auto-correlation functions of the observed and simulated storms at the sampling points showed a good agreement. Later, the authors applied the spatially-variable rainfall to the SHE model to assess the interaction between spatial variability of rainfall, antecedent catchment conditions and runoff production to isolate the component of error in runoff simulations associated with incomplete sampling of the rainfall input to distributed catchment models. Percent errors in peak discharge and in total volume ranged from 1-39% and 1-16%, respectively. The percentage errors were observed to be larger for dry catchment conditions than for wet conditions. The errors increased with decreasing correlation as the rainfall became more spatially variable. Based on the results the authors suggested that under wet conditions, good predictions of runoff could be obtained with a spatially averaged rainfall input, provided that at least one gauge was available in the 10.55 km^2 catchment. But the interpretation of this work was limited by the small catchment size, a few number of storms simulated and a few raingauges used for the conditional simulation.

Faures et al. (1995) examined the effect of various rainfall measurement techniques and spatial rainfall variability on runoff modeling of a small watershed (4.4 ha). The authors demonstrated that the uncertainty in runoff estimation was strongly related to the number of gauges available to measure input rainfall. The spatial variability of rainfall was observed to cause a large variation in modeled runoff. When five model runs were conducted using input from one of the five recording raingauges, one at a time, the coefficient of variation for

peak rate and runoff volume ranged from 9 to 76%, and from 2 to 65%, respectively, over

eight observed storm events. By using four well distributed gauges the variation in modeled

runoff volume was reported to approach the sampling resolution of the raingauges as well

as the estimated accuracy of runoff volume and peak rate observations. The authors

concluded that if distributed catchment modeling was to be conducted at the 5 ha scale in an

environment dominated by convective air-mass thunderstorm rainfall, knowledge of spatial

variability on the same scale was required. A single raingauge with the standard uniform

rainfall assumption could lead to large uncertainties in runoff estimation. In a similar study

conducted on a relatively larger watershed (83 km^2) Hamlin (1983) observed that a rainfall

obtained from a single gauge resulted in underestimation of peak and the errors in the peak

flow estimation exceeded 200%. With the inclusion of an additional gauge the magnitude

of error was sharply reduced to 100%. Use of three gauges gave a significantly better result.

Most of the studies conducted to examine the effect of spatial variability of rainfall

on H/WQ process have focused primarily on runoff volume, time to peak runoff, and peak

runoff rate predictions. Very few attempts have been made to study the effect of input

rainfall spatial variability on the transport of sediment and nutrients. Young et al. (1992)

studied the effect of rainfall spatial variability on N, P and sediment transport using the

AGNPS model. The rainfall spatial variability was captured using a synthetic storm.

Hamlin (1983) mentioned that the use of synthetic rainfalls raises problems which must be

recognized. The results of the gauge density as it affects flow prediction depends not only

on the catchment and number of gauges used but also on the rainfall pattern and choice of

model. Synthetic rainfall data may not model the patterns and amount of real rainfall

adequately. In addition, because of local configuration and site measurement problems of raingauges, there may be causal relationships between rainfall and stream flow which may not be modeled in the synthetic situation. With the availability of radar scanned rainfall data, it is now possible to study the spatial characterization of rainfall and to incorporate this rainfall variability in H/WQ models in order to improve the accuracy of the model predictions.

It is clear from the above discussion that most of the studies conducted to date using spatially variable rainfall were based on relatively smaller watersheds (4 ha - 77 km^2) where only a few raingauges were available to capture the rainfall pattern. Since rainfall spatial variability can be expected to increase with an increase in the watershed size, the results reported in the literature may not be applied to a larger watershed. The knowledge of uncertainty in the estimated parameters due to rainfall spatial variability is also very limited. Only one study conducted by Troutman (1983) attempted to assess the effect of rainfall spatial pattern on estimated model parameters. In that study, the model considered was a rainfall-runoff model. The parameters that affect the transport of sediment, and sediment-attached nutrients were not discussed. The author used a synthetic rainfall to simulate the spatial correlation pattern of an actual rainfall. Because of the simplicity of the stochastic rainfall model used in the study, the results reported may not be expected to define the variability in actual rainfall-runoff modeling applications. The simulation was based on an imaginary watershed and raingauge configuration. The results obtained were not verified using the observed data from a watershed.

In summary, a very few studies have been conducted using rainfall spatial variability to assess model output uncertainty. Most of the studies were focused on runoff volume and peak runoff rate and very limited information exists on the effect of rainfall spatial variation on sediment and nutrient transport. Most of the studies were conducted on a relatively smaller watershed using a few number of raingauges to capture rainfall spatial patterns. The results obtained could not be transferred to the larger watersheds where a large number of gauges may be available to measure rainfall patterns. No study has been conducted to estimate the effect of rainfall spatial variability on estimated model parameters using observed rainfall and output data. Also no attempt has been made to use radar scanned rainfall as an input to assess the effect of rainfall spatial variation on model parameters/outputs.

CHAPTER 3

THEORY

3.1 Interpolation of Rainfall Data

In the application of hydrologic modeling, rainfall often needs to be estimated at a given site because either data are missing or the site is ungauged. Various methods are available to spatially interpolate rainfall at a point based on data available at other sites. A number of techniques for spatial interpolation of rainfall with varying degree of complexity have been suggested in the literature. These techniques can be grouped into the following categories (Tabios and Salas, 1985).

1. Theissen Polygon Method

2. Polynomial Interpolation

3. Inverse Distance Interpolation

4. Multiquadratic interpolation

5. Optimal interpolation, and

6. Kriging

Most of the proposed interpolation techniques are based on a weighted average of surrounding stations. Let x_j and y_j denote the coordinates of a point j in two dimensional space and p_j, a function of x_j and y_j, denotes the observed precipitation depth at n sampling

points, j=1,2,....... n. An estimate of the precipitation depth p_0 at any point with coordinates x_0 and y_0 can be represented as a weighted linear combination of the observed values.

$$p_0 = \sum_{j=1}^{n} w_j \, p_j \qquad (3.1)$$

where w_j = weight of sampling point j. Equation (3.1) is the general form of the interpolation function. The different interpolation techniques differ only in evaluating the weights w_j. In some cases weights are only dependent on distance; in other cases the weights are optimized on the basis of a correlation function. All of the above methods are described in the following sections. The discussion is primarily based on the work reported by Tabios and Salas (1985).

1. Theissen Polygon Method

This method is based on proximal mapping (i.e., nearest distance neighbor). The estimate of the rainfall amount p_0 at any point of interest is equal to the observed value of the nearest sampling point in the area. Let

$$d_{oj} = \sqrt{(x_0 - x_j)^2 + (y_0 - y_j)^2} \qquad (3.2)$$

for j=1,2,3,........ n and $d_{0i} = \min(d_{01}, ..., d_{0n})$. The subscript i is determined by searching for the minimum point-station distance, so that

$$w_j = 0 \text{ for } j \neq i$$

and
$$w_j = 1 \text{ for } j = i$$

27

2. Polynomial Interpolation

Polynomial interpolation requires fitting of a global equation in the rainfall field using either an algebraic or trigonometric polynomial function. The global form of the polynomial function can be written as

$$p_0 = \sum_{k=1}^{m} a_k \varphi_k(x_0, y_0) \qquad (3.3)$$

where p_0 is the interpolated value at any point (x_0, y_0), a_k is the kth polynomial coefficient, $\varphi_k(x_0, y_0)$ the kth monomial in terms of x_0 and y_0 coordinates and m is the total number of monomials determined from the degree of polynomial function fitted in Equation (3.3). Since the interpolation function (3.1) is in terms of weights, it is convenient to express the polynomial equation (3.3) in the form of (3.1). Two approaches available for this purpose are discussed in the following sections.

a. Least Square Approach

This approach provides an estimate of p_0 for processes having a trend surface characteristic. Let p_j be the measured quantity of the rainfall p at sampling station j=1,2,3,... n and p´ be the estimate of the same process based on a model in Equation (3.3). Then

$$p' = \sum_{k=1}^{m} a_k \varphi_k(x_j, y_j) \qquad (3.4)$$

where $\varphi_k(x_j, y_j)$ is the kth monomial in terms of the coordinates x_j and y_j of station j. Parameter set a_k, k=1,2,..... , m is estimated by minimizing the sum of square errors given by

$$F = \Sigma_{j=1}^{n} [p_j - p'_j]^2 \qquad (3.5)$$

b. Lagrange Approach

This approach is an exact interpolation technique. In this case, the coefficients a_k are

evaluated so that the process p will pass through all the observed values. Thus, this approach

requires that the number of monomials be equal to the number of gaging stations (m=n). The

equation for the interpolation estimation is

$$p_0 = \Sigma_{k=1}^{n} [\Sigma_{k=1}^{n} \beta_{kj} \varphi_k(x_0, y_0)] p_j \qquad (3.6)$$

where β_{kj} is an element of the inverse of the n x n matrix with elements $\varphi_k(x_j, y_j)$ for

k=1,2,...,n stations.

3. Inverse Distance Interpolation

This type of interpolation scheme belongs to a family of distance weighting

techniques. The weights of the interpolation function (3.1) are solely a function of the

distance between the point of interest (x_0, y_0) and the sampling points (x_j, y_j) for j=1,2,...,n.

Considering the distance d_{0j} as in Equation (3.2), the weight of a sampling point

(x_j, y_j) is given in general by

$$w_j = \frac{f(d_{oj})}{\Sigma_{i=1}^{n} f(d_{oi})} \qquad (3.7)$$

where $f(d_{oj})$ represents a given function of the distance d_{oj}. A commonly used form of the

29

function f(.) is

$$f(d_{oj}) = \frac{1}{d_{oj}^{b}}$$

(3.8)

where b is an appropriate constant. Here the weight W_j approaches zero as the distance d and/or the parameter b increases. When the parameter b is given the value one or two, the interpolation technique is known as reciprocal distance interpolation and inverse square distance interpolation, respectively.

4. Multiquadratic Interpolation

In multiquadratic interpolation, the influence of each sampling point is represented by quadratic cones as a function of the coordinates of these points. The estimate for a given point (x_0, y_0) is thus obtained by the sum of the contributions from all those quadratic cones. This is mathematically represented as

$$p_0 = \Sigma_{i=1}^{n} c_i d_{oi}$$

(3.9)

where c_i = multiquadratic coefficient of sampling point (x_i, y_i) and d_{oi} is the distance between points (x_o, y_o) and (x_i, y_i).

5. Optimal Interpolation

Let p_o be the rainfall depth to be determined and Equation (3.1) is used to estimate p_o. Let p be the estimate of p_o. Then in the optimal interpolation technique, the weights are

30

determined by minimizing the variance of the error of interpolation σ_e^2 which is given by

$$\sigma_e^2 \;=\; var[p_o - \hat{p}_o] \;=\; var[p_o - \Sigma_{j=1}^{n} w_j p_j] \tag{3.10}$$

Expanding the above equation gives

$$\sigma_e^2 = \sigma^2 - 2 \Sigma_{j=1}^{n} w_j \, cov(p_o, p_j) + \Sigma_{j=1}^{n} \Sigma_{i=1}^{n} w_i w_j cov(p_i p_j) \tag{3.11}$$

where σ^2 is the variance of the process p_o and $cov(p_i, p_j)$ represents the covariance between p_i and p_j.

6. Kriging Interpolation

In hydrologic applications several forms of kriging have been proposed and used. Kriging is similar to the optimal interpolation except that the spatial correlation function is replaced by a variogram. As in optimal interpolation, kriging interpolation requires that the observed process is second order stationary. Essentially, it assumes homogeneity in the means, variances and covariances. In addition, an isotropic spatial covariance structure is assumed. The homogeneous and isotropic semivariogram is defined as

$$\gamma(d_{ij}) \;=\; \frac{1}{2} var[p_i - p_j] = \sigma^2 - cov(d_{ij}) \tag{3.12}$$

for $i,j = 1,2,\ldots,n$ and $\gamma(d_{ij})$ is the semivariogram as a function of the distance d_{ij} between points i and j. Therefore, rewriting equation (3.11) by substituting equation (3.12) for $cov(p_i, p_j) = cov(d_{ij})$ gives

31

$$\sigma_e^2 = \sigma^2 - 2 \sum_{j=1}^{n} w_j [\sigma^2 - \gamma(d_{oj})] + \sum_{j=1}^{n} \sum_{i=1}^{n} w_i w_j [\sigma^2 - \gamma(d_{ij})] \qquad (3.13)$$

Any of the above six methods can be employed to interpolate rainfall at the grid points. But before interpolation is done two issues need to be addressed: (1) how many observed data points will be considered when estimating rainfall at a point and; (2) which interpolation technique should be selected. Several reports exist in the literature describing the spatial correlation pattern of rainfall. Correlation of rainfall decreases with distance and rain gauges situated very far from the reference point may be very weakly correlated or independent (for example Tabios and Salas, 1985; Kruizinga and Yperlaan, 1978). Wilson and Brandes (1979) mentioned that the maximum useful range of a single adjustment gauge varies from storm to storm. Brandes (1975) defined maximum useful range as the distance at which storm total rainfalls become essentially uncorrelated. For Oklahoma convective storms, he found this distance to be approximately 90 km. Kruizinga and Yperlaan (1978) reported on the number of surrounding rain gauges and the calculation of interpolation weights. The authors compared interpolation errors derived from considering seven surrounding stations to errors when all the surrounding stations were considered. When all of the stations were considered, a weight proportional to $\exp(-r/r_o)$ was given to each station and stations with weights less than 0.001 were omitted. Here r was the distance to the reference point and r_o a constant chosen in the order of the mean distance between stations. Based on the results obtained the authors reported that the two methods did not give significantly different results. Thus for Oklahoma rainfalls, either seven surrounding

32

raingauges or all raingauges within a radius of 90 km may be used for interpolation at the grid points.

Selection of the interpolation technique depends on the ability of the technique to estimate rainfall at the grid cell with the maximum possible accuracy. Tabios and Salas (1985) evaluated six techniques by comparing interpolated values with the observed values at the reference point. They suggested 4 different criteria for comparison as follows.

1. Comparison of the mean and variance of the interpolated and observed values.

2. The sum of square errors between the observed and interpolated values.

3. The proportion of the variance of the observed values accounted for by the interpolation, called the coefficient of efficiency

$$E = 1 - \frac{S}{S_o} \tag{3.14}$$

where S_o is the sum of the square differences between the observed values and the mean at point (x_o, y_o) and is given by

$$S_o = \Sigma_{i=1}^{n} [p_o(t) - m_o]^2 \tag{3.15}$$

4. Coefficient of determination obtained by regressing observed and interpolated values.

Based on the results obtained from their study, Tabios and Salas (1985) concluded that polynomial interpolation gave inferior results. The inverse square distance method was found to be somewhat better than the reciprocal distance technique and significantly better than the Theissen polygon method. Based on the criteria of the sum of square errors and the

coefficient of efficiency, the Theissen and reciprocal distance methods gave inferior results. Based on the coefficient of determination only the Theissen method was significantly inferior to the others.

Seed and Austin (1990) mentioned that the distance weighting schemes suffer from a certain arbitrariness in the selection of the parameters and the interpolated surface is not always smooth in the neighborhood of the data points. In order for the interpolated surface to be smooth, the derivative of the weighting function must tend to zero as the distance to the point tends to zero and the function should decay at a rate faster than the inverse square of the distance. Distance weighting schemes also do not cope well with clustered data.

In the inverse distance interpolation, the distance dependence of chosen weights is not very important when the distances are of the same order; in the other case a distance dependence of $1/r^2$ will give a better estimate (Kruizinga and Yperlaan, 1978). One major drawback of the inverse distance interpolation approach is that when two or more sampling points are close to each other, the redundant information from these stations is not discriminated against (Tabios and Salas, 1985).

Optimal interpolation and kriging require that the observed process is second-order stationary. Essentially this assumes homogeneity in the means, variances and covariances. In addition, an isotropic spatial covariance structure is assumed. If these assumptions are not met, the accuracy of the interpolation may be questionable.

Seed and Austin (1990) stated that rainfall and cloud fields are extremely intermittent and variable as compared to some other variables like temperature, pressure and wind. The underlying cause for this extreme variance is drastic non-linearity involved in cloud and rain

34

formation. The response from a hydrological point of view is to exercise extreme caution about the likely accuracy of any interpolation scheme, including those of great mathematical complexity.

In general, it can be expected that as the level of sophistication of an interpolation technique increases, the expected accuracy will also increase. But very sophisticated techniques are more difficult to implement as compared to the relatively simpler schemes. Probably, that is the reason why the Theissen polygon method which is the simplest method and was developed in 1911 is still widely used in hydrology (Seed and Austin, 1990).

3.2 Calibration of NEXRAD Data

Among the rainfall measuring sensors, raingauges and land-based radar are probably the two most important in rainfall estimation. Radar measured rainfall can have both systematic and random errors of 100% or more (Seo et al., 1990). Estimates of precipitation can be improved when raingauge observations are used to calibrate quantitative radar data as well as to estimate precipitation in areas without radar data. Several researchers have suggested that radar estimated rainfall calibrated with raingauges can give a rainfall estimate with the point accuracy of gauges and spatial resolution and coverage of a radar. However, there are several errors associated with radar measured rainfall depth because radar estimates rainfall amount indirectly. Error sources reside in the measurement of radar reflectivity factor, evaporation and advection of precipitation before reaching the ground, and variations in the drop-size distribution and vertical air motions (Wilson and Brandes, 1979).

Seo et al. (1990) grouped the radar calibration techniques into two classes:

35

deterministic and statistical. The deterministic approach involves calibration of radar rainfall against raingauge measurements or the deterministic interpolation of gauge to radar ratio. The statistical approach ranges from multivariate analysis to cokriging.

Radar estimated rainfall depth would be an ideal source to obtain rainfall at grid points but before radar data can be used, they need to be calibrated because of the associated errors. Brandes (1975) suggested the following steps to derive a calibrated rainfall field from radar measurements.

1. First of all an uncalibrated radar rainfall field is obtained. This can be obtained from NEXRAD which is available to the researchers.

2. The radar rainfield is then calibrated with raingauge observations by determining a multiplicative calibration factor at each raingauge site. Jia (1995) used a calibration factor (CF) for NEXRAD data defined as follows.

$$CF = \frac{Gauge\ Rainfall}{Radar\ Rainfall} = \frac{R_g}{R_{rc}} \qquad (3.16)$$

For several raingauge sites, he defined the calibration factor as

$$CF = \frac{1}{n} \Sigma_{i=1}^{n} \left(\frac{R_g}{R_{rc}} \right)_i \qquad (3.17)$$

Where R_g is the raingauge measured rainfall and R_{rc} is the radar estimated rainfall. Gauges recording very small rainfall should not be used because they can lead to very small or very large calibration factors. The calibration factor obtained using Equations (3.16) and (3.17)

can be applied uniformly to rainfall fields. He suggested that either one pixel value or an average of 9 pixels surrounding the raingauge site could be used as the radar measurement (R_i).

Brandes (1975) used an objective analysis scheme to move corrected factors from raingauge sites onto the grid point field. The weight (Wt_i) each gauge calibration $(G)_i$ receives at a particular grid point is

$$Wt_i = \exp(-d^2 / EP) \qquad (3.18)$$

where d is the distance between gauge and grid point (km). EP controls the degree of smoothing and is kept as small as possible to preserve the detail in input observations. Brandes (1975) suggested EP to be 300 km^2 for a gauge density of 1 gauge per 900 km^2. To ensure consideration of more than one gauge-radar comparison at each grid point for rainfalls in Oklahoma, an influence radius of 70 km can be selected for individual calibration factors.

Brandes (1975) suggested two passes through the objective analysis grid with the input data to produce the radar calibration field. On the first pass, a first-guess grid point calibration (F_1) is computed as

$$F_1 = \frac{\sum_{i=1}^{n} Wt_i \, G_i}{\sum_{i=1}^{n} Wt_i} \qquad (3.19)$$

where n is the number of gauges. Differences (D_i) are calculated at each grid location from

$$D_i = G_i - F_1 \qquad (3.20)$$

where the first-guess estimate (F_1) is taken at the grid point nearest the raingauge rather than at the gauge itself.

The second pass uses equation (3.18) with EP reduced by 50% and analyzes the difference at each observation site by the same method. Difference values (corrections) calculated at each grid point are added to the first-guess field and the final grid point calibration is given by

$$F_2 = F_1 + \frac{\sum_{i=1}^{n} W t_i D_i}{\sum_{i=1}^{n} W t_i} \qquad (3.21)$$

When this calibrated field is multiplied with the radar field, the calibrated radar rainfall field is obtained.

In the areas where quality radar data are not available or where radar data are missing, it can be treated as if data from raingauges are available. The rainfall depth at grid points can be obtained by interpolating the raingauge data as outlined in the previous sections.

Corrected radar and gauge derived rainfall distributions can be combined with the emphasis placed on the calibrated radar field. Several researchers have shown that a gauge derived rainfall field is a better estimate of rainfall than either of the two individual methods. Pereira and Crawford (1995) used a statistical objective analysis scheme to show that NEXRAD and Oklahoma Mesonet data could be combined to produce a better estimate of the precipitation than by using either of the two alone.

Brandes (1975) estimated that areal precipitation depth errors for nine rainfalls over a 3000 km^2 watershed averaged 13 and 14% (1.5 and 1.6 mm) when the radar was calibrated

by networks of raingauges having densities of one gauge per 900 and 1600 km², respectively. Areal precipitation estimates derived from rainfalls observed at the gauges alone produced errors of 21 and 24%, respectively. Adjusting the radar data by a single calibration factor resulted in error reduction to 18%. Radar data added to gauge observations also increased the explained variance in point rainfall estimates above that from gauges alone.

Collier (1986) compared the bias and random errors in rainfall measured by a telemetering gauge network alone, and from a radar calibrated by using data from only a few gauges. He suggested that a very dense gauge network was needed to measure point rainfall very accurately. However, a less dense gauge network with a radar system calibrated using the data from a few of the telemetering gauges was capable of producing measurements which had the same or better accuracy as a sparse gauge network over a large area and the calibrated radar estimates were more accurate within 75 km of the radar site than those using the telemetric raingauge network alone. A presence of bright band was found to increase the radar estimated rainfall bias.

Several statistical methods have been suggested in the literature to combine the radar and raingauge data to improve the rainfall field estimates. Pereira and Crawford (1995) developed a Statistical Objective Analysis (SOA) to estimate rainfall accumulations using radar and raingauge estimates of rainfall. Based on the comparisons with the observed data, the authors concluded that the expected error variance of the combined data was less than that obtained from either the error variance of radar estimates or raingauge measurements alone.

39

Seo et al. (1990) and Krajewski (1987) have discussed the use of various cokriging methods, e.g. ordinary, universal, and disjunctive, to utilize both raingauge and radar rainfall data in rainfall estimation. The authors concluded that if the bias in the radar measurement was removed and the error in the radar measured rainfall was low, combining raingauge data with the radar data may not alter rainfall fields significantly. However, if the error in the radar rainfall is high, a substantial improvement could be expected.

It is clear from the above discussion that when both raingauge and NEXRAD data are available, NEXRAD can be calibrated using the raingauge data. Once this calibrated radar rainfall field is obtained, it can be used directly to get rainfall at the grid points. One problem with the estimation of rainfall using NEXRAD is the grid cell size. NEXRAD estimates rainfall at a grid resolution of 4 km x 4 km. The rainfall variability at any finer resolution will be very difficult to obtain using the NEXRAD data.

3.3 Description of NEXRAD Rainfall Algorithms and Techniques

The most basic element common to all the geometric computations is the grid coordinate system used to identify the location of stations and geographical boundaries, such as river basins. The grid used by the NEXRAD rainfall product is the Hydrologic Rainfall Analysis Project or HRAP grid. The primary purpose of HRAP was to develop the objective techniques for preprocessing, quality controlling, and optimally merging rainfall data from multi-radars, raingauges, and satellites for use in various hydrometeorological applications (Greene and Hudlow, 1982). The grid is based on a polar stereographic map projection with a standard longitude of 105 West. The mesh length at 60 North latitude is 4.7625 km. The

mesh length varies between 3.5 and 4.5 km, depending upon latitude, for latitudes of the contiguous United States. The grid is positioned such that the HRAP coordinates at the North Pole are (401, 1601). All grid coordinates are positive over the United States. The mesh lengths for other latitudes can be computed from:

$$Z = \frac{4.7625}{(1 + \sin 60^\circ)/(1 + \sin \varphi)}$$

(3.22)

where Z is the mesh length at latitude φ (km).

The coordinates of a point P(x,y) are computed as follows

$$RE = \frac{\left| EARTHR * (1 + \sin(60^0)) \right|}{ZMESH}$$

(3.23)

$$R = \frac{RE * \cos(XLAT)}{(1 + \sin(XLAT))}$$

(3.24)

$$WLONG = XLON + 75^0$$

(3.25)

$$X = R * \sin(WLONG) + 401$$

(3.26)

$$Y = R * \cos(WLONG) + 1601$$

(3.27)

where EARTHR is the radius of the earth (6371.2 km), ZMESH is the mesh length at 60° latitude (4.7625 km), XLAT is the latitude of the point to be converted (decimal degrees), and XLON is the longitude of the point to be converted (decimal degrees).

The orientation and mesh length of the grid was selected such that it contains the National Meteorological Center (NMC) Limited Fine Mesh I (LFM) and the National Weather Service (NWS) Manually Digitized Radar (MDR) grids as subsets. The HRAP grid mesh length is 1/40th and 1/10th the size of the LFM I and MDR mesh lengths, respectively.

3.4 Bias in Parameter Estimation

Haan (1989) gave a generic representation of hydrologic models as

$$\underline{Q} = f(\underline{I}, \underline{P}, t) + \underline{e} \qquad (3.28)$$

where $\underline{Q}$ is an n x k matrix of hydrologic responses to be modeled, f is a collection of l functional relationships, $\underline{I}$ is an n x m matrix of inputs, $\underline{P}$ is a vector of p parameters, t is time, $\underline{e}$ is an n x m matrix of errors, n is the number of data points, k is the number of responses, and m is the number of inputs.

Generally $\underline{I}$ represents inputs some of which are time varying such as rainfall, temperature, etc., while $\underline{P}$ represents coefficients particular to a watershed which remain constant. The values of the most of the model parameters are seldom known. They must be estimated by calibration before the model can be applied to make predictions. The error term e represents the difference between what actually occurs, $\underline{Q}$, and what the model predicts, $\hat{Q}$.

$$\hat{Q} = f(\underline{I}, \underline{P}, t) \qquad (3.29)$$

$$\underline{e} = \underline{Q} - \hat{Q} \qquad (3.30)$$

If we denote $\underline{I}^*$ as the error free true input and $\underline{P}^*$ as the true parameter value for the model, putting these values in Equation (3.28) will give the relation between actual and predicted output. Here in Equation (3.28), $\underline{I}$ is the erroneous input. An erroneous input will influence the value of $\underline{P}$ and the estimated parameter values may not be the true parameter values ($\underline{P}^*$).

Troutman (1983) classified the modeling errors into two components: (1) model error with correct input $\underline{I}^*$ and $\underline{P}^*$; and (2) error due to erroneous input. The input of interest in this research is rainfall depth. The outputs considered are runoff volume, total sediment, sediment-attached N, and sediment-attached P transport at the watershed outlet. Correct input means that the true rainfall pattern is known as every point in the watershed. Input error is present when measurements from only a small number of gauges are used when a more extensive network might be necessary to give an adequate representation of precipitation over the watershed of interest. Troutman (1983) suggested that even if measured rainfall at the small number of gauges is equal in expected value to areal average rainfall, the variance of watershed average precipitation is always less than that of point rainfall and this difference in variability could result in serious biases in runoff prediction. Even when using this correct input, there would be some error in the predicted results arising from the fact that the model itself is only a simplified approximation of the processes occurring in the nature. This type of error is known as model error or model uncertainty and is not considered in this study. It is only the input error, component (2) above, that is of interest here.

The problem in using an erroneous input in a H/WQ model is that the predicted output is no longer equal to the actual output. Evaluating a model with erroneous input $\underline{I}$

introduces a bias in the output given by the Equation (3.29). On the other hand, if the correct output is known, using an erroneous input in estimating model parameters will result in erroneous model parameters ($\underline{P}$). The bias in model parameters $\underline{e}_p$ can be given as

$$\underline{e}_p = \underline{P}^* - \underline{P} \qquad (3.31)$$

where $\underline{P}$ is parameter estimated using correct input value $\underline{I}^*$. Several parameter estimation techniques such as method of moments, least squares, Bayesian estimation criteria or any other arbitrary objective function defined by the user can be used to estimate the model parameters.

CHAPTER 4

METHODOLOGY

4.1 Description of the Study Area

The study was conducted using data from the Little Washita basin in Southwest Oklahoma. This basin covers 610 km² and is a tributary of the Washita river in Southwest Oklahoma (ARS, 1991). Figure 4.1 shows the location of the watershed in Oklahoma. The watershed is primarily a rural basin. The reasons for selecting the watershed were (1) DEM, soil, and land use data were available in digital form for this watershed; (2) a dense recording raingauge network has been operated by USDA-ARS for a long time; and (3) NEXRAD weather radar is located in Twin Lakes, OK and covers the study area. Moreover, several stream gauges are operated by the USGS within the watershed and a subwatershed of the desired size could be delineated for the purpose of this research.

Climate

The watershed has a typical continental climate. The climate is characterized as moist and subhumid with average annual precipitation of 747 mm (29.42 inches). Approximately 98% of the annual precipitation in the basin is rain and the remainder is snow and sleet (Ma, 1993).

Little Washita Watershed

Figure 4.1. Location of the Little Washita basin in Oklahoma

Summers are typically hot and relatively dry. The average high temperature for July

is 34⁰ C and the average rainfall accumulation for July is 56 mm. Winters are typically short,

temperate, and dry but are usually very cold for a few weeks. The average daily low

temperature for January is -4⁰ C and the average accumulative precipitation for January is

27 mm. Much of the annual precipitation and most of the large floods occur in the spring and

fall (ARS, 1991).

Geology

The primary geological survey of the area was conducted by Davis (1955). The

bedrock exposed in the watershed consists of Permian age sedimentary rocks. The surface

drainage is generally to the east although the formation dips generally to the southwest. The

oldest formation in the watershed is the Chickasha formation which outcrops in the eastern

or outlet side of the watershed and comprises 4.65% of the total watershed area. The

Chickasha formation is several hundred feet thick, is relatively impermeable and consists of

a heterogeneous mixture of sandstones, shales, and silt stones. The Marlow formation

comprises 14.2% of the watershed and consists mostly of even-bedded, brick-red sandy shale

that is gypsiferous. The predominant formation in the catchment is Rush Springs formation

which overlies the Marlow formation, and comprises 45.6% of the watershed area. The Rush

Springs formation consists of fine-grained sand stone and silt stone strata that are evenly to

highly cross-bedded. The Cloud Chief formation overlies the Rush Springs formation and

consists of irregular, impure gypsum beds interbedded with gypsiferous shales. This

formation comprises 16.6% of the watershed. It outcrops the watershed as outliers, so only

47

its lower parts can be seen.

Soils

Figure 4.2 shows the main soil groups of the basin. The Natural Resources Conservation Service (NRCS) have extensively surveyed the soils in the watershed and have classified 64 different soil series. Within these soil series, 162 soil phases have been mapped to reflect differences in characteristics that affect land use. Several other soil characteristics are also defined for each soil group such as depth to bedrock, typical texture found at each depth, permeability, available water capacity, pH, shrink-swell potential, corrosivity, and suitability for use in construction projects such as road fills, pond embankments, building foundations, and septic tank filter fields. Hydrologic soil groups and average crop yield under irrigated and nonirrigated conditions are also listed. The watershed soils are grouped into the following nine associations:

1. Grant-Pond- Creek-Lucien-Minco soils are deep and shallow, loamy and the slope ranges from nearly level to steep on uplands.

2. Port-Pulaski-Gracemont soils are deep, loamy and sandy and the slope is nearly level on flood plains.

3. Konawa-Dougherty-Eufala soils are deep, sandy, well drained to somewhat excessively drained in upland; slope ranges from nearly level to rolling.

4. Cobb soils are prairie soils that are moderately deep, loamy and slope ranges from nearly level to greatly slopping.

48

Figure 4.2. Soil groups of the Little Washita Basin

49

5. Renfrow-Kirkland-Bethany soils are well drained, loamy and slope ranges from nearly level to gently sloping.

6. Dale-Reinach-McLain soils are well drained or moderately well drained, loamy and slope nearly level.

7. Stephenville-Eufala soils are well drained or somewhat excessively drained, loamy or sandy, and slope ranges from gently sloping to moderately steep.

8. Stephenville-Noble-Darnell-Windthorst soils are deep or shallow, moderately well drained to well drained, loamy or sandy on uplands, and slope ranges from very gently sloping to hilly.

9. Nash-Lucien-Stephenville soils are well drained, loamy or sandy, and slope ranges from very gently sloping to moderately steep.

Land use and Cover

Land use and cover is primarily rangeland, winter wheat and woodland. Vegetation is mainly influenced by the underlying Permian Age bedrock. Land use and cover data were obtained from the UDSA-ARS station at El Reno, Oklahoma.

Figure 4.3 shows the land use and cover data for the watershed. Rangeland is the dominant type of land cover accounting for 63% of the total watershed area. Winter wheat, and woodland share about 20, and 12% of the area, respectively. Winter wheat is primarily distributed in the flat and fertile soil areas near flood plains. The next category is summer crops occupying about 4% of the basin area. Quarry and impervious areas comprise less than one percent of the area mainly in the towns of Cyril and Cement. Water bodies are only

▮ (orange)	Range
▮ (tan)	Poor range
▮ (salmon)	Winter wheat
▮ (cream)	Summer crops
▮ (brown)	Bare soil
▮ (navy)	Water
▮ (olive)	Woodland
▮ (mauve)	Quarry/Impervious
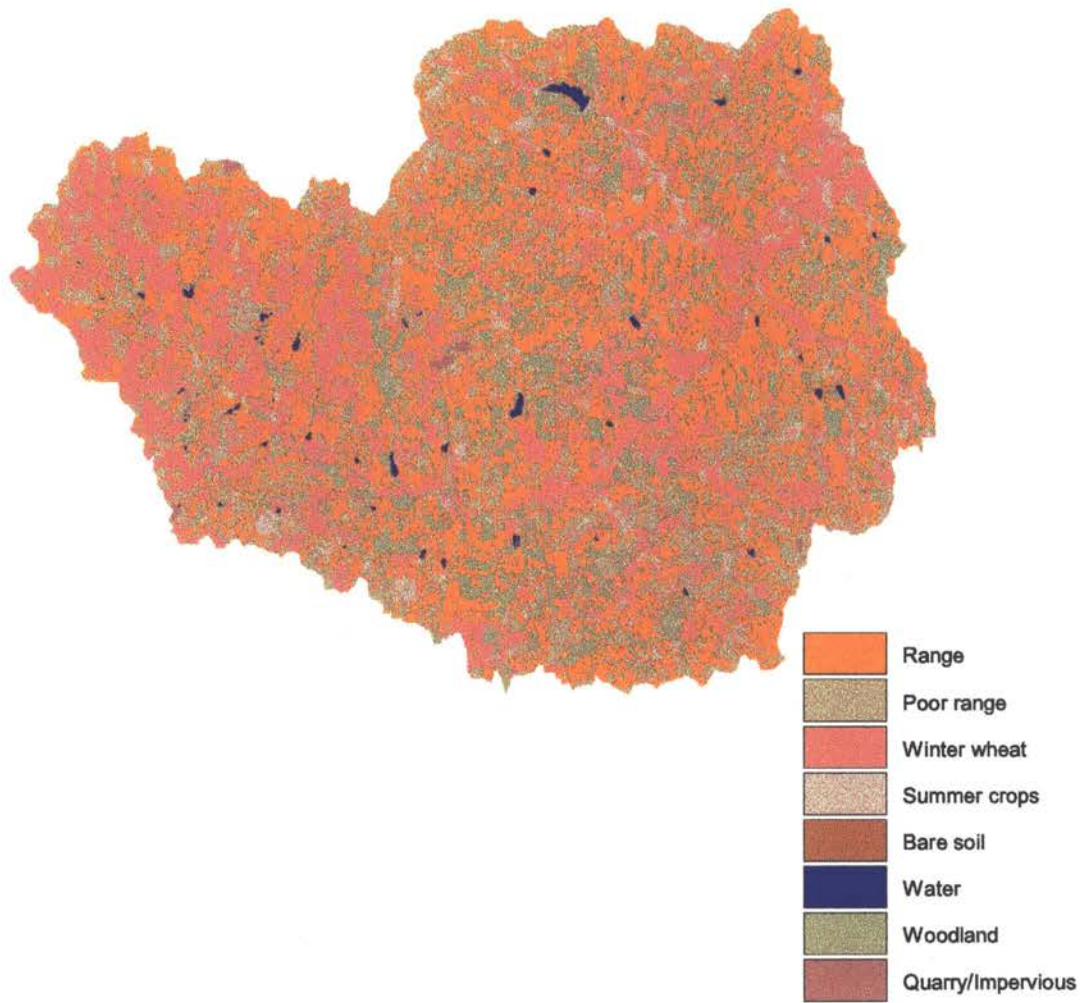
Figure 4.3. Land use and cover of the Little Washita basin

0.4% of the total area.

Topography,

The upland topography of the watershed is gently to moderately rolling, except for a few rocky, steep hills near Cement, OK. Maximum relief in the watershed is about 200 m. Surface slopes are very gentle in most of the watershed. The channel system is very well developed throughout the watershed and extends practically to the drainage divide in most areas. Flatter upland soils are developed from the finer textured Dog Creek Shale and Blaine formation near the eastern part of the watershed, and the western part of the watershed is developed from the Cloud Chief formation (ARS, 1991). The topography of the watershed is shown in Figure 4.4.

At the time of this study, land use and cover data for the entire watershed were not available. This was a major constraint in using the entire watershed for the study. Two subwatersheds were delineated. The first watershed, known as Cyril, was delineated based on the stream gauge station located near Cyril. The stream gauge near Cement was used to delineate the second watershed. The locations of the Cyril and Cement watersheds within the Little Washita basin are shown in Figures 4.5 and 4.6, respectively. The characteristics of these watersheds are shown in Table 4.1. The total area of the Cyril watershed is 30.6 km^2 and of the Cement watershed is 159 km^2.

	1 - 300 m
	301 - 325 m
	326 - 350 m
	351 - 387 m
	388 - 399 m
	400 - 411 m
	412 - 421 m
	422 - 430 m
	431 - 439 m
	440 - 450 m
	451 - 505 m
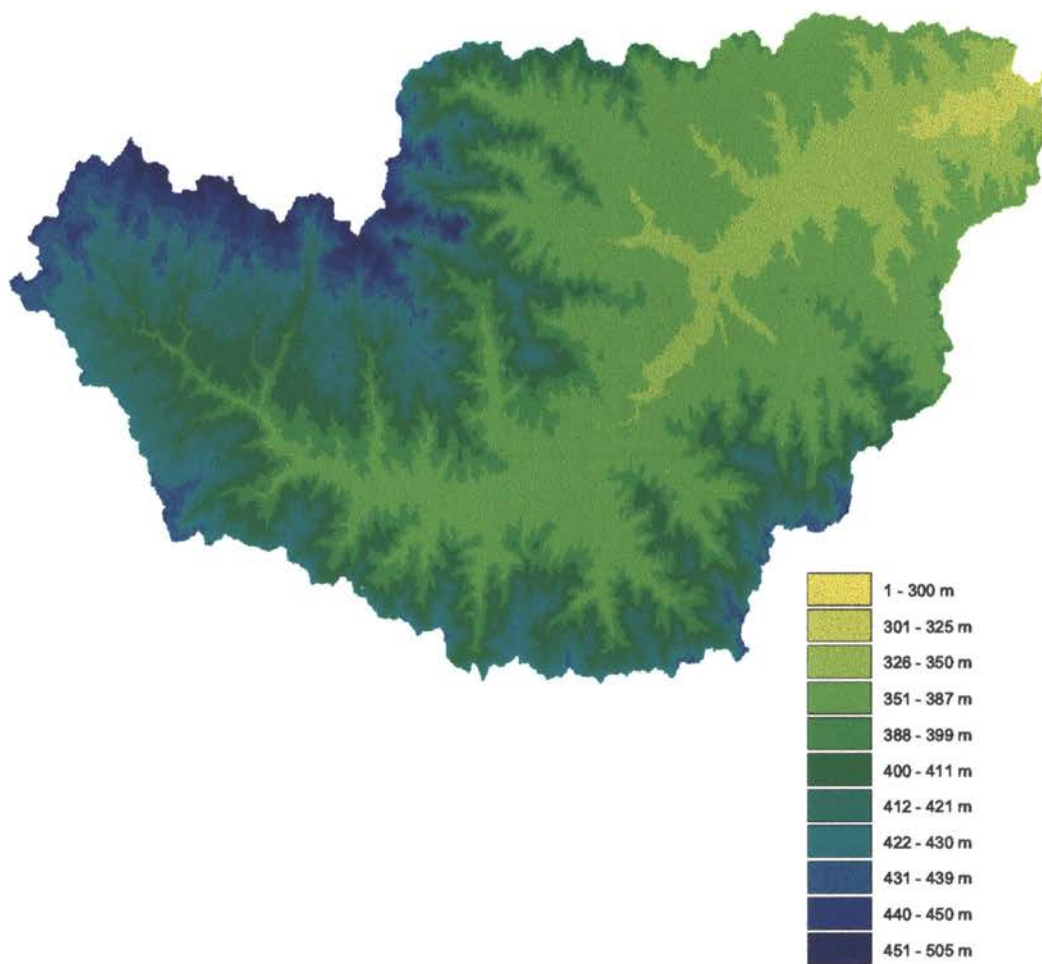
Figure 4.4. DEM data of the Little Washita basin

Figure 4.5. Location of the Cyril watershed in the Little Washita basin
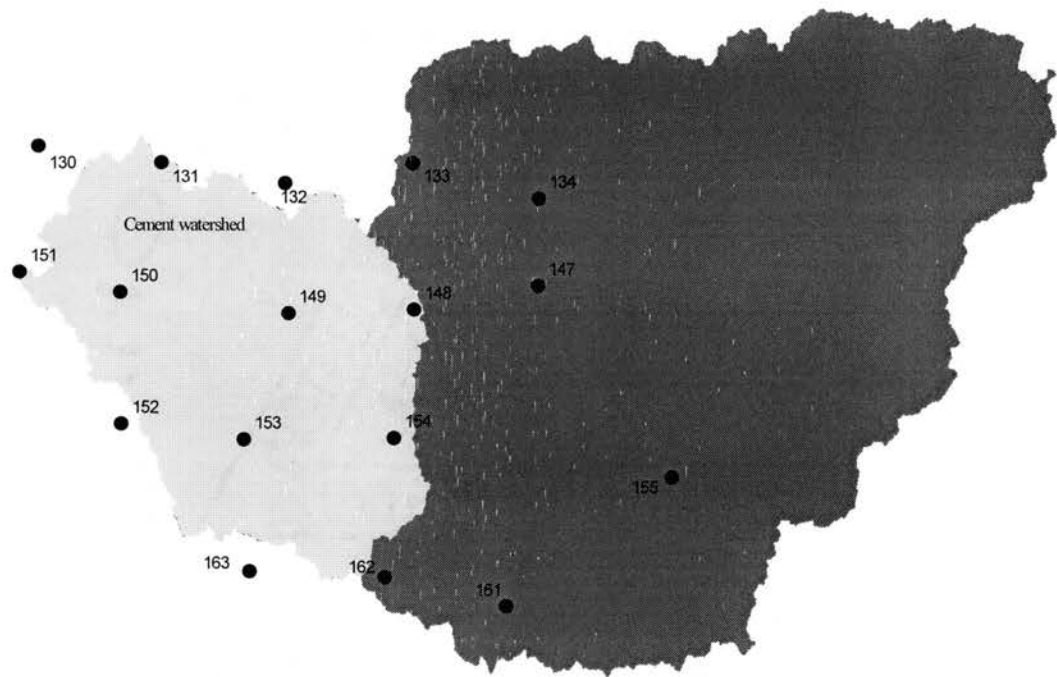
Figure 4.6. Location of the Cement watershed in the Little Washita basin and the

Micronet stations used

Table 4.1. Characteristics of the Cyril and Cement watersheds

Characteristic	Cyril watershed	Cement watershed
Total Area	30.6 km^2	159 km^2
Average slope	1.6%	3.7%
No. of Raingauges	8	17
Land use and Cover (% of the total area)		
Range	25	32
Poor Range	23	26
Winter Wheat	47	31
Summer Crops	2	2
Bare Soil	0.01	0.05
Water	0.13	0.4
Woodland	3	8
Quarry/Impervious	0.01	0.25

4.2. Description of the Model

The hydrology/water quality (H/WQ) model used to assess the effect of rainfall spatial variability was the Agricultural Non-Point Source Pollution model (AGNPS). It is an event-based model that simulates surface runoff, sediment and nutrient transport primarily from agricultural watersheds (Young et al., 1989). The nutrients considered are nitrogen (N) and phosphorus (P). Basic model components include hydrology, erosion, and sediment and chemical transport. In addition, point sources of water, sediment, nutrients, and chemical oxygen demand (COD) from animal feedlots and springs are also considered. Water impoundments such as tile-outlet terraces, are considered as depositional areas of sediment and sediment-bound nutrients. The model can output water quality characteristics at intermediate points throughout the watershed network.

The model operates on a geographic cell basis (Dirichlet tessellation) that is used to represent upland and channel conditions. Dirichlet tessellation is a process of splitting up and grouping a study area into cells or tiles, also known as Theissen or Boronoi polygons. Cells are uniform square areas subdividing the watersheds, allowing analyses at any point within the watershed. Potential pollutants are routed through cells from the watershed divide to the outlet in a stepwise manner so that flow at any point between cells can be examined. All watershed characteristics and inputs are expressed at the cell level. Results from an AGNPS model simulation can be used to provide objective characterization of the water quality conditions in the watershed and to assess the effectiveness of alternative land management practices in enhancing watershed water quality (Young et al., 1989).

The different components of the AGNPS model are discussed in the following paragraphs. More details may be found in Young et al. (1989).

Hydrology

The hydrologic component of the model estimates the runoff volume and peak flow rate. The volume of runoff is calculated using the SCS curve number method

$$Q = \frac{(P - 0.2S)^2}{P + 0.8S} \qquad (4.1)$$

where Q is the runoff volume, P is the rainfall, and S is a retention parameter, all expressed as the depth of water. The retention parameter in mm is defined in terms of a curve number (CN) as follows

57

$$S = \frac{25400}{CN} - 254 \tag{4.2}$$

The CN depends upon land use, soil type, and hydrologic soil conditions (Young et al., 1989).

The peak runoff rate for each cell is estimated using

$$Q_p = 3.79 A^{0.7} CS^{0.16} (RO/25.4)^{(0.903A^{\cdots})} LW^{(-0.19)} \tag{4.3}$$

where Q_p is the peak flow rate (m³/s); A is the drainage area (km²); CS is the channel slope (m/km); RO is the runoff volume (mm); and LW is the watershed length-width ratio, calculated by L^2/A where L is the watershed length.

Erosion and Sediment Transport

Erosion from a single storm at a cell level is calculated using a modified form of the universal soil loss equation (USLE) as follows.

$$SL = (EI) \; KLSCP \; (SSF) \tag{4.4}$$

where SL is the soil loss (kg), EI is the product of the storm total kinetic energy and maximum 30-minute rainfall intensity, K is the soil erodibility factor, LS is the topographic factor, C is the cover factor, P is the supporting practices factor, and SSF is a factor to adjust for slope shape within the cell. Eroded soil and sediment yield are divided into five particle classes-clay, silt, small aggregates, large aggregates and sand.

AGNPS considers only three sources of sediment: (1) sheet and rill erosion from the in-cell processes; (2) channel scour from the in-stream processes; and (3) gullies from the in-

cell processes. After runoff and upland erosion are calculated, detached sediment is routed from cell to cell through the watershed to the outlet. Sediment load for each of the five particle classes leaving the cell is calculated from

$$
Q_s(x) = \left[\frac{2q(x)}{2q(x)+\Delta x V_{ss}}\right]\left[Q_s(o)+Q_{sl}\frac{x}{L}-\frac{w\Delta x}{2}\left[\frac{V_{ss}}{q(o)}+\{q_s(o)-g_s(o)-\frac{V_{ss}}{q(x)}g_s(x)\}\right]\right] \quad (4.5)
$$

where $Q_s(x)$ is the sediment discharge at the downstream end of the channel reach (kg), $Q_s(o)$ is the sediment discharge into the upstream end of the channel reach (kg), Q_{sl} is the lateral sediment flow rate (kg/ha), x is the downstream distance (m), L is the reach length (m), w is the channel width (m), $q(x)$ is the discharge per unit width, and $g_s(x)$ is the effective transport capacity per unit width.

Nutrient Transport

The pollutant transport part of the model estimates transport of N, P, chemical oxygen demand, and pesticides throughout the watershed. Pollutant transport is subdivided into soluble pollutants and sediment-attached pollutants. The following assumptions are made to calculate the nutrient transport:

1. Surface runoff is assumed to interact with a 1 cm soil surface layer.

2. Chemicals on the soil surface are assumed to be uniformly mixed within the surface layer.

3. Infiltration must first pass through the surface layer.

4. The initial abstraction is the first increment of rainfall prior to the surface runoff.

59

Sediment-bound nutrient yield is calculated based on the total sediment yield as follows.

$$Nut_{sed} = Nut_f \, Q_x(x) E_r \qquad (4.6)$$

where Nut_{sed} is the nutrient transported in the sediment-bound form (kg/ha), Nut_f is the nutrient content of the field soil, and E_r is the enrichment ratio, calculated as

$$E_r = 7.4 \, Q_s(x)^{-0.2T_a} \qquad (4.7)$$

where T_f is the correction factor for soil texture.

Effects of nutrient levels in rainfall, fertilization, and leaching are considered while calculating the soluble nutrient transport as follows

$$Nut_{sol} = C_{nut} Nut_{ext} Q \qquad (4.8)$$

where Nut_{sol} is the soluble nutrient concentration in the runoff (ppm), C_{nut} is the mean concentration of soluble N or P at the soil surface during runoff, Nut_{ext} is the extraction coefficient of nutrient by runoff, and Q is the total runoff (mm).

The contributions of soluble N and P from each of the cells are calculated first and routed into the channel. Once soluble nutrients reach concentrated flow, they are assumed to remain constant.

Since its development, the AGNPS model has undergone several modifications. Generally the model requires specification of 20 different input parameters for each grid cell, either manually or through a spreadsheet interface supplied with the program. A summary

of the different input parameters required by the model is shown in Table 4.2. The primary input parameters for version 5.0 of the model consist of two user-supplied categories: program control file header or watershed-level input parameters; and cell-level information.

Various output options available with the model are shown in Table 4.3. Preliminary output includes watershed area and cell size, storm precipitation and erosivity, estimates of runoff volume and peak flow rate at the watershed outlet, and area-weighted erosion, both upland and channel. The model also calculates sediment delivery ratio, mean sediment concentration, and total sediment yield for each of five sediment particle size classes. In the nutrient analysis part, nutrient loss per unit area for the sediment bound and dissolved forms and nutrient concentration are calculated.

4.3 Description of the GRASS-AGNPS Modeling Tool

Preparation of the input parameters for AGNPS is very time intensive. For a relatively large watershed with fine grid cell size (e.g. less than 1 ha), generating, organizing and managing the model input data and analyzing and displaying the model output data can be tedious, time-consuming and problematic. The WATERSHEDSS GRASS-AGNPS modeling tool developed by Osmond et al. (1997) was used to develop the input file. This modeling tool is based on the GRASS-AGNPS interface developed by Srinivasan and Engel (1994). It has some added capabilities of inputting point source, pesticide and channel information.

Table 4.2. Summary of AGNPS (version 5.0) input parameters

---

1. Watershed level input parameters

      Watershed identification
      Description of the watershed
      Area of the watershed
      Number of cells
      Precipitation
      Nitrogen concentration in rainfall
      Energy-intensity value
      Storm duration
      Storm type
      Peak flow calculation
      Geomorphic calculation

2. Cell Level input parameters
      Cell number
      Cell division
      Receiving cell number
      Aspect/flow direction
      SCS curve number
      Average land slope
      Slope shape
      Slope length
      Manning's n
      USLE K factor
      USLE C factor
      USLE P factor
      Surface Condition
      Soil texture number
      Fertilizer indicator
      Pesticide indicator
      Point source indicator
      Additional erosion
      Impoundment indicator
      Channel Indicator

Table 4.3. Summary of AGNPS outputs

1. Hydrology Outputs
      Runoff volume (inches or cm)
      Peak runoff rate (ft^3/s or m^3/s)
      Fraction of runoff generated in the grid cell

2. Sediment Output
      Sediment yield (tons or kg)
      Sediment concentration (mg/L)
      Sediment particle size distribution
      Upland erosion (tons/acre or kg/ha)
      Amount of deposition (percent)
      Sediment generated within the cell (tons or Kg)
      Enrichment ratios by particle size
      Sediment delivery ration by particle size

3. Chemical output
      Sediment bound N (lb/acre or kg/ha)
      Soluble N in cell runoff (lb/acre or kg/ha)
      Soluble N concentration (mg/L)
      Total Soluble N (lb/acre or kg/ha)
      Sediment bound P (lb/acre or kg/ha)
      Soluble P in cell runoff (lb/acre or kg/ha)
      Soluble P concentration (mg/L)
      Total Soluble P (lb/acre or kg/ha)
      Sediment bound pesticide (lb/acre or kg/ha)
      Soluble pesticide in cell runoff (lb/acre or kg/ha)
      Cell chemical oxygen demand (lb/acre or kg/ha)
      Total soluble chemical oxygen demand (lb/acre or kg/ha)
      Soluble chemical oxygen demand concentration (mg/L)

In the WATERSHEDSS modeling tool, AGNPS is loosely coupled with Geographical Resource Analysis Support System (GRASS) to generate, organize and display the model input and output data. GRASS is a raster-based GIS system (USACERL, 1993). Data generated from GRASS is organized as inputs to the model, while the output data from the model are subsequently transferred to the GIS for analysis and display. The data are transferred between the model and GRASS by simply formatting the output data generated by each system.

The GRASS map layers required by the input file generator include the watershed boundary, topography, tillage, USLE C and K factors, nutrient/fertilizer application rate, land use, management practice, hydrologic soil group, percent sand, percent clay, and pesticide application rates. The following is a brief explanation of each map layer unit.

Watershed Boundary: This layer should have a category value of 1 or greater within the watershed area and 0 outside the area. This layer defines the watershed or analysis boundary for all map layers. All other input map layers must extend beyond the boundary of this layer.

Topography: Elevation in meters must be a category value for each cell. For the calculation of slope and aspect, this layer must extend at least 2 cells beyond the watershed boundary all the way around.

USLE K Factor: A raster map layer of the soil series map with K factors as a category value for each map unit is required.

Hydrologic Soil Group: Each map unit should be assigned a category label of A, B, C, or D based on the hydrologic group of the soil.

Percent Sand: Percentage of sand sized soil particles is assigned as one of the category values for each map layer unit for this coverage.

Percent Clay: For this layer, the category values should be the percentage of clay-sized particles in the soil for each map layer unit.

Land Use: One of the following categories should be assigned to each map unit: fallow, row crop, small grain, rotation meadow, close-seeded legumes, pasture (poor), pasture (good), range, meadow, woods, hard surface, farmsteads, roads (dirt), water, and marsh. The poor and good conditions are for the hydrologic conditions and are used to determine the curve number.

Fertilizer/nutrient Application Rate: Four fertilization rates are specified in this layer as follows: 0=none, 1=56 kg/ha N and 22 kg/ha P, 2=112 kg/ha N and 45 kg/ha P, and 3=224 kg/ha N and 90 kg/ha P. The user can also enter custom fertilizer application rates for individual cells, if desired.

Tillage: Each map layer unit should be given one of the following category labels: large offset disk, moldboard plow, lister, chisel plow, disk, field cultivator, row cultivator, anhydrous applicator, rod weeder, planter, smooth, or no till. Urban, water, marsh, and farmstead land use areas can be no till or smooth. These values are used to determine the nutrient availability factor.

Management Practice: One of the following management practices should be specified as the cell label in this layer: straight row, contoured, or contoured and terraced.

USLE C Factor: This map layer should contain the value of USLE C factor as the category label for each cell.

Pesticide application rate: This map layer is optional and is needed only when the user wants to simulate pesticide transport. Up to three pesticide application scenarios can be entered as the category values. A scenario contains a unique set of pesticide type, application rate, application timing, and application method.

Channel Slope: This data layer is optional. The category values for each cell should be the channel slope in percent for each cell. The user also has the option of entering channel information for each cell individually in the interactive part of the input file generator. In the absence of the layer, the channel slope is assumed to be 50% of the overland slope for each cell unless the user changes the value of the cell.

In addition to the maps, several general watershed parameters must be known. These include rainfall depth and duration, soil antecedent moisture condition, N concentration of rainfall, area of each cell, and a short watershed description.

4.4. Modification of the AGNPS to input grid-based rainfall and energy-intensity values

One of the limitations of the AGNPS model, like most of the H/WQ models, is that it allows only one value of rainfall assuming that it is homogeneous across the watershed of interest. The model was modified to input grid-based rainfall and energy-intensity. The modifications were based on the work done by Grunwald and Freede (1996) at the ARS National Sedimentation Laboratory located at Purdue University, West Lafayette, Indiana. The energy-intensity for each cell was calculated from

$$R_{st} = \frac{a_1 P^{f(D)}}{D^{b_\cdot}} \qquad (4.9)$$

where R_{st} is the energy-intensity R factor, P is the cell rainfall in inches corresponding to a duration D in hours, a_1 and b_1 are constants. f(D) was calculated as

$$f(D) = 2.119 D^{0.0086} \qquad (4.10)$$

Values of a_1 and b_1 were taken from Haan et al. (1994). For Oklahoma, a_1 and b_1 are 17.9 and 0.4134, respectively.

The modified AGNPS was verified to see if it produced the same results as the original AGNPS. The model was run using a homogeneous rainfall for all cells and the outputs obtained were compared with the results from the original AGNPS. Under the assumption of rainfall homogeneity, the outputs obtained from the two models were identical.

4.5. Sensitivity Analysis of AGNPS

Sensitivity analysis is the process of identifying model component processes and parameters that have the greatest impact on model output. Majkowski et al. (1981) suggested that sensitivity analysis can be performed to examine the influence of input parameter errors on predictions made by the model. The acceptance level of output uncertainty depends on the system under consideration, the modeling objectives and the modeler's knowledge of the system. Therefore, sensitivity analysis provides a rational method of identifying additional research needs and/or additional data collection to improve parameter estimates and to reduce

67

model uncertainty.

A number of methods have been developed for the purpose of sensitivity analysis. Haan et al. (1995) described a sensitivity coefficient as follows

$$S_a = \frac{\partial O}{\partial P} \qquad (4.11)$$

where S_a is the absolute sensitivity, O is the particular output, and P is the particular input. One of the problems with the absolute sensitivity is that it has the units of the input and output parameters. Parameters can not be ranked on the basis of sensitivity because they may have different units. To overcome this problem, a relative sensitivity index (S_r) can be used as follows

$$S_r = \frac{\partial O}{\partial P} \frac{P}{O} \qquad (4.12)$$

Relative sensitivity index can be used to rank model parameters in terms of their sensitivities because S_r is dimensionless giving the change in O for a unit change in P. The parameters with the highest S_r have the greatest impact on model output. This provides a basis for comparing various parameters and concentrating research and data collection on more sensitive parameters.

When applying this methodology to a H/WQ model, it is impossible to solve $\partial O/\partial P$ directly. Relative sensitivity can be numerically approximated as

$$S_r = \frac{P}{O} \frac{O_2 - O_1}{P_2 - P_1} \qquad (4.13)$$

where P and O are the base values of input and output. The base values are changed by a certain percentage to get P_1, P_2 and the corresponding O_1, and O_2. When applying Equation 4.13 to calculate S_r, it is assumed that the model response is linear in the range of interest. A H/WQ model may be linear for certain processes and/or over limited ranges. When a H/WQ model is nonlinear, an extensive sensitivity analysis using this method can be done to estimate relative sensitivity over a variety of conditions.

The outputs considered were runoff volume, total sediment, sediment-bound N, and sediment-bound P. Sensitivity analysis of AGNPS was performed using 26 parameters. The base parameter values were changed by ±10% to estimate S_r. The relative sensitivity values for these outputs are shown in Table 4.4. The relative sensitivity of total soluble N and total soluble P is not shown in Table 4.4. For these nutrients, the output obtained was zero and the relative sensitivity values could not be calculated.

4.6. Description of the rainfall events and the data set

There are 36 continuous recording gauges operating since 1962 and 12 additional gauges were installed and have been operational since May 1994. Figure 4.7 shows the location of these Micronet stations within the Little Washita watershed. The characteristics of the Micronet stations are shown in Table 4.5. Also a NEXRAD (WSR-88D) radar is located northeast of the basin in Twin Lakes, near Oklahoma City, and covers the study area.

Rainfall data for the Micronet stations were obtained from USDA-ARS. The raingauges used in the Micronet are Belfort 5-780 series dual-traverse weighing bucket raingauges. An automatic data logger is used to measure the rainfall amounts.

Table 4.4. Relative sensitivity of the AGNPS parameters for the output considered.

Output	Parameter	Relative Sensitivity
Runoff Volume	CN	3.03
Total Sediment	CN	1.91
	Land Slope	0.31
	K factor	0.35
	C factor	0.35
	P factor	0.34
Sediment-N	CN	1.53
	Land Slope	0.24
	K factor	0.36
	C factor	0.36
	P factor	0.36
	Soil N	1.07
Sediment-P	CN	1.53
	Land Slope	0.25
	K factor	0.28
	C factor	0.28
	P factor	0.28
	Soil P	0.50

For each gauge location, cumulative rainfall depths were available at 5 minute intervals. The rainfall data start at 0 GMT hour and end at 2355 GMT hour. All the rainfall data were converted to CDT time.

Stream flow data for the Cyril and Cement watersheds were obtained from the USGS. Daily discharge in cubic meter per second at both sites was available. USGS classifies stream flow data as excellent, good, fair, and poor. The accuracy of the stream flow records depends primarily on two factors: (1) the stability of the stage-discharge relation or, if the control is unstable, the frequency of discharge measurements; and (2) the accuracy of
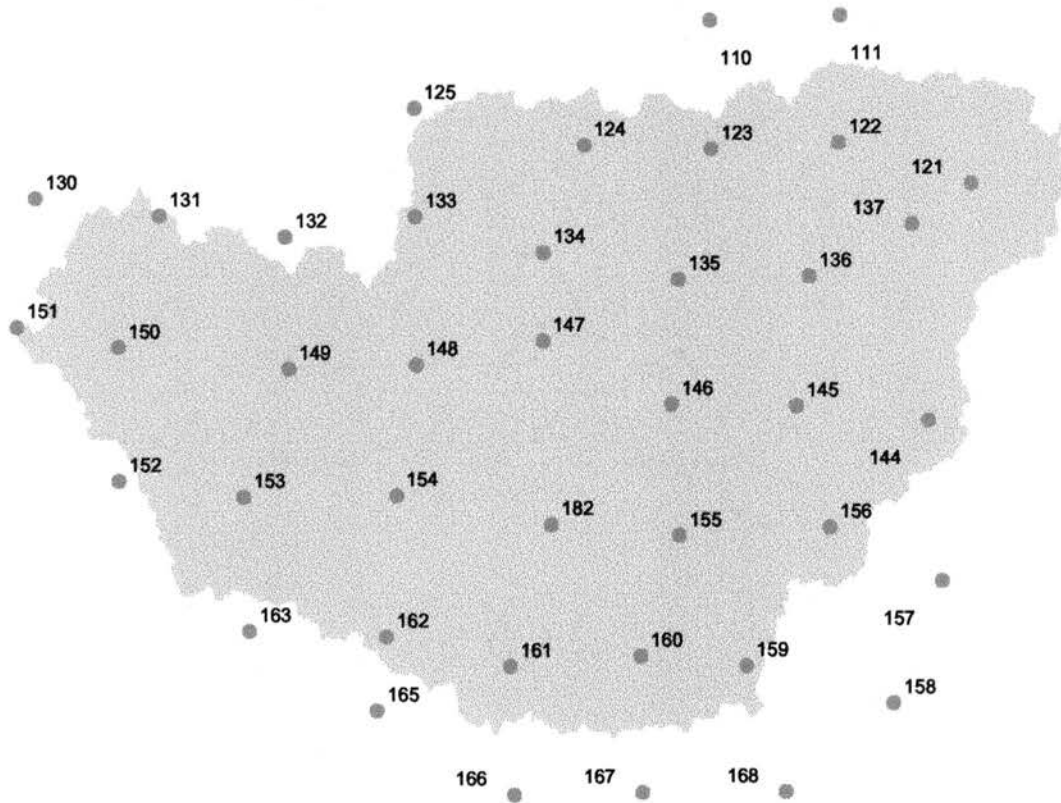
Figure 4.7. Location of the Micronet stations in the Little Washita basin

Table 4.5. Characteristics of the Micronet Stations

Number	Station ID	Name	City	North Lat.*	East Long.*
501	A110	110	Norge	35.0144	-98.0096
502	A111	111	Chickasha	35.0158	-97.9517
503	A121	121	Ninnekah	34.9586	-97.8986
504	A122	122	Ninnekah	34.9728	-97.9528
505	A123	123	Norge	34.9711	-98.0056
506	A124	124	Norge	34.9728	-98.0581
507	A125	125	Cement	34.9858	-98.1281
508	A130	130	Stecker	34.9564	-98.2847
509	A131	131	Cyril	34.9503	-98.2336
510	A132	132	Cement'	34.9428	-98.1819
511	A133	133	Cement	34.9492	-98.1281
512	A134	134	Cement	34.9367	-98.0753
513	A135	135	Cement	34.9272	-98.0197
514	A136	136	Ninnekah	34.9278	-97.9656
515	A137	137	Ninnekah	34.9450	-97.9231
516	A144	144	Agawam	34.8789	-97.9172
517	A145	145	Agawam	34.8842	-97.9714
518	A146	146	Agawam	34.8853	-98.0231
519	A147	147	Cement	34.9069	-98.0758
520	A148	148	Cement	34.8992	-98.1281
521	A149	149	Cyril	34.8983	-98.1808
522	A150	150	Cyril	34.9061	-98.2511
523	A151	151	Stecker	34.9133	-98.2928
524	A152	152	Fletcher	34.8611	-98.2511
525	A153	153	Cyril	34.8553	-98.2000
526	A154	154	Cyril	34.8553	-98.1369
527	A155	155	Agawam	34.8408	-98.0203
528	A156	156	Agawam	34.8431	-97.9583
529	A157	157	Rush Springs	34.8247	-97.9122
530	A158	158	Rush Springs	34.7836	-97.9328
531	A159	159	Rush Springs	34.7967	-97.9933
532	A160	160	Rush Springs	34.8003	-98.0369
533	A161	161	Sterling	34.7972	-98.0906
534	A162	162	Sterling	34.8075	-98.1414
535	A163	163	Fletcher	34.8100	-98.1981
536	A164	164	Fletcher	34.8207	-98.2789
537	A165	165	Sterling	34.7828	-98.1456
538	A166	166	Sterling	34.7539	-98.0894
539	A167	167	Rush Springs	34.7544	-98.0367
540	A168	168	Rush Springs	34.7542	-97.9775
541	A181	181	Apache	34.8697	-98.3014
542	A182	182	Cement	34.8450	-98.0731

* North Lat = North Lattitude; East Long = East Longitude

72

measurements of stage, measurements of discharge, and interpretation of records. A record classified as "excellent", "good", and "fair" means that about 95% of the daily discharges are within 5, 10, and 15% of the true values, respectively. Records that do not meet this criteria are rated "poor". The USGS has not classified the data for the watersheds used in this study.

A total of 12 rainfall dates were selected for the year 1996. For the Cyril watershed, 8 raingauges located within and around the watershed were used. For the Cement watershed, 17 raingauges were used for the analysis of the rainfall. The location of the 17 gauges used with the Cement watershed are shown in Figure 4.6. The base flow was separated from the total flow to get the surface runoff. In the computation of the runoff, a horizontal line from the start of the rainfall event was drawn until it intersected the storm hydrograph. This was termed as the base flow line. Total volume above the base flow line was considered as the runoff volume. Often several days elapsed as this runoff volume was occurring. This method of runoff computation minimized the effect of various flood retardation structured present in the watershed. For March 27 and 28, April 21 and 23, August 1 and 3, May 31 and June 1, and July 9 and 10, it was not possible to separate the base flow from the total flow for the rainfall on each day. The total rainfall for the two days was considered as one rainfall event and was used in the analysis. Thus, the total number of rainfall events considered was seven. The events are indicated by the first day of the event. For the Cement watershed, the rainfall observed at several gauges within the watershed was erroneous on 8/1/96. The rainfall on this date was discarded from the analysis for this watershed. The rainfall on 11/6/96 observed at the majority of the gauges was too small to run the AGNPS model. Since AGNPS was developed to predict the erosion losses, it does not work very well for the very small rainfall

73

events. This event was also not considered for the Cement watershed. The rainfall on 4/21/96 was then included in the analysis to have at least five different rainfall events analyzed. Rainfall four days preceding the event date were also obtained to characterize the antecedent moisture conditions used in CN calculations.

The GRASS-AGNPS modeling tool (Osmond et al., 1997) was used to generate the input file for AGNPS. The GIS layers required were watershed boundary, topography, tillage practices, USLE K factor, USLE C factor, hydrologic soil group, percent sand, percent clay, nutrient application rate, land use, and management practice map. Soil type, land use and elevation data were obtained from the USDA-ARS station at El-Reno, Oklahoma. All the input layers required by the GRASS-AGNPS modeling tool were prepared in raster format using a 30 m cell resolution. The input layers needed for the Cement watershed are shown in Figures 4.8-4.17. Information about the tillage practices, nutrient application rate, and management practice were obtained from personnel at the USDA-ARS station at Chickasha, Oklahoma. Watershed boundary and topographic maps were prepared from the digital elevation model (DEM) data. USLE K factor, hydrologic soil group, percent sand, and percent clay coverages were prepared from the soil data of the watershed. USLE C factor was based on the watershed land use information. The cell size used in AGNPS modeling was 200m x 200m. This cell size was used to insure the adequate representation of the watershed properties without increasing the complexity of the input file and the AGNPS run time. In a study done on the Upper Little Washita basin which encompasses the two watersheds used in this study, Ma (1993) concluded that spatial structure of the landscape complexity had a significant impact on the spatial scaling and high runoff-generating areas played an important

74

role in surface runoff processing. The author concluded that a cell size less than 300 m X 300 m should be used to preserve the presence of high runoff generating areas.

Once the input file for AGNPS was prepared using the GRASS-AGNPS modeling tool, the cell-based rainfall values were added to the input file. For any rainfall event, if a gauge had erroneous rainfall or did not seem to be functional, then the data from that gauge were completely discarded and it was assumed that the gauge was not present for the event. Erroneous rainfall data were indicated by large negative numbers. A nonfunctional gauge was indicated by the rainfall of -998.

Figure 4.8. Boundary of the Cement watershed

![yellow]	1 - 360 m
![dotted1]	361 - 370 m
![dotted2]	371 - 385 m
![blue1]	386 - 400 m
![blue2]	401 - 425 m
![blue3]	426 - 455 m
![blue4]	456 - 490 m
![red]	491 - 505 m
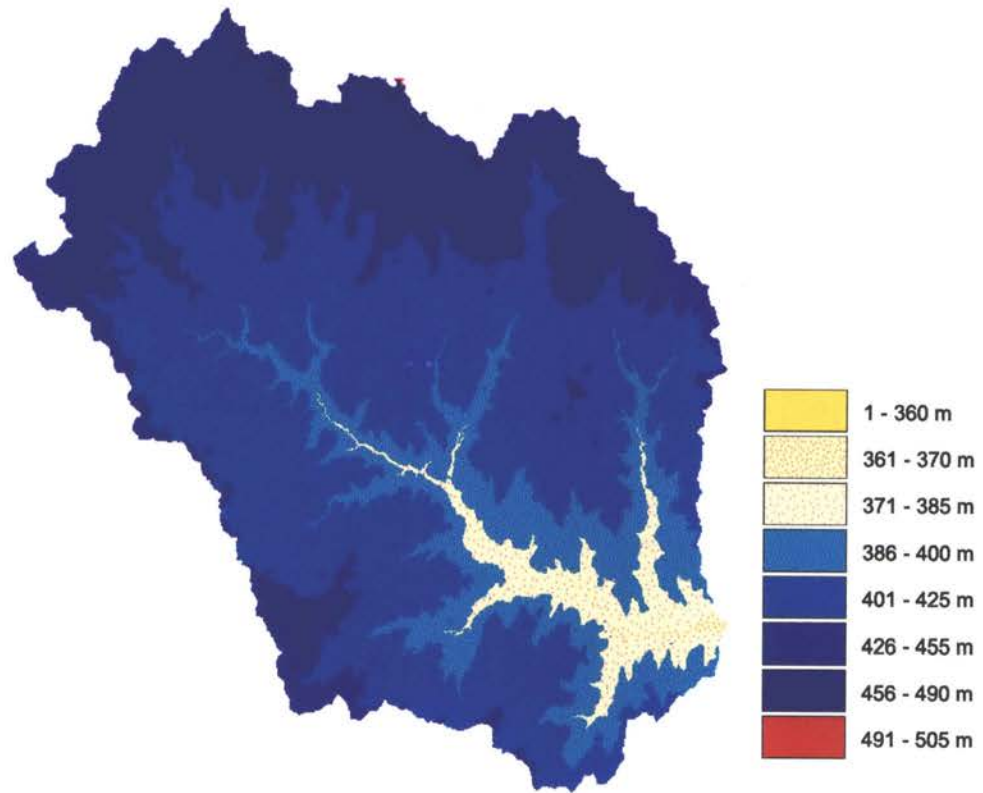
Figure 4.9. Elevation map of the Cement watershed
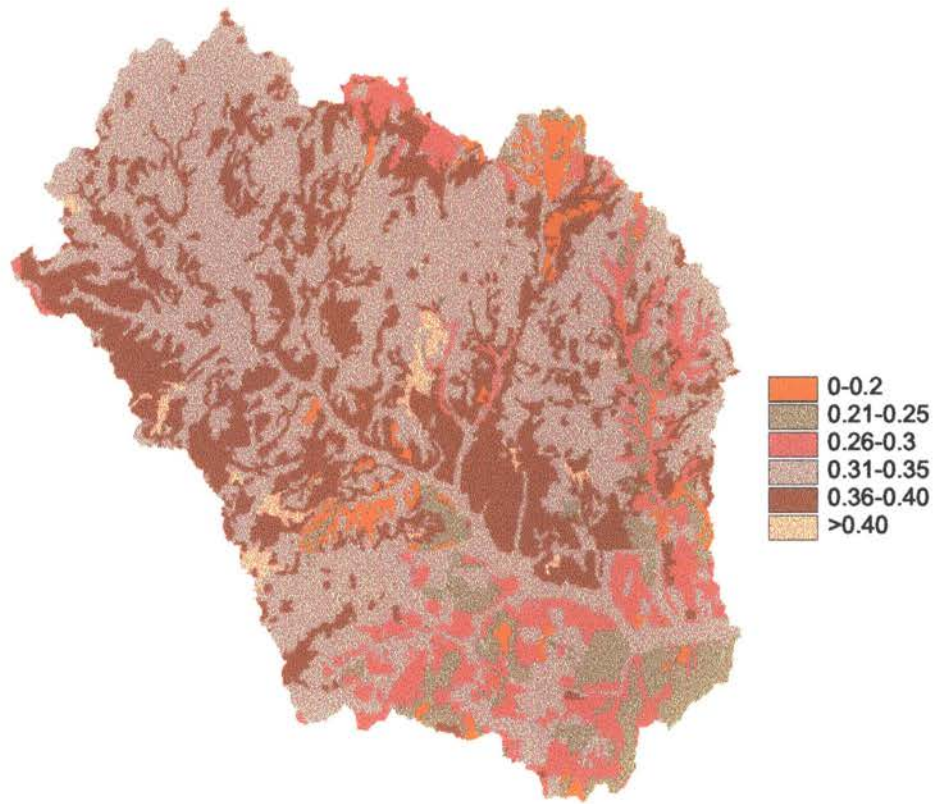
Figure 4.10. USLE K factors for the Cement Watershed
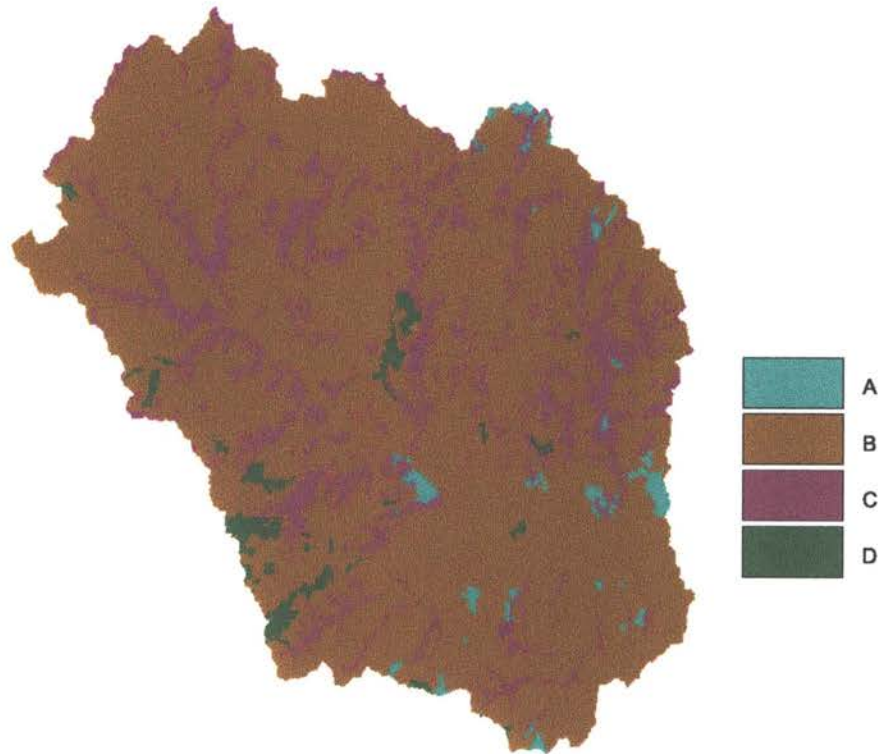
Figure 4.11. Hydrologic groups of the Cement watershed
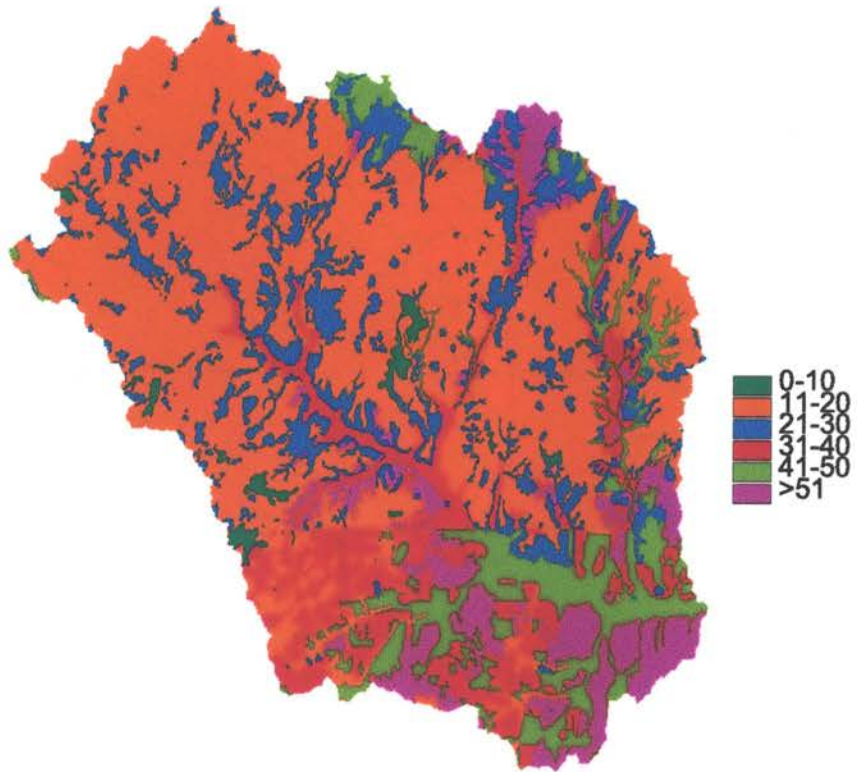
Figure 4.12. Percent sand for the Cement watershed
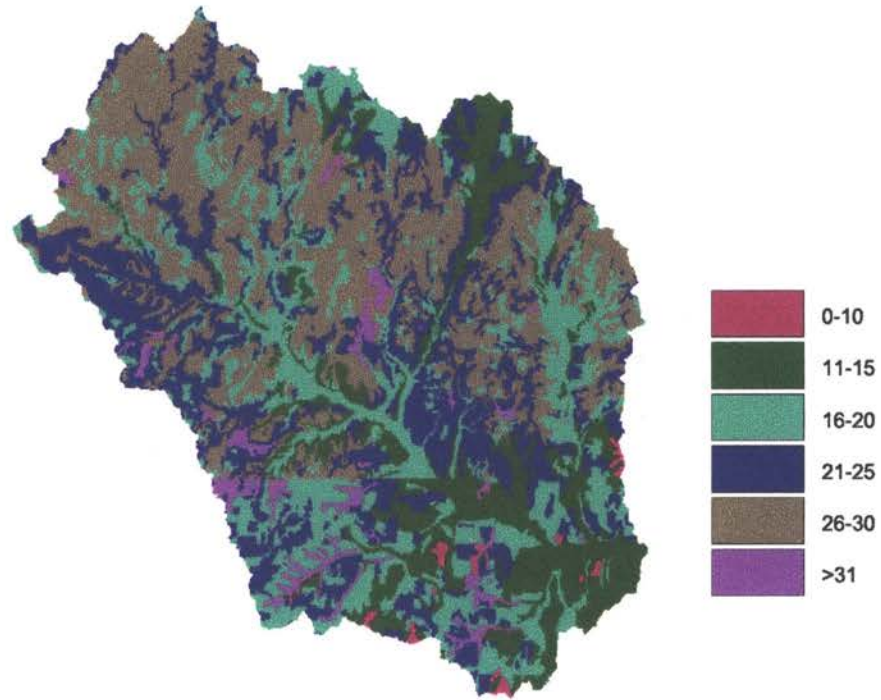
Figure 4.13. Percent clay for the Cement watershed
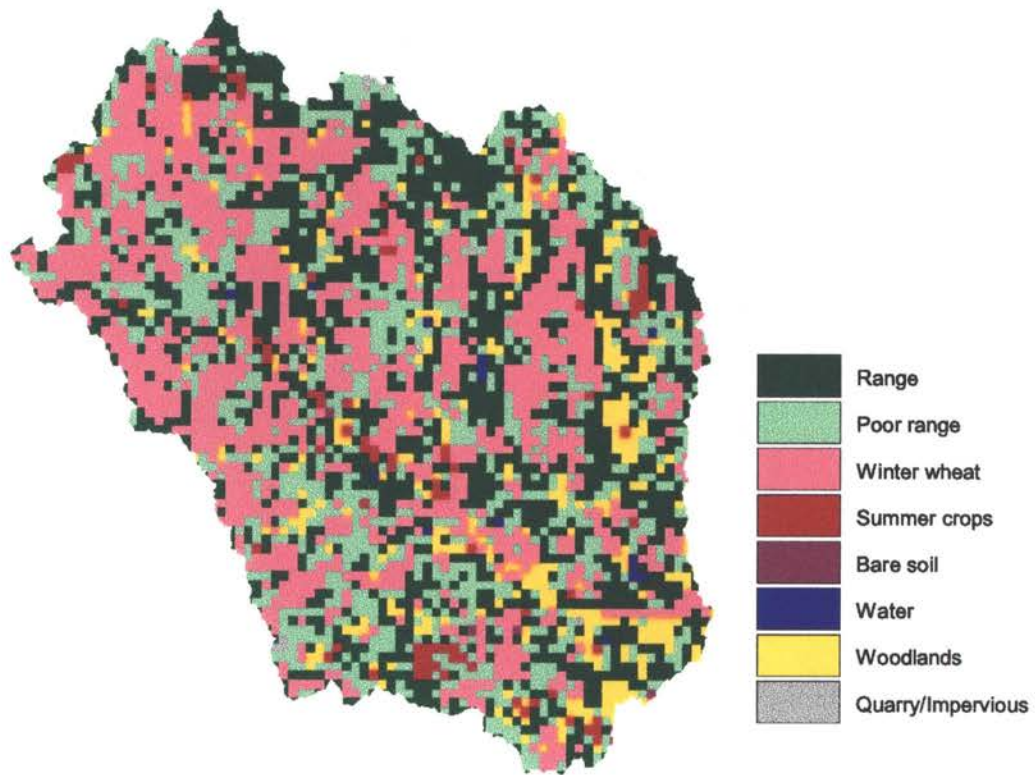
Figure 4.14. Land use and cover of the Cement watershed
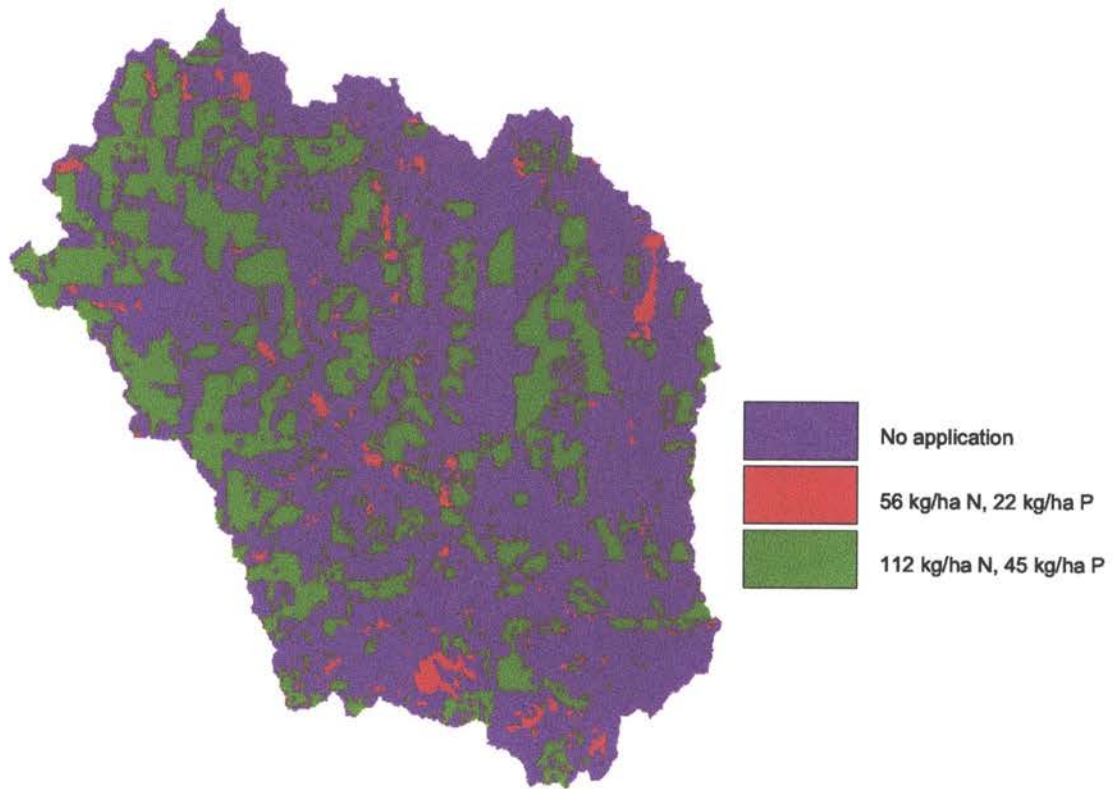
Figure 4.15. Fertilizer/nutrient application rates for the Cement watershed

Figure 4.16. Tillage practices for the Cement watershed
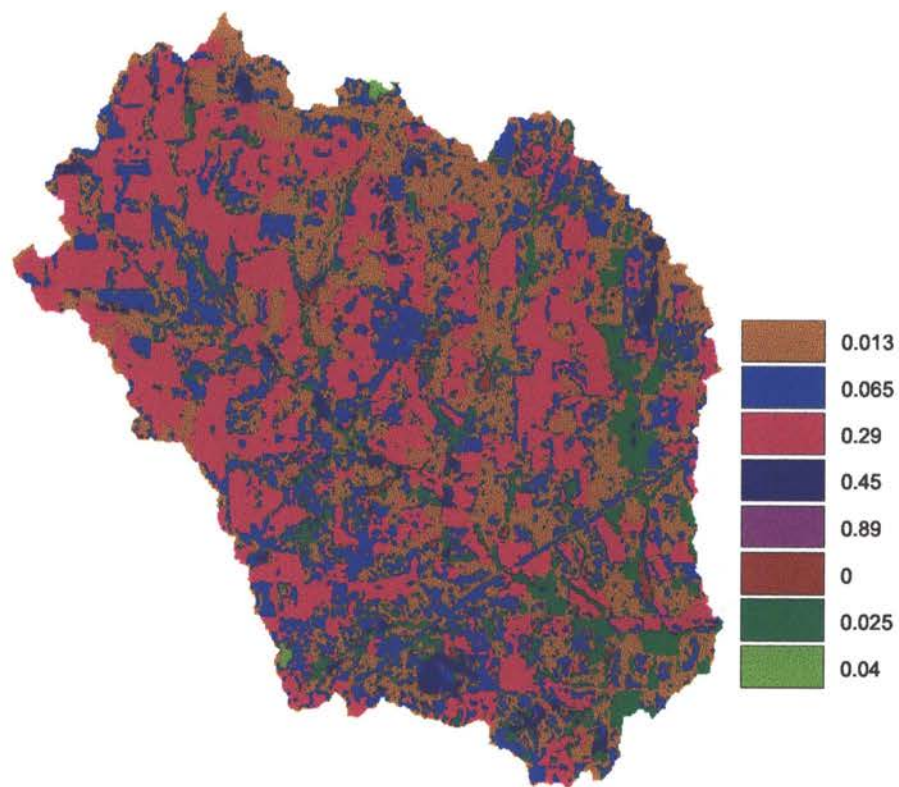
Figure 4.17. USLE C factors for the Cement watershed

4.7 Description of the Radar Data

NEXRAD products are available either in graphical format or in digital format with polar coordinates. The NEXRAD rainfall data were Digital Precipitation Array (DPA) data stored in a binary format. The coordinate system used with the DPA data is HRAP as described in the previous chapter. Rainfall in the DPA data is available at five minute intervals with hourly cumulative rainfall preceding the time at which the rainfall was scanned. For each date, the time specified is GMT. For example, the rainfall at 1200 hours will give the cumulative rainfall that occurred over a one hour period preceding 1200 GMT.

The DPA data are in a two dimensional array format with 131 rows and 131 columns. The radar rainfall was obtained for the rainfall on 7/9/96 for the radar located at Twin Lakes, Oklahoma. This radar covers the Little Washita watershed. The DPA data were converted to the corresponding rainfall values for each cell using the following equation.

$$EXP = \frac{(DPA\ value\ *\ 0.125\ -\ 6)}{10} \tag{4.14}$$

$$Rainfall = 10^{EXP} \tag{4.15}$$

The unit of rainfall obtained by Equation (4.15) is mm.

The geographic location of each radar rainfall cell was not known directly. Instead the location of the radar was known and the location of each rainfall cell was determined indirectly from this information. The radar was located at the center of the rainfall area scanned. In the HRAP coordinate system, it captures the rainfall values that extend 65 cells

86

in all directions. The size of the cells varies with latitude in the HRAP coordinate system. Since all of the input layers were prepared in GRASS, it was not possible to use the rainfall information in HRAP coordinate system directly because the GRASS requires a uniform cell size. The cell size was calculated at the Northeast and Southwest corner of the Little Washita watershed using Equation (3.22). The cell sizes at these corners were 3.95 and 4.05 km, respectively. This gives the minimum and maximum cell size for the watershed. In this research the average cell size (4 km) from these two values was calculated and used as the uniform cell size in all calculations. Although this is an approximation of the rainfall occurring in each grid, it was assumed that the error introduced was not significant. Hourly cumulative rainfall was added for the event to get the daily total rainfall values for each cell.

The cell size used in AGNPS was 200 m X 200 m. The rainfall information was available at a cell size 4000 m X 4000 m. Thus, 400 cells in the watershed were assigned rainfall value that occurred within one radar cell. Rainfall at a resolution of 200 m X 200 m was used for all analyses.

4.8 Calibration of Radar Rainfall

The calibration factor for radar rainfall values at each gauge location was determined using Equation (3.16). Rainfall observed at only one cell that contained the raingauge was used to determine the calibration factor. A calibration factor at each of the 13 gauges used to capture the rainfall pattern for the Cement watershed was calculated. The calibrated radar rainfall field was obtained using

$$R_c = CF_i * R_r \qquad\qquad (4.16)$$

where R_c is the calibrated radar-scanned rainfall value for any particular cell, and R_r is the uncalibrated radar rainfall value for that cell, and CF_i is the appropriate calibration factor for the cell under consideration.

An arbitrary lower and upper limit of 0.1 and 10.0 for the calibration factor was fixed to insure that a very small or large calibration factor was not used. The parameter and output uncertainty induced in the AGNPS model was estimated by using the data from the Cement watershed only. The rainfall event on 7/9/96 consisted of rainfall occurring on 7/9/96 and 7/10/96. The gauge measured rainfall was available for these two dates. The hourly rainfall on each date was added to get the total daily rainfall. Then the calibration factors for rainfall on these two dates were determined separately. Equation (4.16) was used to calibrate the radar rainfall values. The calibration factor corresponding to each gauge location was used for all cells falling within the area associated with that gauge as delineated by the Theissen polygon method. The calibrated rainfall for the two days at each grid was then added to get the total rainfall for the event.

4.9 Estimation of parameter uncertainty due to spatial variability of rainfall

AGNPS requires 26 input parameters. The variability induced in all parameters due to the spatial variability of rainfall was not studied because it would have been very time intensive. Also the output of the model is not equally sensitive to all parameters. To reduce the time of the analysis, only the most sensitive parameters that affect runoff volume, total

sediment transport, sediment-N, and sediment-P transport at the outlet of the watershed based on the sensitivity analysis of AGNPS were used. The most sensitive parameters were curve number (CN), USLE K, C, P factors, and land slope (S). For the AGNPS model, USLE K, C, and P factors always appear as the product KCP and thus can not be separated for parameter estimation. Therefore, for the parameter variability analysis, only one of the three parameters can be considered and the other two parameters will show the same variability. The K factor was used for this study. Thus the three parameters considered were CN, S, and K.

The only available observed data were the rainfall and runoff volume. No observed water quality or sediment data were available. Two steps were used to estimate the parameter uncertainty due to the spatial variability of rainfall. In the first step, grid-based rainfall depths, considered as the 'true' rainfall, were captured using the Theissen polygon method. AGNPS was calibrated for CN using observed 'true' rainfall and runoff volume by adjusting the individual cell curve numbers either all upward or downward by a constant percentage until predicted runoff volume equaled observed runoff volume. The AMC was assumed to be II for CN throughout the parameter estimation process for all rainfall events. All other parameters were estimated based on the observed watershed characteristics. Runoff volume, total sediment, sediment-N, and sediment-P were obtained by running the model using calibrated CN, and 'true' rainfall values for each event. These outputs were considered as the 'observed' values for the further analysis. Characteristics of rainfall, runoff, sediment, and nutrient data for all events analyzed are shown in Table 4.6.

Table 4.6. "Observed" rainfall, runoff, sediment and nutrient values

Rainfall Date	Rainfall (mm)	Runoff (mm)	Total Sediment (Mg)	Sediment-N (kg/ha)	Sediment-P (kg/ha)
Cyril Watershed					
3/27/96	31	0.3	13.6	0.02	0.01
5/31/96	78	0.8	128	0.15	0.07
7/9/96	112	3	401	0.36	0.18
8/1/96	26	4.1	67.1	0.09	0.04
10/27/96	12	0.3	5.44	0.01	0.01
11/6/96	12	0.3	10.9	0.02	0.01
Cement Watershed					
3/27/96	33	0.5	242	0.07	0.03
4/21/96	25	0.8	443	0.1	0.06
5/31/96	83	3	3395	0.53	0.27
7/9/96	64	1.5	2367	0.39	0.2
10/27/96	23	0.3	68	0.02	0.01
Radar (7/9/96)	65	1.5	3338	0.53	0.26

In the second step, parameter uncertainty due to spatial variability of rainfall was estimated. It was assumed that each of the eight raingauges, considered one at a time, in the case of the Cyril watershed, and 17 gauges in the case of the Cement watershed, was the only gauge available for the rainfall measurement and the rainfall depth recorded by that gauge was spatially homogeneous across the watershed. Model parameters were estimated using the rainfall observed at each gauge location, one at a time, and the 'observed' runoff, total sediment, sediment-bound N, and sediment-bound P values. The objective function used in the parameter estimation was the sum of absolute value of relative errors for runoff, sediment and nutrients. The relative error was defined as

$$Relative\ Error\ =\ \frac{(Observed\ value\ -\ Predicted\ value)}{Observed\ value} \tag{4.17}$$

A two stage "brute force" optimization procedure described by Allred and Haan (1996) was used the find the optimum parameter values. In the first optimization stage, a rough estimate of the optimum parameter set was obtained by setting a percentage by which each parameter was to be changed. The parameter values in each cell were increased or decreased by this percentage. Eight increments or decrements were performed for each parameter. Curve numbers were always increased or decreased by a whole number. For three parameters a total of 512 model runs were performed and objective function values calculated for every possible permutation of the parameters. If the optimum values of any of the three parameters were obtained at the upper or lower boundary of the parameter values, the step sizes of the parameter values were increased and the same procedure was repeated to insure

91

that the optimum parameter estimates did not fall at the boundary values. Mathematically, the optimum parameter value can be represented as $(P_i)_j$, where P_i is the average optimum value of parameter i obtained at step j (j=1,2,.....8). If j was equal to one or eight, then the range of the step size was increased, and the optimization procedure was repeated. The first estimate of the optimum parameter set was chosen that had the minimum objective function value.

The second optimization was conducted in a similar manner as the first one by further refining the parameter values. Refinement was accomplished using a much narrower range of parameters obtained from the first optimization. If the optimum parameter obtained by the first approximation was $(P_i)_j$, then the range of the parameters in the second optimization was $(P_i)_{j-1}$ to $(P_i)_{j+1}$. At some instances, more than one set of parameter values, very close to each other, were obtained that minimized the objective function. In that case, the range was set such that all the parameters minimizing the objective function were bracketed. In the second optimization, a step size in the form of a fraction for each parameter was calculated that divided the range of the parameter into 10 evenly distributed values. Each parameter at the cell level was then increased or decreased by this fraction and model runs were performed. In this step also, the curve numbers were increased or decreased by a whole number. A total of 1000 model simulations were performed for each possible permutation of the parameter values. The set of parameters that minimized the objective function were considered as the final optimum parameter set. This "brute force" optimization procedure, although being computationally less efficient than other methods, has the advantage of not being affected by local minimums in the objective function (Allred and Haan, 1996).

92

For the Cyril watershed, eight sets of parameters, one for each gauge-measured rainfall, that minimized the objective function were obtained for each rainfall event. For the Cement watershed, 17 sets of parameters were obtained. Since the parameter values were different at the cell level, the values shown in the subsequent sections represent the average parameter values for the watershed.

The same procedure was repeated for the radar data. The calibrated radar rainfall was assumed to be the "true" rainfall for the Cement watershed. The parameters were estimated using the two steps described in the previous paragraphs and the parameter uncertainty induced by the spatial variability of rainfall was estimated when the "true" rainfall pattern was captured using the calibrated radar rainfall. The parameters were estimated using the calibrated rainfall at the gauge locations only. This gave 17 sets of different parameters for the calibrated radar rainfall field.

4.10 Estimation of output uncertainty due to spatial variability of rainfall

AGNPS was run using the rainfall observed at each gauge location, one at a time, assuming that the rainfall depth was uniform across the watershed. Calibrated values of CN using 'true' rainfall pattern and other best estimates of parameters for each event obtained from the previous section were used. The parameters were fixed for each event. Eight and 17 sets of outputs for the Cyril and Cement watersheds, respectively, were obtained for each rainfall event.

For the calibrated radar rainfall, two sets of the model output uncertainty were obtained. In the first set, the model was run using the rainfall value observed at each gauge

93

location as described in the previous paragraph and the output uncertainty was estimated using the 17 sets of outputs for the Cement watershed for rainfall on 7/9/96. In the second set, the model was run using all of the different rainfall values from the calibrated radar rainfall field. This gave 43 sets of outputs for the watershed representing 43 different rainfall values. A summary flow chart of parameter/output uncertainty estimation is shown in Figure 4.18.

The variability in the model parameters and outputs induced by the spatial variability of rainfall is termed the parameter/output uncertainty. The uncertainty in the model parameters and outputs was quantitatively estimated using Average Error (AE), Relative Error (RE), Standard Error (SE), and Coefficient of Variation (C.V.). These error statistics can be defined as follows

$$AE = \frac{1}{n} \sum_{i}^{n} (|P_i - O|) \tag{4.18}$$

$$RE = \frac{AE}{\overline{O}} \tag{4.19}$$

$$SE = \sqrt{\frac{1}{n} \sum_{i}^{n} (P_i - O)^2} \tag{4.20}$$

$$CV = \frac{SE}{\overline{O}} \tag{4.21}$$

where P_i is the predicted value, O is an observed output or the parameter value, $\bar{O}$ is the mean of the observed data, and n (i=1,2,3,....,n) is the number of data pairs. In this case, since the observed value of parameter/output is fixed for each event, O is equal to $\bar{O}$. The average error quantifies parameter/output variability in the units of O and P (e.g., kg, m/m, mg/L). In order to compare the parameters/outputs having different units, Average Error must be expressed in unitless terms. The relative error, RE, gives the percent deviation of the parameter/output value from the mean observed value. The standard error, SE, and the coefficient of variation, C.V., are numerical indicators of the variability in predicted data.

The variability in the rainfall amounts observed at each location was quantified using Equations 4.18-4.21. Here P_i is the rainfall observed at the gauge i, O is the average rainfall for the area, and n is the number of gauges used to capture the rainfall spatial variability.
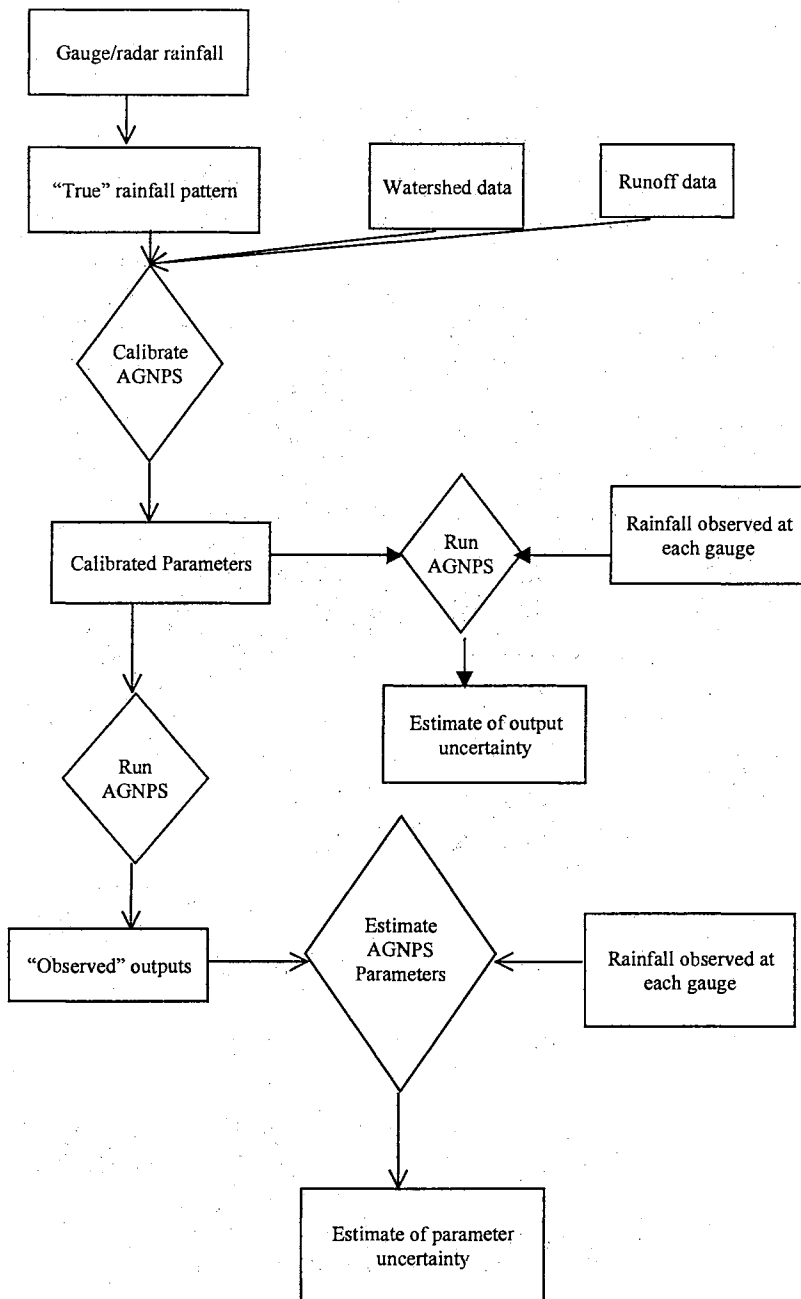
Figure 4.18. Summary flow chart of parameter/output uncertainty estimation

CHAPTER 5

RESULTS AND DISCUSSION

5.1 Spatial Variability of Rainfall

Consideration of spatial variability of rainfall is very important in studying the process

of generation and transport of runoff, sediment, and nutrients from a watershed. In modeling

the hydrologic behavior of watersheds, most of the models available to date assume spatial

homogeneity of rainfall. Figure 5.1 shows the hourly distribution of rainfall that occurred on

8/3/97 over the Little Washita watershed as recorded at 42 Micronet stations. Total area of

the watershed is 610 km². A large variation in the cumulative rainfall depth over the area is

evident. The event rainfall depth varied from almost zero to 43 mm. Traditionally, rainfall

is measured at a few gauges (possibly only one) scattered throughout the basin and these point

measured values are used to determine the average rainfall depth for use in hydrologic/water

quality (H/WQ) models. In an ideal condition, where the density and distribution of gauges

are adequate, rainfall depth can be estimated with sufficient accuracy at any point in the basin

by using a spatial interpolation technique. Unfortunately, this ideal condition rarely exists.

In fact, it is not uncommon to have no rain gauge within the basin of interest. If each of the

42 gauges in the Figure 1 is assumed to be the representative gauge for the watershed, the

result obtained using the rainfall recorded at each gauge location, one at a time, will have a
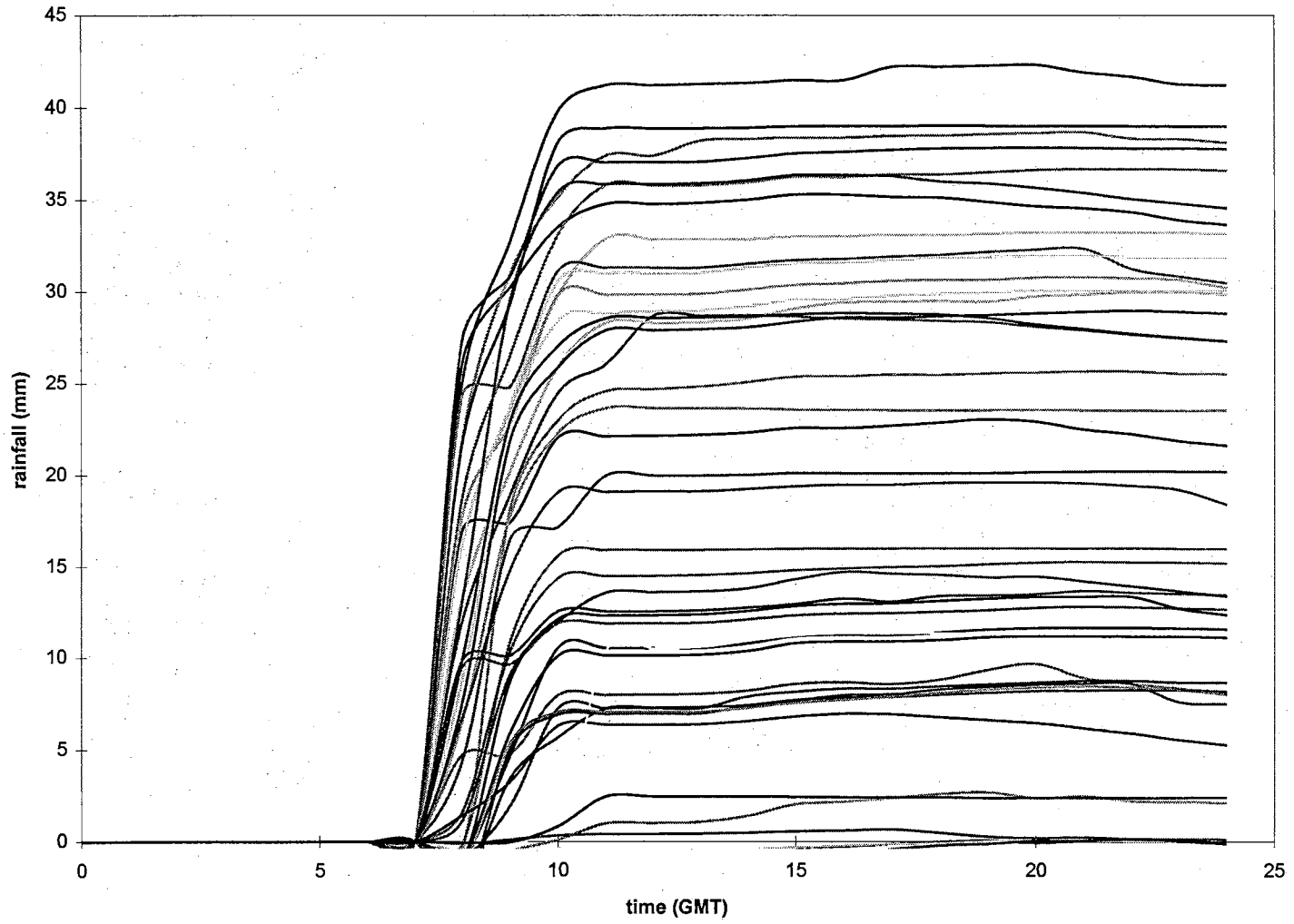
Figure 5.1. Hourly distribution of rainfall on 8/3/96 over Little Washita watershed

large variability. A H/WQ model like AGNPS may not predict any significant output using the low rainfall values as compared to a larger rainfall depth (>30 mm) observed at some other gauge locations.

Eight gauges located within and around the Cyril watershed were used in the analysis of rainfall spatial variability. Figure 5.2 shows the location of these gauges. The characteristics of the rainfall observed by the eight gauges are shown in Table 5.1. Table 5.2 shows the rainfall characteristics for the five events analyzed for the Cement watershed. Spatial variability of rainfall for the Little Washita basin is shown in the Table 5.3. For the Cement watershed, eight of the 17 gauges had erroneous rainfall amounts recorded on 8/1/96. Most of these gauges were located within the basin. This event was not considered for this watershed. However, this problem was not encountered with the Cyril watershed, because the watershed size was small, and gauges considered for this watershed did not have any problem. When analyzing the results with the Little Washita basin, all gauges which did not seem to be functional for any of the two days that made an event were discarded from the analysis. The number of gauges considered to capture the rainfall spatial variability ranged from 13 to 17 for the Cement watershed, and 23 to 42 for the Little Washita basin.

For the Cyril watershed, the six events analyzed varied in terms of the rainfall depth. The average rainfall varied from 11 mm to 84 mm. The range of the rainfall recorded by eight gauges, average error, relative error, standard error, and C.V. were calculated for all events. The C.V. ranged from 0.07 to 0.7 for the five events. The rainfall on 5/31/96 was most homogeneous in nature which is evident by the smallest C.V., standard error and relative error (Table 5.1). The rainfall on 8/1/96 was the most heterogenous as shown by the largest C.V.
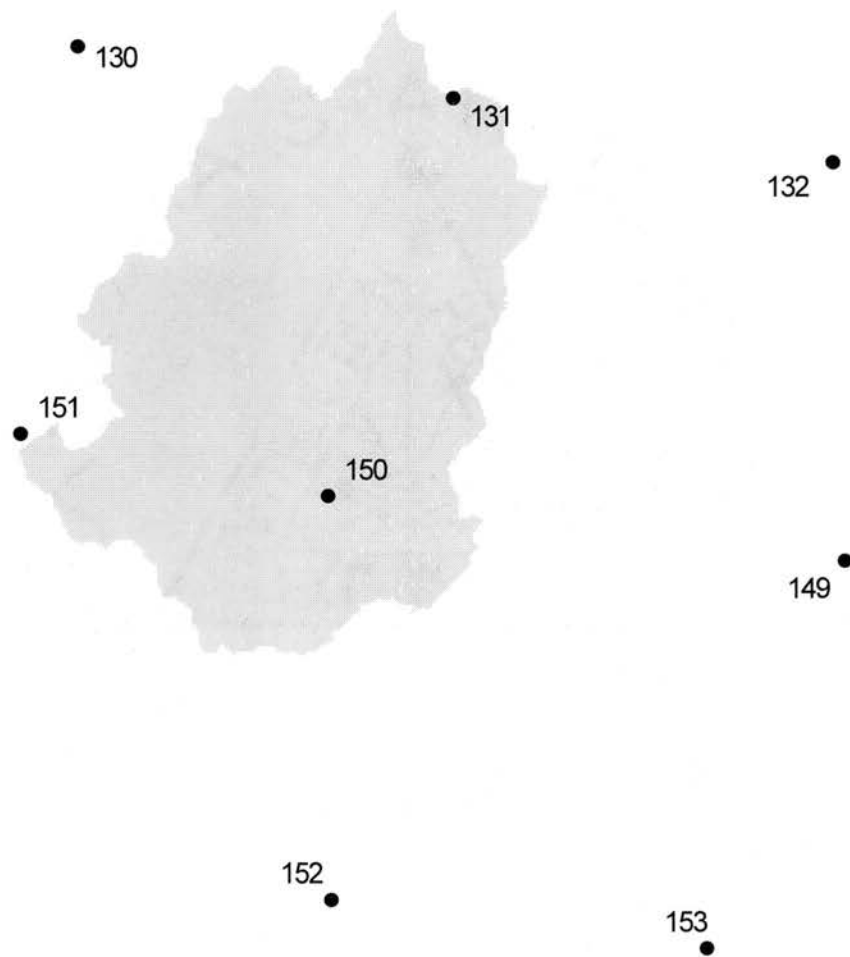
Figure 5.2. Micronet stations used with the Cyril watershed

Table 5.1. Spatial Variability of rainfall for the Cyril watershed

Stastistic	Rainfall Date					
	3/27/96	5/31/96	7/9/96	8/1/96	10/27/96	11/6/96
Average (mm)	29.21	83.06	84.20	27.18	20.03	10.80
A.W. Avg. (mm)	30.92	78.57	111	26.95	12.88	12.06
Range (mm)	18.0-40.9	76.5-94.5	42.4-137	5.33-68.1	9.65-38.4	1.27-21.8
Avg. Error (mm)	8.13	5.21	31.56	14.92	8.28	5.05
Rel. Error	0.28	0.06	0.37	0.55	0.41	0.47
Std. Error (mm)	8.90	5.91	34.7	19.0	9.33	6.00
C.V.	0.30	0.07	0.41	0.70	0.47	0.56
No. of Gauges	8	8	8	8	8	8

Table 5.2. Spatial variability of rainfall for the Cement watershed

Statistic	Rainfall Date				
	3/27/96	4/21/96	5/31/96	7/9/96	10/27/96
Average (mm)	32.0	26.2	77.8	69.2	18.5
A.W. Avg. (mm)	32.5	24.6	83.3	64.3	23.4
Range (mm)	18.0-40.9	16.7-50.3	57.15-94.5	30.7-137	0-44.5
Avg. Error (mm)	6.35	7.15	6.47	27.0	9.34
Rel. Error	0.20	0.27	0.08	0.39	0.51
Std. Error (mm)	7.95	9.08	8.87	31.6	11.7
C.V.	0.25	0.35	0.11	0.46	0.64
No. of Gauges	13	16	17	17	17

A.W. Average = area weighted average; Avg. Error = average error
Rel. Error = relative error; Std. Error = standard error
No. of Gauges = Number of gauges used within and around the watershed

Table 5.3. Spatial Variability of rainfall for the Little Washita basin

Statistic	Rainfall Date						
	3/27/96	4/21/96	5/31/96	7/9/96	8/1/96	10/27/96	11/6/96
Average (mm)	27.8	30.3	74.1	66.2	38.0	15.8	16.0
Range (mm)	1.02-40.9	0.76-57.7	0.25-103	14.7-137	11.7-59.9	0-44.5	0-44.7
vg. Error (mm)	9.48	9.17	10.3	27.4	11.7	7.84	10.0
Rel. Error	0.34	0.30	0.14	0.41	0.31	0.50	0.63
Std. Error (mm)	10.9	11.8	15.5	31.7	14.0	10.2	12.4
C.V.	0.40	0.39	0.21	0.48	0.37	0.65	0.78
No. of Gauges	23	41	42	42	26	42	37

A.W. Average = area weighted average; Avg. Error = average error

Rel. Error = relative error; Std. Error = standard error

No. of Gauges = Number of gauges used within and around the watershed

For the Cement watershed, the average rainfall ranged from 19 to 78 mm for the five events analyzed (Table 5.2). The C.V. ranged from 0.11 to 0.64. The smallest C.V. and relative error were associated with the rainfall on 5/31/96 and largest with the rainfall on 10/27/96. The standard error was smallest for the rainfall on 3/27/96.

The average rainfall for the Little Washita basin ranged from 16 to 74 mm for the seven events (Table 5.3). The range of C.V. was 0.21 to 0.78. The smallest and largest standard errors resulted on 10/27/96 and 7/1/96, respectively. The rainfall on 5/31/96 resulted in the smallest relative error, while the rainfall on 11/6/96 resulted in the largest relative error. For this watershed, the rainfall on 5/31/96 was also the most homogeneous in nature as shown by the smallest C.V. (Table 5.3).

For the Cyril watershed a true rainfall pattern was captured using four gauges and the Theissen polygon method. For the Cement watershed rainfall observed by 13 gauges was used to capture the true rainfall pattern. The area weighted rainfall shown in Tables 5.1 and 5.2 were obtained from the rainfall observed by these gauges and the Theissen polygon method. The average rainfall was obtained from the 8 gauges in Cyril watershed and 17 gauges in Cement watershed. The average rainfall and the area-weighted average rainfall were not same for all events, except 8/1/96 for the Cyril watershed. For the Cement watershed, the area-weighted rainfall was different from the average rainfall for all dates, except 3/27/96. Inclusion of additional gauges that were in the vicinity of the watershed introduced a bias in the average rainfall estimate. In actual conditions, it is not uncommon to have a raingauge located outside the watershed of interest. As the number of raingauges

available to estimate the area-weighted rainfall increases, this bias can be expected to decrease.

The common events analyzed for the Cyril and Cement watersheds were 3/27/96, 5/31/96, 7/9/96, and 10/27/96. For Cement watershed, C.V., relative error, and range of rainfall was larger for all dates except 3/27/96. Standard error was larger for the events on 5/31/96 and 10/27/96. For the event on 3/27/96, the range of rainfall observed by 8 gauges for Cyril watershed and 17 gauges for Cement watershed was same. The inclusion of additional gauges that had rainfall within the same range decreased the C.V., standard, and relative errors.

For the Little Washita basin, when range and error statistics of rainfall are compared with the Cyril and Cement watersheds, a larger variation in the rainfall is evident. The range and C.V. of rainfall are larger for Little Washita basin as compared to the two smaller watersheds. As compared to the Cyril watershed, standard error was larger for all events, except 8/1/96. Average error was larger for 3/27/96, 5/31/96, and 11/6/96. When compared to the Cement watershed, standard error was larger for all events except on 7/9/96, and 10/27/96. The average rainfall was also different for the three watersheds.

In general, the rainfall spatial variability increased with an increase in the watershed size. This is evident from the fact that the rainfall range increased with the watershed area. The minimum rainfall observed by raingauges decreased as the size of the watershed increased. For the Little Washita basin, the minimum rainfall observed was very close to zero for five of the seven events analyzed. These rainfall data will not predict any significant output as compared to the output obtained when the maximum rainfall was used. This shows

104

that the use of a single gauge to measure rainfall for application in H/WQ models can introduce significant errors in model results.

Contour maps of the rainfall depth for all the seven dates are shown in Figures 5.3-5.9. The contour map was made using inverse distance interpolation. The rainfall was interpolated at each point using seven surrounding gauges. Considerable variation in the rainfall depth is evident. Here for the area shown in these figures, the maximum distance in the East-West direction is 41 km and in the North-South direction is 25 km. The rainfall depth gradient and the direction of the rainfall depth gradient is different for each storm.

For four of the six events analyzed for the Cyril watershed, rainfall observed by gauge 150 was closest to the area-weighted rainfall. For rainfall on 11/6/96, gauge 131 recorded a rainfall depth similar to the area-weighted rainfall. Figure 5.2 shows that gauge 150 is located near the center of the watershed. There are only two gauges, 131 and 150, located within the watershed (Figure 5.2). Together these two gauges observed a rainfall depth similar to the area-weighted rainfall for all events analyzed, except on 8/1/96. For the rainfall on 8/1/96, gauge 132 was the best representative gauge from the area-weighted rainfall point of view.

For the Cement watershed, gauges 149 and 150 recorded a rainfall similar to the area-weighted rainfall on 3/27/96. For the rainfall on 4/21/96 and 5/31/96, gauge 147 was the best representative gauge for the watershed. Gauge 154 on 4/21/96 and 152 and 154 on 5/31/96 also observed rainfall depth similar to the area-weighted rainfall. Gauges 148 and 154 were the most representative gauge for the rainfall on 7/9/96 and 10/27/96, respectively.
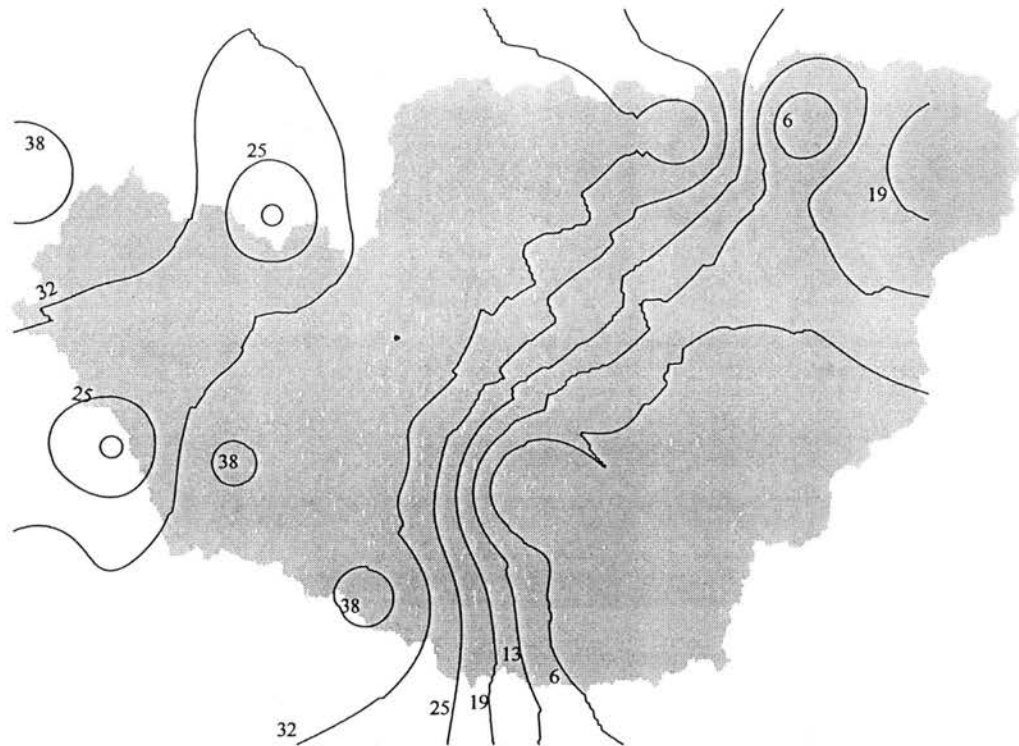
Figure 5.3. Contour map of rainfall depth (mm) for storm on 3/27/96

106
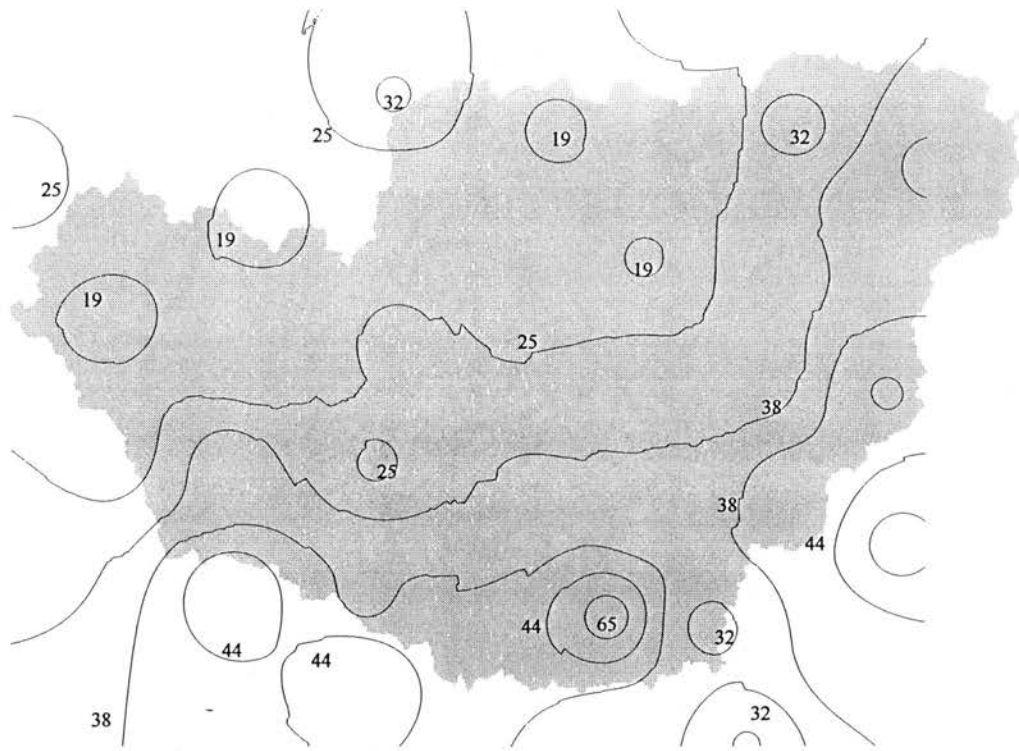
Figure 5.4. Contour map of rainfall depth (mm) for storm on 4/21/96
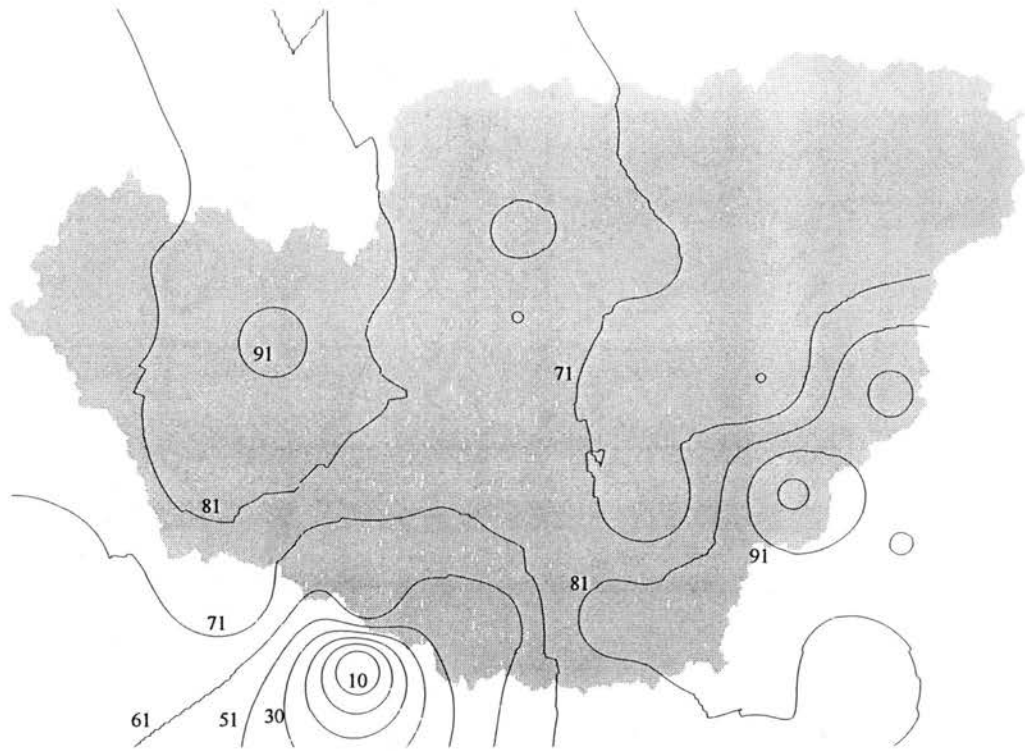
Figure 5.5. Contour map of rainfall depth (mm) for storm on 5/31/96

Figure 5.6. Contour map of rainfall depth (mm) for storm on 7/9/96
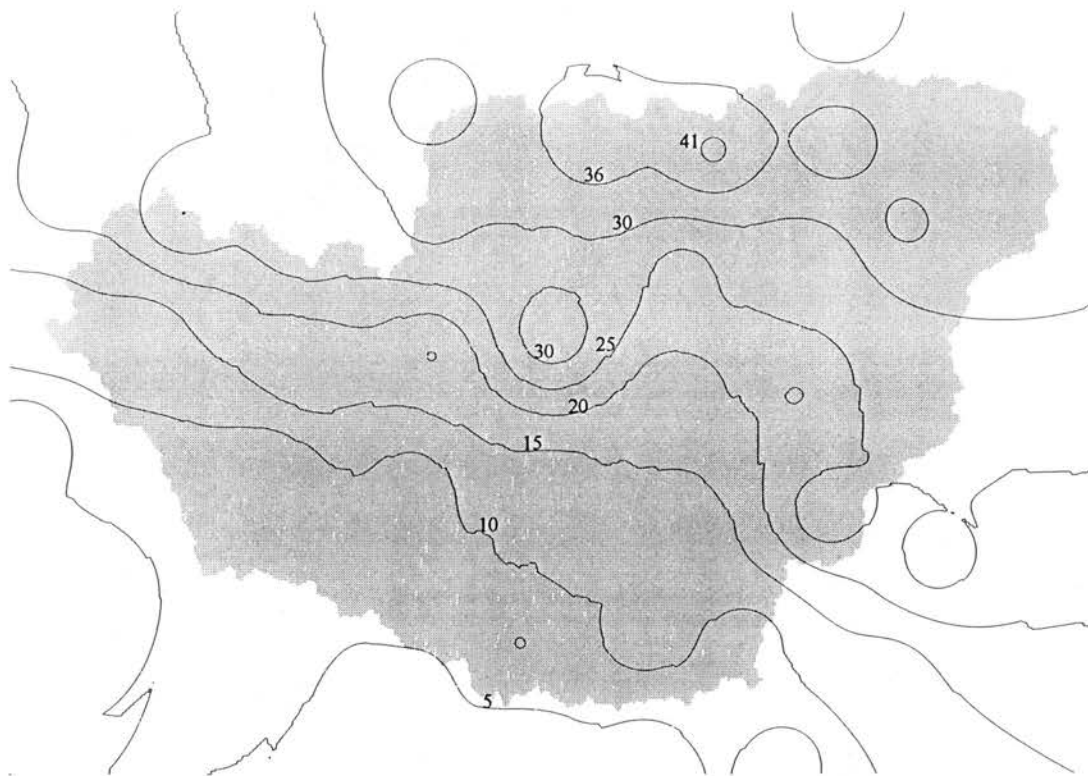
Figure 5.7. Contour map of rainfall depth (mm) for storm on 8/3/96

Figure 5.8. Contour map of rainfall depth (mm) for storm on 10/27/96

Figure 5.9. Contour map of rainfall depth (mm) for storm on 11/6/96

In general, for the Cyril watershed, the gauges located within the basin were the most representative gauges for the rainfall in the watershed for the most of the events. For the Cement watershed, although the gauges located near the center of the watershed had rainfall recorded that was a better representation of the area-weighted rainfall, the best representative gauge was not always located near the center of the watershed. Gauges 149 and 153 are located near the center of the watershed, however, gauge 149 was the most representative gauge for only one of the five events analyzed.

5.2 Calibration of Radar Rainfall Data

Table 5.4 shows that for the rainfall on 7/9/96, the calibration factor ranged from 0.08 to 7.45. Since the lower limit for the calibration factor was 0.1, the radar rainfall corresponding to the calibration factor 0.08 was not used. As compared to the gauge measured rainfall the radar over estimated the rainfall at six gauge locations and under estimated the rainfall at seven gauge locations. For the rainfall on 7/10/96, the calibration factor ranged from 1.125 to 3.93 (Table 5.5). Radar underestimated the rainfall at all gauge locations for the rainfall on this date. For the rainfalls in Oklahoma, Smith et al. (1996) concluded that underestimation of rainfall was pronounced beyond 150 km in spring-summer and beyond 100 km in winter-fall due to incomplete beam filling and overshooting of precipitation. For the warm season the raingauge observations were found to be 48% larger than radar rainfall estimates in the range 0-40 km, 18% larger in the range 40-160 km, and 40% larger in the range greater than 160 km. The maximum and minimum distance between a raingauge and radar for the watershed Cement is 104 km and 85 km, respectively. The

Table 5.4. Radar rainfall calibration factors for rainfall on 7/9/96

Gauge #	Radar value (mm)	Gauge value (mm)	C.F.
130	9	45	5
131	11	82	7.45
132	13	43	3.31
133	12	36	3
148	37	26	0.7
149	33	19	0.58
150	24	50	2.08
151	13	57	4.38
152	42	12	0.29
153	45	7	0.16
154	38	5	0.13
162	17	23	1.35
163	49	4	0.08

Table 5.5. Radar rainfall calibration factors for rainfall on 7/10/96

Gauge #	Radar value (mm)	Gauge value (mm)	C.F.
130	19	57	3
131	14	55	3.93
132	20	31	1.55
133	23	42	1.83
148	23	41	1.78
149	19	28	1.47
150	23	48	2.09
151	19	69	3.63
152	18	35	1.94
153	24	36	1.5
154	21	31	1.48
162	13	23	1.77
163	16	18	1.125

raingauges corresponding to the maximum and minimum distances were 151 and 134, respectively. The results obtained here were consistent with the results reported by Smith et al. (1996) except that the underestimation of rainfall by radar was more pronounced for the events analyzed in this research. If the radar rainfall is not calibrated using the raingauge data, the calibration factors show the error in the rainfall one may expect. For example, the uncalibrated radar rainfall on 7/9/96 has a range of error from 0.08 to 7.45 factors. This rainfall should be corrected before it can be used in any hydrologic applications.

The average and range in the radar scanned rainfall over the watershed were 65 mm, and 21-189 mm, respectively. The area weighted rainfall using data from raingauges alone and the Theissen polygon method was 64 mm. This shows that the calibrated rainfall produced an average rainfall over the Cement Watershed similar to the area-weighted rainfall obtained using 13 raingauges. The standard deviation and C.V. were 37.5, and 0.59, respectively. The variability in the radar-scanned rainfall as indicated by range and C.V. is larger than the corresponding rainfall variability when the rainfall was captured using the raingauges alone. It shows that when only a limited number of raingauges are used to capture the rainfall, the variation in the rainfall may be lower than the true but unknown variation. A calibrated radar rainfall may give a better estimate of true rainfall pattern over the watershed area.

5.3 Effect of Rainfall Spatial Variability on Parameter Estimation

5.3.1 Effect of Rainfall Spatial Variability on Model Parameter Uncertainty

Parameter variability induced by spatial variability of rainfall is shown in Table 5.6

for the Cyril watershed. AGNPS is a distributed parameter model. The model parameters

vary from cell to cell. The parameter estimates discussed here represent the average

parameter value and all the statistics were based on the average parameter estimates for the

watershed. In AGNPS, land slope is used to calculate the amount of sediment and nutrients

eroded within each cell and the subsequent routing of the sediment and nutrients from each

cell to the watershed outlet. The K factor is used in Universal Soil Loss Equation (USLE) to

calculate the amount of sediment and nutrients eroded at each cell. CN indicates the runoff

potential of an area. Coefficient of variation (C.V.) in estimated CN ranged from 0.06 to 0.54

for the six events considered. The largest standard error (SE) in CN was produced by the

rainfall that had the largest standard error (7/9/96). The smallest C.V. and SE in CN were

associated with the rainfall with the smallest C.V. and SE (5/31/96). Coefficient of variation

and SE are numerical representations of the variability in the data. It means that a rainfall

with a large variation in observed depth will produce a higher variability in CN. This can be

expected since for a fixed runoff there is a one-to-one correspondence between rainfall and

CN. For a small observed rainfall value, CN must be higher to produce a volume of runoff

equal to the measured runoff and vice-versa.

Table 5.7 shows the parameter variability induced by rainfall spatial variability for the

Cement watershed. The C.V. in CN ranged from 0.11 to 0.51 for the five events considered.

The SE ranged from 4.85 to 16.85. Here again the largest SE in the rainfall was associated

117

with the largest SE in CN. In general, the standard error in CN decreased with a decrease in the SE for rainfall depth.

The C.V. in the estimated slope ranged from 0.06 to 1.64 for the Cyril watershed and 0.12 to 0.58 for the Cement watershed. The range of SE were 0.09 to 2.62 for the Cyril watershed and 0.46 to 2.15 for the Cement watershed, respectively. Out of the total six rainfall events analyzed, the rainfall on 7/9/96 and 8/1/96 were the most heterogeneous in nature for the Cyril watershed. These two events produced the highest variation in the estimated slope for the Cyril watershed. For the Cement watershed, although the largest C.V. and SE in the estimated slope were not associated with the rainfall having largest C.V. and SE, in general a higher variability in rainfall resulted in a higher variability in estimated slope. The rainfall on 5/31/96 was the most homogeneous in nature. This resulted in the smallest C.V. in the slope estimates.

For the Cyril watershed, C.V. and SE in the K factor ranged from 0.08 to 0.79, and 0.03 to 0.27, respectively. Here again, the smallest C.V. and SE were associated with the rainfall event most uniform in nature (5/31/96). The variability in the estimated K factor increased with an increase in rainfall heterogeneity. For the Cement watershed, the C.V. ranged from 0.08 to 0.85 for K factor. The corresponding range in SE was 0.03 to 0.28.

Coefficient of variation in retention parameter (S) ranged from 0.11 to 0.81 for the Cyril watershed and 0.17 to 0.49 for the Cement watershed, respectively. The corresponding ranges in SE were 28.2 to 84.1 mm, and 46.7 to 251 mm, respectively. Similar to the CN, the smallest variation in S resulted from the rainfall most homogeneous in nature (5/31/96).

Table 5.6. Parameter variability induced by spatial variability of rainfall for Cyril watershed

Statistic	Parameter values for rainfall dates					
	3/27/96	5/31/96	7/9/96	8/1/96	10/27/96	11/6/96
CN						
Average	62	36	46	73	68	77
Range	52-71	32-38	32-62	46-90	52-77	66-82
C.V.	0.15	0.06	0.54	0.19	0.14	0.08
Std. Error	8.42	2.37	17.7	13.6	10.6	6.31
Avg. Error	6.63	1.63	13.1	11.0	7.75	5.57
Rel. Error	0.11	0.04	0.4	0.15	0.10	0.07
Slope						
Average	1.69	1.50	2.52	2.44	1.14	1.54
Range	0.93-2.75	1.2-1.87	1-4.05	0.4-8.2	0.55-1.8	1.44-1.6
C.V.	0.45	0.16	0.92	1.64	0.43	0.06
Std. Error	0.73	0.25	1.47	2.62	0.69	0.09
Avg. Error	0.66	0.21	1.19	1.53	0.57	0.06
Rel. Error	0.41	0.13	0.75	0.96	0.36	0.04
K factor						
Average	0.41	0.33	0.50	0.30	0.25	0.23
Range	0.32-0.58	0.29-0.36	0.28-0.79	0.09-0.87	0.05-0.48	0.19-0.38
C.V.	0.40	0.08	0.72	0.79	0.50	0.37
Std. Error	0.13	0.03	0.25	0.27	0.17	0.13
Avg. Error	0.09	0.03	0.18	0.23	0.14	0.12
Rel. Error	0.26	0.07	0.53	0.67	0.4	0.36
Retention Parameter (S)						
Average	164	461	344	108	128	75.9
Range	103-234	415-540	156-540	27.9-298	75.9-234	55.9-132
C.V.	0.29	0.11	0.45	0.81	0.73	0.33
Std. Error	54.1	49.5	232	84.1	65.3	28.2
Avg. Error	44.2	33.3	183	60.5	45.0	24.4
Rel. Error	0.24	0.08	0.36	0.58	0.5	0.29

Std. Error = stadard error; Avg. Error = average error
Rel. Error = relative error

Table 5.7. Parameter variability induced by spatial variability of rainfall
for Cement watershed

Statistic	Parameter values for the rainfall dates				
	3/27/96	4/21/96	5/31/96	7/9/96	10/27/96
CN					
Average	58	65	43	44	66
Range	51-70	47-72	36-52	23-64	47-76
C.V.	0.12	0.11	0.12	0.51	0.26
Std. Error	6.83	6.98	4.85	16.9	14.2
Avg. Error	4.38	5.81	3.75	13.8	12.7
Rel. Error	0.07	0.09	0.1	0.42	0.23
Slope					
Average	3.96	5.69	3.93	4.12	3.62
Range	3.11-5.24	3.33-6.79	3.32-5.14	2.07-6.22	2.1-5.54
C.V.	0.20	0.58	0.12	0.33	0.26
Std. Error	0.75	2.15	0.46	1.24	0.95
Avg. Error	0.48	2.02	0.30	1.02	0.77
Rel. Error	0.13	0.55	0.09	0.28	0.21
K factor					
Average	0.35	0.44	0.32	0.51	0.36
Range	0.23-0.58	0.25-0.68	0.28-0.38	0.27-0.87	0.14-0.59
C.V.	0.38	0.54	0.08	0.85	0.50
Std. Error	0.13	0.18	0.03	0.28	0.16
Avg. Error	0.08	0.14	0.02	0.21	0.15
Rel. Error	0.23	0.43	0.08	0.62	0.45
Retention Parameter (S)					
Average	188	144	351	388	139
Range	109-244	98.9-287	234-452	143-850	80.3-287
C.V.	0.23	0.33	0.17	0.49	0.44
Std. Error	46.7	48.5	67.1	251	92.2
Avg. Error	31.2	37.6	54.9	223	84.6
Rel. Error	0.16	0.25	0.14	0.43	0.41

Std. Error = stadard error; Avg. Error = average error
Rel. Error = relative error

In general, a wide range in estimated parameters resulted when the rainfall measured at each gauge location was used individually, one at a time. None of the parameters can be considered unlikely when viewed individually for each event. Together the sets of parameter values obtained illustrate the possible range depending upon the rainfall variability across the watershed.

A larger range in the rainfall values within a single event resulted in a higher range in all estimated parameters. When compared to the true parameter values, the variation was very large for all events. For slope, K, and S the range was several orders of magnitude for some events for both watersheds. Parameter uncertainty comes into play when developing and testing a model. One might have several observed events and use each to estimate model parameters. The result may be quite inconsistent estimates. Usually the uncertainty in the model parameters is attributed to the structure of the model because the mathematical models are simplified description of the processes occurring in the nature. Results of this study indicate that even in the case of physically-based distributed-parameter models, an uncertainty in the parameter estimates would be observed because of the input error coming from the spatial variability of rainfall. The input error is present when measurements from only one gauge or a small number of gauges is used when a more extensive network might be necessary to give an adequate representation of the rainfall pattern over a basin.

5.3.2 Biases in the Estimated Parameters Due to Rainfall Spatial Variability

Biases in the estimated parameters obtained are shown in Table 5.8. Here a bias is defined as the difference between true and estimated average parameter value. A positive bias means the parameter was underestimated and a negative bias mean that the parameter was overestimated. The parameters were estimated using observed output and rainfall measured at each gauge location, one at a time. The objective function used to estimate the parameters was the sum of absolute values of relative errors defined by Equation 4.17. For the Cyril watershed, the values shown in the Table 5.8 represent the average of the 8 sets of parameters obtained for 8 different rainfall measurement for each event. For the Cement watershed, the parameter values shown are the average of 17 different realizations of the parameters, each corresponding to one gauge location for each event.

Here it should be noted that the true parameter values for slope and K factor were obtained using the observed characteristics of the watershed. CN were obtained by using the true pattern of rainfall captured by 4 gauges using Theissen polygon method for Cyril watershed, and 13 gauges for Cement watershed. Retention parameter (S) was derived from CN. Here it was assumed that CN obtained using a spatially variable rainfall pattern for the two watersheds gave the true CN and S estimates. In the case of Slope and K, it was assumed that the observed watershed characteristics yielded the true estimates of these parameters.

For the Cyril watershed, for all events except on 8/1/96, area-weighted rainfall is different from the average rainfall obtained using 8 gauges. This bias in rainfall produced a bias in CN and S. For the Cement watershed, a bias is evident in average and area-

122

Table 5.8. Biases in the estimated parameters induced by the rainfall spatial variablity

Rainfall date	CN	S (mm)	Slope (%)	K
Cyril Watershed				
3/27/96	-4	19.6	-0.09	-0.07
5/31/96	1	-28.4	0.11	0.02
7/9/96	-13	171	-0.92	-0.16
8/1/96	-2	-4.57	-0.84	0.04
10/27/96	6	-29.3	0.46	0.09
11/6/96	-2	8.64	0.06	0.11
Cement Watershed				
3/27/96[a]	-2	11.2	-0.25	-0.02
4/21/96[b]	-2	5.33	-1.98	-0.11
5/31/96[c]	-3	46.0	-0.22	0.01
7/9/96[c]	-11	128	-0.41	-0.18
10/27/96[c]	-11	69.1	0.09	-0.03

a = Average of 13 gauges
b = Average of 16 gauges
c = Average of 17 gauges

weighted rainfall for all rainfall events. This resulted in a biased average estimate of CN and S for all events.

The true parameter values of slope and K did not depend on the true rainfall pattern. They were derived from the watershed characteristics. When the slope and K factors were estimated using the rainfall depth observed at each gauge location one at a time, the bias in the recorded rainfall at each gauge location was compensated for by adjusting the parameter values to get the model predictions closer to the observed output values. In this case, a bias in the amount of recorded rainfall was translated to parameter bias and affected the resulting parameter estimates. As the number of rainfall observations for a watershed increases, the bias in the estimated parameters can be expected to decrease.

5.3.3 Relative Errors in Estimated Parameters Due to Rainfall Spatial Variability

Relative errors for estimated parameters as compared to the calibrated parameter values were calculated for all events for the two watersheds. Table 5.9 shows the relative errors in estimated parameters as compared to the calibrated parameter values for the Cyril watershed. The corresponding parameter relative errors for the Cement watershed are shown in Table 5.10. The maximum and minimum relative errors as compared to the area-weighted average rainfall for all events analyzed are shown in Table 5.11. For each event, parameters were estimated using eight raingauges for the Cyril watershed and 13 to 17 raingauges for Cement watershed. Rainfall observed at each gauge location gave a different set of parameters that minimized the objective function defined by Equation 4.17.

124

Table 5.9. Relative errors in estimated parameters for Cyril watershed

Rainfall Date	Parameter	Relative Error	
		Maximum	Minimum
3/27/96	CN	0.22	0
	S	0.44	0
	Slope	0.72	0.17
	K	0.71	0
5/31/96	CN	0.14	0
	S	0.25	0
	Slope	0.25	0.03
	K	1.32	0
7/9/96	CN	0.88	0.03
	S	0.7	0.05
	Slope	1.53	0.03
	K	1.32	0
8/1/96	CN	0.35	0.04
	S	1.87	0.14
	Slope	4.13	0
	K	1.56	0.11
10/27/96	CN	0.3	0
	S	1.63	0
	Slope	0.66	0.05
	K	0.85	0.03
11/6/96	CN	0.12	0.01
	S	0.55	0.05
	Slope	0.1	0
	K	0.44	0.12

Table 5.10. Relative errors in estimated parameters for Cement watershed

Rainfall Date	Parameter	Relative Error	
		Maximum	Minimum
3/27/96	CN	0.23	0.02
	S	0.46	0.04
	Slope	0.41	0.01
	K	0.75	0
4/21/96	CN	0.25	0
	S	0.92	0
	Slope	0.83	0.1
	K	1.06	0.03
5/31/96	CN	0.33	0
	S	0.4	0
	Slope	0.39	0.02
	K	0.15	0.03
7/9/96	CN	0.94	0.03
	S	0.72	0.04
	Slope	0.67	0.01
	K	1.63	0
10/27/96	CN	0.38	0.03
	S	0.61	0.08
	Slope	0.49	0
	K	0.78	0.03

Table 5.11. Relative errors in rainfall values

Rainfall Date	Relative Error	
	Maximum	Minimum
Cyril Watershed		
3/27/96	0.42	0.01
5/31/96	0.2	0
7/9/96	0.62	0.09
8/1/96	1.57	0.15
10/27/96	2.08	0.02
11/6/96	0.89	0.17
Cement Watershed		
3/27/96	0.45	0.01
4/21/96	1.04	0
5/31/96	0.31	0.02
7/9/96	1.13	0.05
10/27/96	0.9	0.13

The minimum and maximum relative errors shown in the Table 5.9 for each parameter are the minimum and maximum relative errors obtained from the eight sets of parameters for each event. For the Cement watershed (Table 5.10), the minimum and maximum relative errors for the parameters represent the minimum and maximum relative error values from 13 to 17 sets of parameters for each event. For the Cyril watershed, the maximum relative error in CN, S, Slope and K factor were 0.88, 1.87, 4.13, and 1.56, respectively, for all events considered. The maximum relative error in CN occurred for rainfall observed at gauge location 153 on 7/9/96. The maximum relative error in the slope estimates resulted from the rainfall observed at gauge 152 on 8/1/96. The minimum relative error for these parameters was zero. Table 5.9 shows that the minimum relative error was very near to zero for all of the events for all parameters. The corresponding rainfall error observed at these gauge location was also relatively smaller. For the rainfall observed at gauge 151, the relative error in slope estimate was zero although the relative error in rainfall at this gauge location was highest for the event.

For the Cement watershed, the maximum relative error in CN, S, slope, and K factor were 0.94, 0.92, 0.83 and 1.63, respectively, for all events considered. The corresponding rainfall relative errors were 0.52, 1.04, 0.32, and 0.52, respectively. Maximum relative error in CN was obtained at the gauge 161 for rainfall on 7/9/96. The rainfall obtained at this gauge location was minimum for this event. For S, the maximum relative error occurred at gauge 163 on 4/21/96. For this event, rainfall relative error was maximum at this gauge location. Also, the rainfall observed at this gauge was the maximum for the event. Maximum relative error in slope estimate was at the gauges 132 and 150 on 4/21/96. The rainfall observed by these gauges was the minimum for the event. The maximum relative error in estimated K

128

factor was associated with the minimum rainfall observed at the gauge 161 on 7/9/96.

The minimum relative errors for CN, S, slope, and K factor for the Cement watershed were zero. The corresponding rainfall relative errors were 0.09, 0.26, 0.09, and 0.15, respectively. The minimum relative error was close to zero for all events for all parameters. Here it should be noted that the minimum relative errors were not associated with the rainfall minimum relative errors. For example, rainfall on 4/21/96 had the rainfall measured at the gauge 147 very similar to the area-weighted rainfall value. But the relative errors in the parameters were not minimum at this gauge location. This might have come from the routing of the runoff from cell to cell, and subsequently to the watershed outlet. For a large watershed, if the center of the storm is located towards the watershed outlet, the spatially variable rainfall will produce larger runoff volume than a spatially homogeneous rainfall equal to the area-weighted rainfall depth. This was evident from the fact that the average CN for the watershed for rainfall at gauge 147 was higher than the average true CN obtained using true rainfall pattern on 4/21/96, although the rainfall observed at this gauge was very close to the area-weighted mean rainfall. In other words, in order to produce the given amount of runoff with a given CN, rainfall observed at the gauge location should be higher than the area-weighted rainfall. It means that for large watersheds, an area-weighted average rainfall may not result in the true parameter estimates. However, a bias in the parameter using area-weighted rainfall will be smaller as compared to the parameter estimated using rainfall observed at only one gauge location. This bias can be expected to decrease with a decrease in the watershed size. Similar results were obtained for other events for this watershed.

129

Maximum relative errors in CN and S were associated with the minimum rainfall observed at a gauge location for all events, except on 4/21/96. For the rainfall on 4/21/96, the maximum rainfall observed at the gauge 163 produced the maximum relative error in CN, and S. For estimated slope and K factor, the maximum relative error resulted from the gauges that observed the minimum rainfall. This shows that if the rainfall is observed by several gauges, and the parameters of the model are estimated using rainfall one gauge at time, the maximum relative error may result from the minimum rainfall recorded for the event. However, this result should be tested with other models before it can be extrapolated for all H/WQ models. Since AGNPS is designed to predict erosion events, not low flow events, the bias and relative errors in parameter estimates can be expected to be large for smaller rainfall events.

5.3.4 Correlation Structure Among the Parameters

The correlation among the parameters and the input rainfall was calculated for all events for the two watersheds. The results of the correlation analysis for the Cyril watershed are shown in Table 5.12. Table 5.13 shows the correlation among the input parameters for the Cement watershed. The correlation of S with other parameters is not shown in these Tables. S is derived from CN, and hence its correlation will be similar to that shown for CN.

The correlation analysis shows that rainfall, CN, slope, and K factors are highly correlated. In the parameter estimation process, rainfall was the only input variable, and the values of CN, slope and K factor were adjusted to get the best estimates of parameters that met the objective function given by Equation 4.17. For the Cyril watershed, the maximum and minimum correlation between CN-slope was -0.99, and -0.28, respectively.

130

Table 5.12. Correlation among the estimated parameters for Cyril watershed

	Rainfall	Slope	CN	K
3/27/96				
Rainfall	1			
Slope	-0.99	1		
CN	-1	0.99	1	
K	-0.92	0.94	0.94	1
5/31/96				
Rainfall	1			
Slope	-0.9	1		
CN	-0.99	0.92	1	
K	-0.27*	-0.12*	0.15*	1
7/9/96				
Rainfall	1			
Slope	-0.99	1		
CN	-0.97	0.98	1	
K	-0.95	0.96	0.98	1
8/1/96				
Rainfall	1			
Slope	-0.48*	1		
CN	-1	0.47*	1	
K	-0.68	0.91	0.68	1
10/27/96				
Rainfall	1			
Slope	-0.71	1		
CN	-1	0.73	1	
K	-0.73	0.81	0.7	1
11/6/96				
Rainfall	1			
Slope	0.23*	1		
CN	-0.99	-0.28*	1	
K	0.71	0.6*	-0.76	1
Overall				
Rainfall	1			
Slope	-0.14*	1		
CN	-0.93	0.25*	1	
K	0.71	0.8	0.06*	1

* Not significant at α =0.05.

131

Table 5.13. Correlation among estimation parameters for Cement watershed

	Rainfall	Slope	CN	K
3/27/96				
Rainfall	1			
Slope	-0.96	1		
CN	-1	0.96	1	
K	-0.99	0.97	0.99	1
4/21/96				
Rainfall	1			
Slope	-0.98	1		
CN	-1	0.98	1	
K	-0.86	0.87	0.89	1
5/31/96				
Rainfall	1			
Slope	-0.98	1		
CN	-1	0.98	1	
K	-0.91	0.86	0.91	1
7/9/96				
Rainfall	1			
Slope	-0.97	1		
CN	-0.97	0.98	1	
K	-0.89	0.91	0.96	1
10/27/96				
Rainfall	1			
Slope	-0.94	1		
CN	-1	0.95	1	
K	-0.87	0.92	0.89	1
Overall				
Rainfall	1			
Slope	-0.54	1		
CN	-0.97	0.64	1	
K	-0.38	0.73	0.48	1
Radar				
Rainfall	1			
Slope	-0.94	1		
CN	-0.98	0.99	1	
K	-0.92	0.92	0.95	1

The maximum correlation between CN-K, and CN-rainfall were found to be 0.98, and -1.0, respectively. The minimum correlation between these parameter pairs were 0.15, and -0.97, respectively. Although there is a one to one correlation between rainfall and CN for a fixed runoff, the relation between rainfall and CN is nonlinear. A high correlation between optimized CN and rainfall was expected. The maximum correlation between slope-rainfall and slope-K were -0.99, and 0.96, respectively. The minimum correlation between these parameter pairs were 0.23, and -0.12, respectively. The maximum and minimum correlation between rainfall-K factor were -0.95, and -0.27, respectively.

A t-test was performed to see if the correlation coefficients among the parameters were significantly different from zero. The t-test assumes the data to be normally distributed. Because some of the parameters may not have a normal distribution, the results obtained here are approximations of the true results. Nevertheless, it gives an idea about the association among different parameters. Table 5.12 shows that for the Cyril watershed, the correlation between K-rainfall, K-CN, and K-slope was not significantly different from zero (α=0.05) for rainfall on 5/31/96. The correlation between slope-rainfall, and slope-CN was not significant (α=0.05) for the rainfall on 8/1/97. Slope-rainfall, slope-CN, and K-CN were not significantly correlated (α=0.05) for the rainfall event that occurred on 11/6/96.

For the Cement watershed, the maximum correlation between CN-rainfall, CN-slope, and CN-K factor was, -1.0, 0.98, and 0.99, respectively. The corresponding minimum correlation between these parameters were -0.97, 0.95, and 0.88, respectively. Slope-rainfall and slope-K factor had a maximum correlation of -0.98, and 0.97, respectively. The minimum correlation between these parameters were -0.94, and 0.88, respectively. Rainfall-K

133

factor had a maximum and minimum correlation of -0.99, and -0.86, respectively. For the Cement watershed, all correlation coefficients were significantly different from zero (α=0.05) for all events analyzed (Table 5.13).

In AGNPS, land slope is used to calculate the amount of sediment and nutrients eroded within each cell and the subsequent routing of the sediment and nutrients from each cell to the watershed outlet. A high significant negative correlation between slope-rainfall means for a given amount of sediment and nutrient transported at the watershed outlet, if the rainfall is higher, slope should be lower, and vice-versa to predict the sediment/nutrient transport equal to the observed output. The K factor is used in the Universal Soil Loss Equation (USLE) to calculate the amount of sediment and nutrients eroded at each cell. A high correlation between slope-K factor was expected.

The correlation among the parameters for the six events combined together for the Cyril watershed and for five events for the Cements watershed were calculated. The correlation among parameters for all events in the Table 5.12 were based on 46 different estimates for each parameter. The correlations among parameters shown for all events together were derived from 77 parameter estimates. Tables 5.12 and 5.13 show that the correlations were less when the parameters for all events were combined together. For the Cyril watershed only CN-rainfall, and slope-K were significantly correlated (α=0.05). All parameters were significantly correlated (α=0.05) for the Cement watershed (Table 5.11).

In general, rainfall, CN, slope, and K factors were highly correlated for all events analyzed for both watersheds. This correlation is a major contributor to the difficulty of estimating parameters for H/WQ models. A high correlation between two parameters means

that one parameter can not be estimated without adjusting the value of other. At the same time there can exist a large number of combinations that will give similar outputs.

5.3.5 Probability structure of the estimated parameters

Probability plots of estimated parameters for all events for the Cement watershed are shown in Figures 5.10-5.12. The assumption made in the probability plotting was that the individual observations are independent of each other and that the sample data obtained here are representative of the population. Figures 5.10 and 5.11 show that the estimates of the slopes and the K factors are not normally distributed. Retention parameter (S) is plotted on a lognormal scale (Figure 5.12) because S is assumed to have a lognormal distribution. It shows that the estimated S does not follow a lognormal distribution. The total number of data points available for all events ranged from 13 to 17. These numbers of data points are relatively small to show the probability distribution function of the parameters.

In all figures, the probability on the Y-axis represents the percent cumulative probability that a value of the parameter obtained will be less than a given value. Mathematically it can be represented as $P(X \leq x)$. Here X is the parameter for which the cumulative probability is desired and x is the value of the parameter. The probability of getting the parameter estimate less than or equal to the true parameter value can be calculated. If this probability is less than 0.5, then it can be concluded that the parameter was overestimated using the rainfall observed at a majority of the gauges. On the other hand, if the probability is more than 0.50 then the parameter was underestimated for the majority of the gauge rainfall values.

135
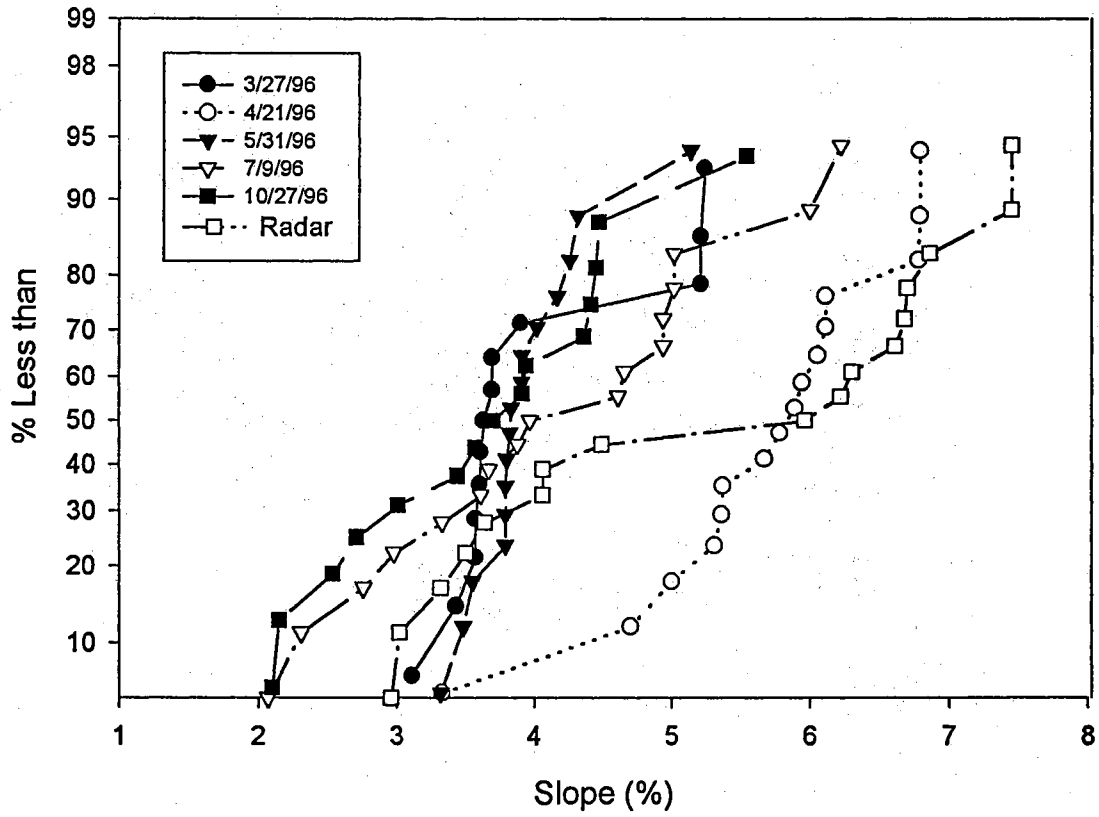
Figure 5.10. Probability plot of estimated slopes for Cement watershed
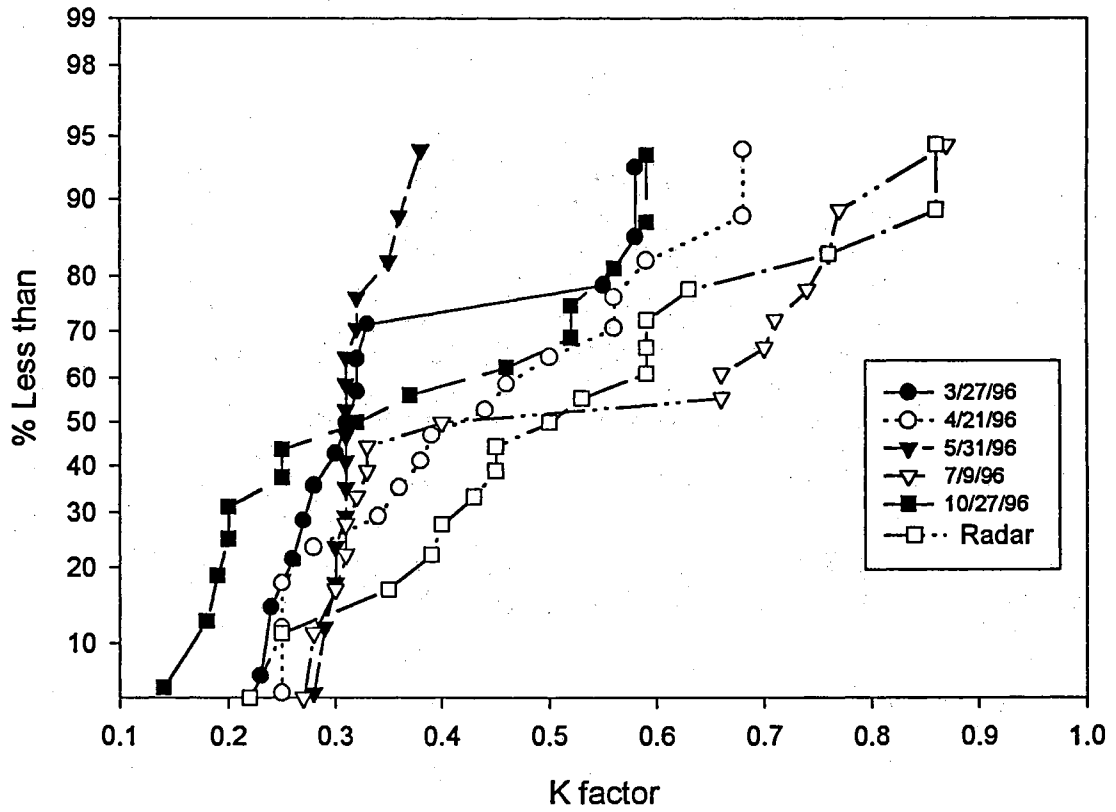
Figure 5.11. Probability plot of estimated K factors for Cement watershed
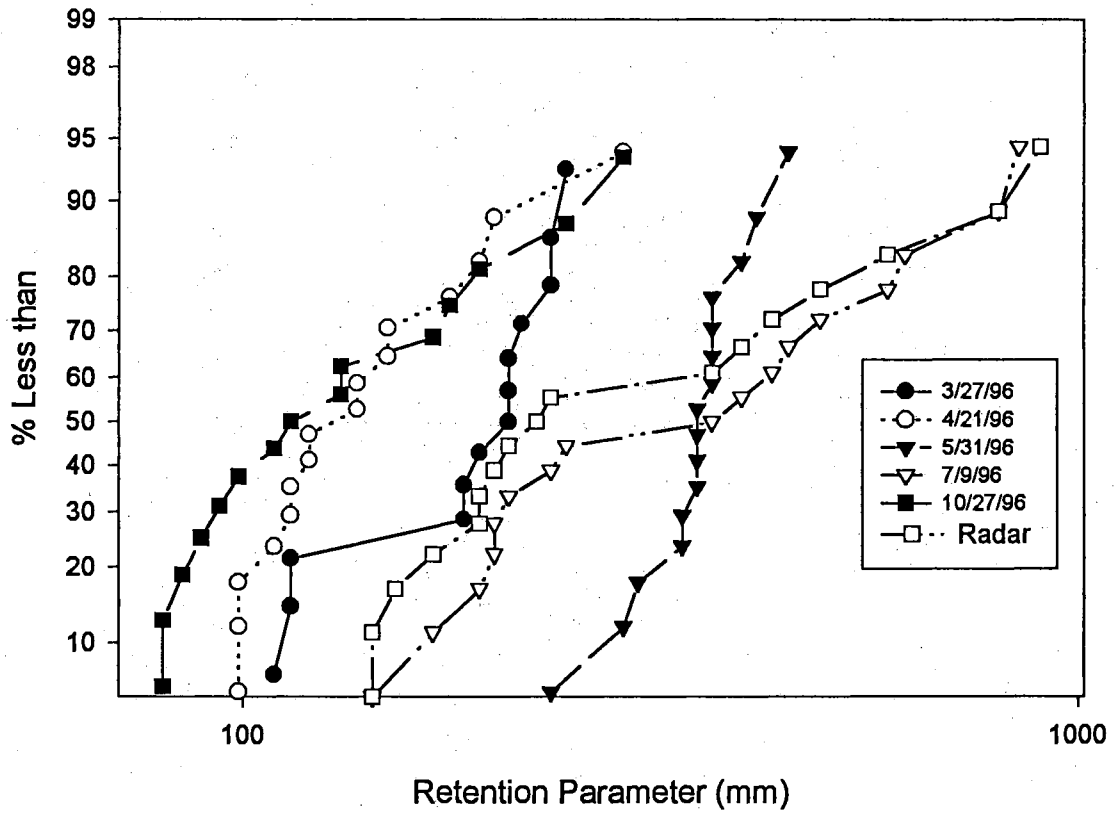
Figure 5.12. Probability plot of estimated retention parameters for Cement watershed

Figure 5.10 shows that the probability of estimating a slope less than the true slope (3.71%) is greater than 0.50 for the rainfalls on 3/27/96 and 10/27/96. It means that for a rainfall pattern like this slope will be underestimated using the rainfall observed at majority of the gauges. For the other events analyzed, Figure 5.10 shows that the probability of estimating a slope less than the true slope is less than 0.50 and the slope is overestimated using the rainfall observed at the majority of the gauges.

The true parameter value for the K factor was 0.33. Figure 5.11 shows that K factor is overestimated for the rainfalls on 4/21/96 and 7/9/96 using the rainfall at a majority of the gauges. For the other events, the K factor is underestimated. The base values for the retention parameter were 188, 144, 351, 410, and 139 mm, respectively, for the rainfalls on 3/27/96, 4/21/96, 5/31/96, 7/9/96, and 10/27/96. The retention parameter was overestimated for the rainfall on 3/27/96, and underestimated for the rainfalls on the other events when the rainfall at each gauge location was used, one at a time, to estimate the parameter.

5.3.6 Model Parameter Uncertainty Obtained with Radar Rainfall Data

For the rainfall on 7/9/96, the variability induced in estimated parameters due to rainfall spatial variability is shown in Table 5.14 when the true rainfall pattern was captured using radar. The results presented here are based on the 17 sets of different parameter values each corresponding to the calibrated rainfall at gauge locations. The average CN, S factor (mm), slope (%), and K factor obtained were 44, 390, 5.02, and 0.49, respectively. A comparison of the statistics of estimated parameters obtained from radar data and from raingauge data shows that the average, range, C.V., standard error, average error, and relative

139

error were larger for estimated CN and slope when the parameter estimates were obtained using the radar data (Tables 5.7 and 5.14). For retention factor (S), the average was less when radar rainfall was used. The range and C.V. in radar-scanned rainfall was higher than the corresponding values obtained when the rainfall variability was captured using raingauges alone. When compared with the error estimates from raingauge data, a higher variability in the radar-scanned rainfall resulted in a higher variation and errors in the estimated parameters. For the K factor, the average and range were larger when the radar rainfall was used. The C.V., standard error, average error, and relative error in estimated K were very similar when the radar rainfall was used.

Although the average rainfall for the watershed using the radar was very similar to the area-weighted rainfall obtained from gauges alone, the average CN, retention factor, and slope were different. The estimates of average CN, slope and K factor were larger than the corresponding estimates obtained using data from gauges alone. Table 4.6 shows that the observed values of total sediment, sediment-attached N, and sediment-attached P were higher when the radar data was used. When the parameters were estimated using these higher observed values, the average parameter values had to be higher to minimize the objective function defined by Equation 4.17. A larger range in the rainfall resulted in a larger range in the estimated parameters

Table 5.14 Parameter variability induced by rainfall spatial variability
with radar measurement of rainfall

Statistic	CN	S factor (mm)	Slope (%)	K factor
Average	44	390	5.02	0.49
Range	22-64	143-900	2.96-7.45	0.22-0.86
C.V.	0.64	0.51	0.55	0.7
Std. Error	19.15	303	2.03	0.23
Avg. Error	15.65	268	1.59	0.18
Rel. Error	0.52	0.45	0.43	0.56

Std. Error = standard error; Avg. Error = average error
Rel. Error = relative error

5.4 Effect of Rainfall Spatial Variability on Model Outputs

5.4.1. Uncertainty in the Model Outputs due to Rainfall Spatial Variability

The effect of rainfall spatial variability on model outputs for watersheds Cyril and Cement are shown in Tables 5.15 and 5.16, respectively. For all rainfall events, variability in the measured rainfall resulted in variability in the model outputs based on a fixed set of parameters. Table 5.15 shows that for the Cyril watershed, five of the six events considered had rainfall at some of the gauge locations too small to produce any significant runoff, sediment, and nutrient transport at the watershed outlet.

In case of the modeled runoff volume, the C.V. ranged from 0.52 to 1.82 for the six events. Ranges of C.V. for total sediment, sediment-attached N, and sediment-attached P were 0.34-1.64, 0.56-1.7, and 0.27-1.44, respectively. The smallest C.V. for all outputs was obtained with rainfall on 5/31/96. Rainfall on this date was most uniform in nature as indicated by the lowest C.V. (Table 5.1). For all events, the C.V. in output was larger than the C.V. in the rainfall.

The ranges of SE and RE for runoff volume, total sediment, sediment-attached N, and sediment-attached P are shown in Table 5.15. In general, a larger SE in rainfall resulted in a larger SE in outputs, except for rainfall on 3/27/96. A larger RE in output was associated with a larger RE in input rainfall.

For the Cement watershed, range in C.V. in estimated runoff volume, total sediment, sediment-attached N, and sediment-attached P was 0.5-2.29, 0.43-2.4, 0.36-2.15, and 0.37-2.17, respectively (Table 5.16). For modeled outputs, the smallest C.V. was obtained for rainfall on 5/31/96 which had the smallest C.V. and was most uniform in nature (Table 5.2).

142

The largest C.V. in output occurred on 10/27/96. Table 5.2 shows that this event had the largest rainfall C.V. The range of SE for runoff volume, total sediment, sediment-attached N, and sediment attached P was 0.51-2.54 mm, 211-3930 Mg, 0.04-0.48 kg/ha, and 0.02-0.25 kg/ha, respectively. For all outputs the smallest SE in rainfall resulted in the smallest SE in outputs. The SE in estimated output increased with an increase in rainfall SE. The same result is evident with the relative error. The smallest RE in output occurred on 5/31/96 and was associated with the rainfall with the smallest RE.

Coefficient of variation and RE in estimated outputs were larger than the corresponding C.V. and RE in rainfall for all events. This shows that the uncertainty in estimated runoff, total-sediment, sediment-attached N, and sediment-attached P using a single raingauge as measured by C.V. and RE can be expected to exceed the input rainfall uncertainty. A similar result was reported by Faures et al. (1995) on a small watershed (<5 ha). This has an important implication for parameter estimation during model calibration if a single raingauge is used to measure input rainfall. If the spatial homogeneity of rainfall is assumed during the parameter estimation process, the variation in the modeled outputs could be mistakenly attributed to the model shortcomings.

Table 5.15. Output uncertainty induced by the spatial variability of rainfall in Cyril watershed

Output	Statistic	Output values for rainfall dates					
		3/27/96	5/31/96	7/9/96	8/1/96	10/27/96	11/6/96
Runoff Volume	Observed	0.33	0.76	3.05	4.06	0.15	0.30
(mm)	Average	0.51	1.27	2.03	4.06	1.78	0.25
	Range	0-1.27	0.51-2.29	0-7.37	0-19.8	0-7.62	0-2.03
	C.V.	1.13	0.52	1.42	1.65	1.42	1.82
	Std. Error	0.51	0.76	2.8	6.35	2.79	0.76
	Rel. Error	1.04	0.65	0.85	1.1	13.0	1.41
Total Sediment	Observed	13.9	128	401	67.0	4.99	10.4
(Mg)	Average	16.2	169	233	72.7	34.9	9.43
	Range	0-44.2	110-271	0-732	0-317	1.81-124	0-44.8
	C.V.	1.05	0.34	1.23	1.46	1.24	1.64
	Std. Error	17.8	73.3	350	110	55.5	16.0
	Rel. Error	1.01	0.39	0.68	1.03	7.14	1.06
Sediment-N	Observed	0.02	0.15	0.36	0.09	0.01	0.02
(kg/ha)	Average	0.02	0.18	0.20	0.08	0.04	0.01
	Range	0-0.07	0.12-0.26	0-0.58	0-0.30	0-0.15	0-0.67
	C.V.	1.03	0.26	1.16	1.24	1.12	1.7
	Std. Error	0.02	0.06	0.27	0.09	0.06	0.02
	Rel. Error	0.89	0.28	0.63	0.8	3.9	0.83
Sediment-P	Observed	0.01	0.07	0.18	0.04	0.01	0.01
(kg/ha)	Average	0.01	0.09	0.10	0.04	0.02	0.01
	Range	0-0.03	0.07-0.13	0-0.29	0-0.15	0-0.07	0-0.03
	C.V.	0.99	0.27	1.16	1.25	1.06	1.44
	Std. Error	0.01	0.02	0.13	0.04	0.03	0.01
	Rel. Error	0.82	0.29	0.62	0.81	3.96	0.87

Std. Error = standard error; Rel. Error = relative error

144

Table 5.16. Output uncertainty induced by the spatial variability of rainfall in Cement watershed

Output	Statistic	output values for rainfall dates				
		3/27/96	4/21/96	5/31/96	7/9/96	10/27/96
Runoff Volume	Observed	0.51	0.76	3.05	1.52	0.25
(mm)	Average	0.51	1.02	2.03	1.52	0.25
	Range	0-1.27	0-6.10	0.25-4.32	0-9.14	0-1.52
	C.V.	0.75	1.56	0.5	1.84	2.29
	Std. Error	0.51	1.52	1.52	2.54	0.51
	Rel. Error	0.67	1.15	0.41	1.27	1.09
Total Sediment	Observed	242	443	3390	2370	68.0
(Mg)	Average	282	267	2760	2450	93.4
	Range	0-621	9-1610	398-5240	0-13580	0-802
	C.V.	0.76	1.54	0.43	1.65	2.4
	Std. Error	211	436	1320	3930	219
	Rel. Error	0.75	0.82	0.3	1.23	1.82
Sediment-N	Observed	0.07	0.10	0.53	0.39	0.02
(kg/ha)	Average	0.07	0.06	0.44	0.34	0.02
	Range	0-0.13	0-0.29	0.10-0.75	0-1.60	0-0.17
	C.V.	0.71	1.29	0.36	1.47	2.15
	Std. Error	0.04	0.09	0.18	0.48	0.04
	Rel. Error	0.59	0.73	0.25	1.01	1.4
Sediment-P	Observed	0.03	0.06	0.27	0.20	0.01
(kg/ha)	Average	0.03	0.03	0.22	0.17	0.01
	Range	0-0.07	0-0.15	0.04-0.37	0-0.81	0-0.08
	C.V.	0.7	1.24	0.37	1.47	2.17
	Std. Error	0.02	0.04	0.09	0.25	0.02
	Rel. Error	0.61	0.72	0.26	1	1.36

Std. Error = standard error; Rel. Error = relative error

The SE in modeled outputs were less than the SE in rainfall values. It shows that if the uncertainty in the input rainfall value is quantified in terms of SE, this uncertainty will be damped out in the modeled runoff volume, total sediment, sediment-attached N, and sediment-attached P.

In general, a larger range in input rainfall values in a single event resulted in a larger range in modeled runoff volume, total sediment, sediment-attached N, and sediment-attached P transport. When compared with the observed output values, a large variability in the estimated output is evident for all events for both watersheds. All of the events, except on 5/31/96, had rainfall measured by at least one gauge which was too small to produce any significant output. Rainfall input error measured as C.V. and RE resulted in magnified output errors with a fixed set of parameters. Estimated output varied from one to several orders of magnitude when compared with the observed outputs.

Faures et al. (1995) demonstrated that the use of the data from the non-recording gauges could improve the results of the modeled runoff when only one recording gauge was available for the rainfall measurement. The authors suggested that if several gauges were available, their measurements could help reduce the uncertainties resulting from measurement error and spatial variability of rainfall.

5.4.2 Bias in Modeled Output due to Rainfall Spatial Variability

Biases in modeled runoff volume, total sediment, sediment-attached N, and sediment-attached P are shown in Table 5.17. The bias was obtained by taking the difference between the observed output and the average modeled output. For the Cyril watershed, the modeled

average outputs represented are the average of 8 model runs, using rainfall observed at each gauge location one at a time. For the Cement watershed, the modeled average outputs are the average of 17 model outputs, each corresponding to one rainfall at a time. The positive values of bias represent the underestimation and negative values represent the overestimation of the modeled outputs as compared to the observed outputs.

In general, a bias in input rainfall resulted in a bias in model outputs. For both watersheds, the runoff bias was very small for all events analyzed. For the Cyril watershed, the minimum and maximum bias in total sediment was 1.81 Mg and 168 Mg, respectively. The minimum and maximum bias in modeled sediment-attached N was 0 and 0.16 kg/ha, respectively. The corresponding values for sediment-attached P were 0, and 0.08 kg/ha, respectively. For the Cement watershed, the biases in modeled runoff volume, sediment-attached N, and sediment-attached P were also very small. For the sediment transport prediction, the minimum and maximum bias was -25.4 Mg and 632 Mg, respectively. These biases can be compared to the observed outputs shown in Tables 5.15 and 5.16 to assess their importance. The bias in predicted results can be expected to decrease with an increase in the number of raingauges to capture the rainfall pattern.

Table 5.17. Bias in modeled output due to rainfall spatial variability

Rainfall Date	Runoff (mm)	Total Sediment (Mg)	Sediment-N (kg/ha)	Sediment-P (kg/ha)
Cyril Watershed				
3/27/96	0	-2.72	0	0
5/31/96	-0.51	-40.8	-0.03	-0.02
7/9/96	1.02	168	0.16	0.08
8/1/96	0	-5.44	0.01	0
10/27/96	-1.52	-29.9	-0.03	0.02
11/6/96	0	1.81	0.01	0
Cement Watershed				
3/27/96	0	-39.9	0	0
4/21/96	-0.25	176	0.04	0.02
5/31/96	1.02	632	0.09	0.04
7/9/96	0	-84.4	0.06	0.03
10/27/96	0	-25.4	0	0

5.4.3 Relative Errors in Modeled outputs due to Rainfall Spatial Variability

Relative errors in modeled runoff volume, total sediment, sediment-attached N, and sediment-attached P are shown in Table 5.18 for the Cyril watershed. Outputs were obtained by running the AGNPS model with the calibrated parameter values and rainfall observed at each gauge location, one at a time. For the Cyril watershed, for each rainfall event eight sets of outputs were obtained, each corresponding to the rainfall observed at one gauge location. Thirteen to 17 sets of outputs were obtained for the Cement watershed for each rainfall event. The maximum and minimum relative errors shown in Table 5.18 represent the maximum and minimum relative error from the eight sets of outputs for each rainfall event. Table 5.19 represent the maximum and minimum error obtained from 13 to 17 different sets of output for each rainfall event. The maximum relative errors in runoff volume, total sediment, sediment-attached N, and sediment-attached P were 49.1, 24.1, 12, and 12.1, respectively. All of these values were obtained on 10/27/96 at the gauge 153. Area-weighted average rainfall for this event was 12.4 mm. Rainfall depth recorded at gauge 153 was 38.4 mm. This represents more than 300% more rain than the area-weighted average rainfall depth. The relative error in the rainfall depth at this gauge location was the highest for all the rainfall events analyzed. The largest relative error in rainfall resulted in the largest output error. For other events, the maximum relative error was considerably smaller than the relative error on 10/27/97. When no rainfall was recorded at a gauge location, the relative error at that location was one.

Table 5.18. Relative errors in modeled outputs due to rainfall spatial
variability for the Cyril watershed

Rainfall Date	Output	Relative Error	
		Maximum	Minimum
3/27/96	Runoff Volume	2.54	0.03
	Total Sediment	2.17	0.14
	Sediment-N	2	0
	Sediment-P	1.52	0.11
5/31/96	Runoff Volume	2.07	0
	Total Sediment	1.11	0.01
	Sediment-N	0.77	0
	Sediment-P	0.82	0
7/9/96	Runoff Volume	1.42	0.45
	Total Sediment	1	0.28
	Sediment-N	1	0.22
	Sediment-P	1	0.23
8/1/96	Runoff Volume	3.87	0.33
	Total Sediment	3.73	0.11
	Sediment-N	2.38	0.13
	Sediment-P	2.46	0.09
10/27/96	Runoff Volume	49.2	0.05
	Total Sediment	24.1	0.04
	Sediment-N	12	0
	Sediment-P	12.1	0.04
11/6/96	Runoff Volume	5.53	0.45
	Total Sediment	3.28	0.3
	Sediment-N	2	0
	Sediment-P	2.2	0.23

Table 5.19. Relative errors in modeled outputs due to rainfall spatial
variability for the Cement watershed

Rainfall Date	Output	Relative Error	
		Maximum	Minimum
3/27/96	Runoff Volume	1.42	0.16
	Total Sediment	1.57	0.15
	Sediment-N	1	0.17
	Sediment-P	1.13	0.12
4/21/96	Runoff Volume	6.74	0.04
	Total Sediment	2.64	0.07
	Sediment-N	1.89	0
	Sediment-P	1.81	0.06
5/31/96	Runoff Volume	0.91	0.03
	Total Sediment	0.88	0.07
	Sediment-N	0.81	0.04
	Sediment-P	0.82	0.05
7/9/96	Runoff Volume	5.39	0.16
	Total Sediment	4.73	0.17
	Sediment-N	3.09	0.14
	Sediment-P	3.05	0.13
10/27/96	Runoff Volume	3.47	0.38
	Total Sediment	10.74	0.29
	Sediment-N	6.5	0
	Sediment-P	6.16	0.24

The minimum relative errors in runoff volume, total sediment, sediment-attached N, and sediment-attached P were 0, 0.01, 0, and 0, respectively. The relative error in rainfall at these gauge locations was very close to zero. In other words, the rainfall depths observed at the gauge locations corresponding to the minimum output error were very similar to the area-weighted average rainfall value.

For the Cement watershed, the relative errors in predicted outputs due to the rainfall spatial variability are shown in Table 5.19. The maximum relative errors in predicted runoff volume, total sediment, sediment-attached N, and sediment-attached P were 6.74, 10.74, 6.5, and 6.16, respectively, for all events analyzed. The maximum relative error in runoff volume occurred at gauge location 163 on 4/21/96. The rainfall relative error in total sediment, sediment-attached N, and sediment-attached P occurred at the gauge 133 on 10/27/96. This gauge also observed the maximum rainfall relative error and the maximum rainfall depth for the event.

The smallest relative errors in runoff volume, total sediment, sediment-attached N, and sediment-attached P were 0.03, 0.07, 0, and 0.05, respectively. The corresponding rainfall relative errors were 0.03, 0.29, 0.29, and 0.29, respectively. The minimum relative error in runoff volume occurred on 5/31/96 at gauge 153. The rainfall relative error at this gauge location was not minimum for the event. The smallest relative error in total sediment, sediment-attached N, and sediment-attached P occurred at gauge 155 on 4/21/96. Here again the rainfall relative error at this gauge location was not minimum. For the Cement watershed, the rainfall minimum relative error did not result in the output minimum relative error. For example, a rainfall relative error very close to zero was observed at gauge 154 on 4/21/96.

However, this rainfall did not produce the minimum output relative error. A gauge-observed rainfall higher than the area-weighted rainfall was needed to get the minimum output relative error. This may have been due to the routing of the output from cell to cell, and subsequently to the watershed outlet. When the model was run using the correct parameter values and true rainfall pattern, the output observed was termed as the observed output in the case of total sediment, sediment-attached N, and sediment-attached P. The area-weighted average rainfall was obtained from the true rainfall pattern. When the model was run, assuming the rainfall to be spatially homogeneous and using area-weighted rainfall depth, the runoff volume, total sediment, sediment-attached N, and sediment-attached P were lower than the observed values. It may be because (1) weighted average rainfall averages out the spatial variability of rainfall, and (2) a watershed responds to a spatially distributed input of rainfall rather than a spatially averaged input. This may also come from the non-linearity of the model under consideration. Assuming that the output modeled by Equation (3.28) is non-linear in terms of input I, and parameters P, the average response of the non linear systems will not be equal to the average of the responses evaluated at average input parameter values. Mathematically it can be represented as

$$\bar{O} \neq f(\bar{I}, \bar{P}, t) \tag{4.22}$$

where $\bar{O}$ is the modeled average output, $\bar{I}$ is the average input values and $\bar{P}$ is the average parameter values. In other words, the expected value of the output is not equal to the functional relationship of the expected values of the input variables.

153

This shows if the spatial homogeneity of the rainfall is assumed, a rainfall greater than the area-weighted rainfall is needed to produce the output similar to the observed output for a fixed set of parameters. However, when the sum of relative errors in runoff volume, total sediment, sediment-attached N, and sediment-attached P was considered, rainfall similar to the area-weighted rainfall produced the minimum total relative error in two of the five events analyzed for the Cement watershed. For other events also it gave a relatively better result.

However, the same result was not true for the Cyril watershed. A gauge-measured rainfall very similar to the area-weighted average rainfall produced the minimum relative error in all of the predicted outputs. The sum of the relative errors in the predicted outputs was also minimum for the gauge-observed rainfall values similar to the area-weighted rainfall depth. This shows that with an increase in the size of the watershed, a rainfall higher than the area-weighted average rainfall is needed to produce a given output for a fixed set of parameters. A similar result was evident in the case of the estimated parameters. For the Cement watershed, for a given output a rainfall higher than the area-weighted rainfall was needed to produce the parameter estimates similar to the true parameter values.

Similar relative errors in the model outputs are reported in a limited number of studies conducted using spatially variable rainfall inputs. Faures et al. (1995) reported that even for a very small watershed (<5 ha), spatial variability in input rainfall could translate into a large variation in the modeled runoff. The C.V. in runoff rate was found to range from 2 to 65% when five model outputs were obtained using input from one of the five recording gauges, one at a time. Goodrich (1995) reported a relative variation in modeled runoff volume up to 0.43

154

when two gauges were used independently as input for a runoff model in three small catchments 0.4 to 4.4 ha in size.

Young et al. (1992) applied a spatially variable synthetic storm on a 6475 ha watershed. The maximum relative errors in runoff volume, sediment yield, total N, and total P transport predicted by AGNPS were found to be 0.85, 3.26, 3.29, and 5.15, respectively. Luzio and Lenzi (1995) applied grid-based rainfall values on a 77 km^2 watershed. The true rainfall pattern was captured using five raingauges and a spline method of interpolation. The authors reported maximum relative errors in predicted runoff volume, total sediment, total N, and total P as 0.84, 0.17, 0.21, and 0.19, respectively, using the AGNPS model. The main difference between this study and the research reported by Young et al. (1992) and Luzio and Lenzi (1995) is the size of the watershed and number of gauges available to capture the rainfall spatial variability. The results reported by Young et al. (1992) were based on the synthetic rainfall data. Synthetic rainfall data may not model the patterns and amounts of real rainfall adequately. In addition, because of the local configuration and site measurement problems of real gauges, there is a causal relationship between rainfall and stream flow which may not be modeled in the synthetic situation (Hamlin, 1983). The study of Luzio and Lenzi was based on a small watershed with a small number of gauges available to measure the true rainfall pattern. In this study a larger number of raingauges were available to measure the true rainfall pattern. The results of this study indicate that the rainfall spatial variability increases with an increase in the watershed size. Since the errors in the modeled outputs are magnified when an erroneous rainfall from observation made at a single gauge location is input, the results obtained by Luzio and Lenzi (1995) may not be generalized for larger watersheds.

The variability in the modeled runoff volume, total sediment, sediment-attached N, and sediment-attached P was significantly larger than the variability reported by Faures et al. (1995) and Luzio and Lenzi (1995). This could be a better representation of the relative errors in the predicted output for a watershed size studied in this research. This variability can be expected to increase with an increase in the watershed size because the rainfall variability increases with watershed size and the rainfall input error is magnified in the modeled outputs.

5.4.4. Impact of Gauge Location on Output Uncertainty

Troutman (1983) reported that one source of uncertainty in the model outputs may be the lack of information about the location of storm center. When the rainfall information at only a single gauge is available, it is not known whether the overall storm magnitude was small or whether the storm was large with a center located at some distance from the gauge. The author speculated that this could result in considerable error in predicted runoff, especially if the gauge was not centrally located. Based on the simulation results from a 25.1 km^2 watershed, Dawdy and Bergman (1969) reported that the most representative gauge was that closest to the center of the basin; the least representative was on the perimeter and at the highest elevation of the basin.

In this research, the effect of gauge location on model predictions was analyzed for the Cyril and the Cement watersheds. The sum of relative errors in predicted runoff volume, total sediment, sediment-attached N, and sediment-attached P was considered. The sum of the relative errors was termed the total error.

156

For the Cyril watershed, the minimum total error was obtained for the gauge 149 on 3/27/96. Figure 5.2 shows that this gauge is not centrally located within the watershed. For the rainfall on 5/31/96 the minimum total error occurred at gauge 150. The total errors at gauges 131, 150, and 151 were considerably less than the total errors at other gauge locations. For rainfall on 7/9/96, relatively lower total errors were obtained at gauges 130, 150, and 151. Gauge 130 had the minimum total error for this event. Gauges 130 and 131 on 8/9/96 and gauge 150 on 10/27/96 had the minimum total error, respectively. For the rainfall on 11/6/96, gauge 131 had the minimum total error. The centrally located gauge (151) had the minimum total error for only two of the six events analyzed.

For the Cement watershed, the gauges located within the watershed are 131, 148, 149, 150, 153, and 154 (Figure 4.6). For rainfall on 3/21/96 the minimum total error was observed at gauge 154. Gauges 149 and 153 also had relatively lower total errors. The maximum total error was observed at gauge 130. The minimum and maximum total error on 4/21/96 occurred at gauges 155 and 163, respectively. Figure 4.6 shows that neither of these two gauges is located within the watershed. In fact gauge 155 is the farthest gauge from the center of the watershed. Gauges 147 and 152 observed the minimum total error on 5/31/96. These gauges are also not located within the watershed, although for this event, gauge 153 also had relatively lower total error. For the rainfall on 7/9/96, gauge 134 had the lowest total output error. Gauge 149 showed the minimum total error on 10/27/96.

In general for the two watersheds, the gauges located within the watershed had relatively smaller total error in predicted outputs. The minimum total error did not always occur at the gauge located at the center of the watershed. At least for one event, a gauge

157

located outside the watershed area had a better predicted output than the gauges located within the basin. The representativeness of the gauge will depend upon the size of the watershed as well as on the size and orientation of the storm event. Based on the results of this study no definite conclusion can be made regarding the best location of a gauge if the rainfall is measured using only one gauge. In the midst of the rainfall spatial variability, it will be better to capture the rainfall spatial variability using more than one gauge. If several gauges are available to measure rainfall, and model outputs are obtained using the rainfall observed at each gauge location, one at a time, the average of the multiple realizations of the outputs for each event will also improve the accuracy of the predicted results.

5.4.5 Model Output Uncertainty Obtained with Radar Rainfall Data

The effect of rainfall spatial variability on modeled outputs is shown in Table 5.20 when the true rainfall pattern was captured by radar. The third column represents the results of the model simulation when the rainfall data at the 17 gauge locations were used, one at a time. The calibrated radar rainfall had 43 different rainfall values. Some of these values were observed at the cells where no gauge was available. The last column in Table 5.20 shows the model results when all different rainfall values from the calibrated radar were used to predict output, one at a time. Here the outputs were obtained by running the model using rainfall observed at each gauge location, one at a time. The parameters used were the true parameter values. The true estimate of CN was obtained by calibrating the model for CN using calibrated radar rainfall and observed runoff volume. True values of slopes and K factors were obtained from the observed watershed characteristics.

Table 5.20 Output uncertainty induced by spatial variability of rainfall when radar data was used

Output	Statistic	Estimated outputs using	
		17 gauges	Radar rainfall
Runoff Volume	Observed	1.52	1.52
(mm)	Average	1.02	1.78
	Range	0-6.60	0-18.8
	C.V.	2.01	2.22
	Std. Error	1.78	4.06
	Rel. Error	1.06	0.04
Total Sediment	Observed	3340	3340
(Mg)	Average	2050	3570
	Range	0-12760	0-31230
	C.V.	1.84	2.03
	Std. Error	3890	7150
	Rel. Error	1.01	0.11
Sediment-N	Observed	0.53	0.53
(kg/ha)	Average	0.28	0.43
	Range	0-1.52	0-3.13
	C.V.	1.65	1.85
	Std. Error	0.52	0.77
	Rel. Error	0.89	0.22
Sediment-P	Observed	0.26	0.26
(kg/ha)	Average	0.15	0.21
	Range	0-0.76	0-1.57
	C.V.	1.65	1.85
	Std. Error	0.26	0.39
	Rel. Error	0.89	0.11

Std. Error = standard error; Rel. Error = Relative error

The minimum estimates of runoff volume, total sediment, sediment-attached N, and

sediment-attached P were zero. At least 15 of the 43 different rainfall values from the

calibrated radar rainfall were too small to predict any significant output with AGNPS. Six

of these rainfall values were observed at different gauge locations. Average, range, C.V., and

standard error for all the outputs were larger when all the different rainfall values were used

to estimate the outputs. Output uncertainty, when measured in terms of the relative error, was

less for all of the outputs when all different rainfall values were used. The variability in the

rainfall as measured by C.V. and range was larger when all 43 different rainfall values were

used. This larger variability in the rainfall field resulted in larger average, range, and C.V.

in all estimated outputs.

Table 5.21 shows the bias in the modeled runoff volume, total sediment, sediment-

attached N, and sediment-attached P when using the calibrated radar data. In general the bias

in the modeled outputs decreased when the outputs were obtained by running the model using

all the different rainfall values. This shows that as the number of gauges available to capture

the rainfall pattern increases, the bias in the modeled outputs decreases.

Table 5.21. Bias in estimated parameters with calibrated radar data

Output	Bias obtained using	
	17 gauges	Radar rainfall
Runoff Volume (mm)	0.51	-0.25
Total Sediment (Mg)	1280	-234
Sediment-N (kg/ha)	0.25	0.1
Sediment-P (kg/ha)	0.11	0.04

The maximum relative errors in runoff volume, total sediment, sediment-attached N, and sediment-attached P were 12.1, 8.4, 4.9, and 5.1, respectively. All of these errors occurred at one location where the rainfall observed was maximum for the event. The relative error in rainfall at this location was 1.93. The corresponding minimum errors for these outputs were 0.08, 0.07, 0.06, and 0.04, respectively. The rainfall errors at these locations were 0.52, 0.46, 0.46, and 0.46, respectively. The minimum output errors were not associated with the minimum rainfall errors for all outputs.

The output uncertainty due to rainfall spatial variability is shown in Table 5.16 when the true rainfall pattern was captured using the rainfall observed at 13 gauges and Theissen polygon method. The comparison of the outputs obtained using the two estimates of true rainfall pattern shows that a larger variability in the outputs, as indicated by C.V., is obtained when calibrated radar rainfall is used. This may have resulted from the fact that the range and C.V. of the true rainfall pattern were larger when the rainfall variability was captured using calibrated radar data. This difference can be expected to decrease with an increase in the number of gauges available to capture the rainfall. For example, in the case of radar scanned rainfall, if the raingauges were located at each cell in the rainfall field where a different rainfall value was observed, the results obtained from the raingauge data would be similar to the results from the calibrated radar data. However, installation and maintenance of such a high density of raingauge network would be cost prohibitive. In that case, the radar-scanned rainfall field calibrated with the raingauge data would be an ideal resort to capture the true rainfall pattern for application in H/WQ models.

CHAPTER 6

SUMMARY, CONCLUSIONS, AND RECOMMENDATIONS

6.1 Summary

Impact of various agricultural activities on surface water quality has been reported to be a serious problem. One of the most convenient ways to study the pollution of surface water from agricultural activities is the use of hydrologic/water quality (H/WQ) models. Historically, in the application of H/WQ models, rainfall is assumed to be a homogeneous process and is assumed not to contribute to parameter and output uncertainty. Consequently, a single rainfall depth is input in the models. With the advent of modern precipitation measurement techniques like radar and dense networks of raingauges, it is now known that rainfall is not spatially uniform, but it varies from place to place. This spatial variability in the rainfall may introduce significant errors in model parameters and outputs when the spatial homogeneity of rainfall is assumed in the application of H/WQ models.

The overall goal of this study was to assess the variability induced in H/WQ model parameters and outputs solely due to the spatial variability of rainfall. This will help isolate the variability in the model parameters/outputs caused by the spatial variability of rainfall which is otherwise assumed to be a homogeneous process and is usually assumed not to contribute to the model parameter/output uncertainty.

This study was conducted on the Little Washita basin. Two subwatersheds of area 30.6 km² and 159 km², known as Cyril and Cement watersheds, were delineated and used. A dense network of 42 raingauges, known as a Micronet, is operated within the Little Washita basin. In addition, the stream flow data were obtained from the USGS. The H/WQ model used was the Agricultural Non-Point Source Pollution (AGNPS) model. It is an event-based, distributed parameter model that simulates surface runoff, sediment and nutrient transport primarily from agricultural watersheds. The model was modified to input grid-based rainfall and energy intensity values. The WATERSHEDSS GRASS-AGNPS modeling tool was used to generate the input file for the model.

Six rainfall events in 1996 were selected and used with the Cyril watershed. The total number of rainfall events used with the Cement watershed was five. The outputs considered were runoff volume, total sediment transport, sediment-attached N, and sediment-attached P. Curve Number (CN), land slope, and USLE K factor were the model parameters selected for the study based on the sensitivity analysis of the model.

The only observed data were the rainfall and runoff volume. The uncertainty induced in the model parameters/outputs was estimated in two steps. In the first step, grid-based rainfall depths, considered as the true rainfall pattern, were captured using the Theissen polygon method. AGNPS was calibrated for CN based on observed runoff and true rainfall pattern. All other model parameters were estimated using observed watershed characteristics. The outputs obtained using the true rainfall pattern and calibrated parameters were termed as 'observed' outputs.

In the second step, parameter and output uncertainty due to spatial variability of rainfall was estimated. It was assumed that each of the raingauges was the only raingauge available and the rainfall depth was homogeneous across the watersheds. Model parameters were estimated using the rainfall observed at each gauge location, one at a time, and the 'observed' outputs. For each rainfall event, eight sets of parameters for the Cyril watershed and 17 sets of parameters for the Cement watershed were obtained.

Uncertainty in the model output was estimated by running the model using rainfall observed at each gauge location, one at a time, assuming that the rainfall was homogenous across the watershed. The calibrated values of parameters for each rainfall were used. For each rainfall event, eight sets of outputs for the Cyril watershed and 17 sets of outputs for the Cement watershed were obtained. The variability observed in the model parameters and outputs was termed the parameter/output uncertainty.

NEXRAD rainfall data were obtained for the rainfall on 7/9/96 and 7/10/96 from the WSR-88D radar located at Twin Lakes, Oklahoma. This rainfall was calibrated using the data from the Micronet stations. Calibrated radar rainfall data were then used as the input in the AGNPS model and the model parameter/output uncertainty due to rainfall spatial variability was estimated when the true rainfall pattern was captured using the radar data. The methods outlined in the previous sections were used.

A summary of the findings related to each objective of this study are discussed in the following sections.

Objective 1. To combine raingauge and radar data to capture spatial variability of rainfall.

The calibration factor of radar rainfall at each gauge location was determined. The calibration factor ranged from 0.08 to 7.45. For the rainfall on 7/9/96, the radar underestimated the rainfall at seven gauge locations and overestimated it at six gauge locations. For the rainfall on 7/10/96, the radar underestimated the rainfall at all gauge locations. The results from the comparison of raingauge data to the radar data indicate the need for the calibration of radar-scanned rainfall before it can be applied in H/WQ models. However, after the radar rainfall was calibrated, the area weighted rainfall from the radar data was very similar to the area weighted rainfall obtained using a network of 13 raingauges and the Theissen polygon method. The variability in the radar rainfall was larger than the corresponding variability when the rainfall was captured using the raingauges alone. It shows that when only a limited number of raingauges are used to capture the rainfall, the observed variation in the rainfall may be lower than the true variation.

Objective 2. To estimate parameter uncertainty in H/WQ models solely due to the spatial variability of rainfall.

In general, a wide range in estimated parameters resulted when the rainfall measured at each gauge location was used individually, one at a time, to estimate the model parameters. A larger range in the rainfall values within a single event resulted in a higher range in all estimated parameters. The smallest parameter uncertainty resulted from the rainfall that was most spatially homogeneous in nature. The variations were very large when compared to the

166

true parameter values. For slope, K, and retention parameter the range was several orders of magnitude for some events for both watersheds. Traditionally, variability in the estimated parameters is considered as the model uncertainty because the models are simplified descriptions of the processes occurring in the field. Results of this study indicate that even in the case of physically-based distributed parameter models, uncertainty in the parameter estimates would be observed because of the input error coming from the spatial variability of rainfall. To eliminate this input error, a "true" rainfall pattern should be captured and used in H/WQ models.

For the Cyril watershed, the true rainfall pattern was captured using four raingauges. However, the parameter uncertainty was estimated by using the rainfall from eight gauges located within and around the watershed. For the Cement watershed, 13 raingauges were used to capture the true rainfall pattern and 17 raingauges were used to estimate the parameter uncertainty. A bias in the average and area-weighted rainfall resulted in a bias in the estimated parameters. As the number of raingauges used to capture the rainfall increases in a watershed, the bias in the estimated parameters can be expected to decrease.

Relative errors for estimated parameters as compared to the calibrated parameter values were calculated for the two watersheds. For the Cyril watershed, the minimum relative errors were observed at the gauges which recorded a rainfall very similar to the area-weighted rainfall. This result was not true for the Cement watershed. A rainfall larger than the area-weighted rainfall was needed to best estimate the parameters. In general, a gauge located at or near the center of the watershed resulted in a lower total relative error in the parameter estimates.

The correlation analysis among input rainfall and parameters showed that rainfall, CN, slope, K factors were highly correlated. For the Cyril watershed CN-rainfall, and slope-K were found to be significantly correlated when the correlation was estimated for all the parameter estimates combined together for the six events. For the Cement watershed all of the parameters were significantly correlated. This correlation is a major contributor to the difficulty of estimating parameters in H/WQ models. A high correlation between two parameters means that one parameter can not be estimated without adjusting the value of the other.

When the model parameters were estimated using the calibrated radar rainfall, the variability in the estimated parameters was larger as compared to the parameter variability obtained when the true rainfall pattern was captured using gauge data alone. The estimated average CN, slope, and K factor were larger than the corresponding estimates obtained using data from gauges alone. The observed values of the runoff volume, total sediment, sediment-attached N, and sediment-attached P were also higher when the true rainfall pattern was captured by calibrated radar rainfall field.

Objective 3. To study the impact of spatial variability of rainfall on model outputs i.e., runoff, sediment and nutrient losses.

For all events, variability in the measured rainfall resulted in variability in the model outputs based on a fixed set of parameters. Five of the six events considered for the Cyril watershed and four of the five events considered for the Cement watershed had rainfall at some of the gauge locations too small to produce any significant output. Rainfall error

168

measured as C.V. and relative error resulted in magnified output errors. Estimated output varied from one to several orders of magnitude when compared with the observed outputs. In general, a bias in the input rainfall resulted in a bias in the model outputs. This bias can be expected to decrease with an increase in the number of raingauges to capture the rainfall pattern.

For the Cyril watershed, raingauges that resulted in the minimum output relative error had a rainfall very similar to the area-weighted rainfall value. But for the Cement watershed, a rainfall larger than the area-weighted rainfall was needed to produce the minimum output relative error. The maximum relative error in rainfall measurement was associated with the maximum relative errors in model outputs.

In general for the two watersheds, the gauges located within the watershed area had relatively smaller total error in predicted results. The minimum total error did not always occur at the gauge located at the center of the watershed. Based on the results of this study, no definite conclusion could be drawn regarding the best location of a gauge if the rainfall was measured using only one gauge. If several gauges are available to measure rainfall, and the model outputs are obtained using the rainfall observed at each gauge location, one at a time, the average of all the outputs for each event will improve the accuracy of the predicted results.

A larger variability in the outputs as indicated by C.V. was obtained when the true rainfall pattern was captured using calibrated radar data. In general, the bias in the modeled outputs decreased when the outputs were obtained by running the model using all the different rainfall values with the calibrated radar rainfall field. This shows that as the number of

gauges available to capture the rainfall pattern increases, the bias in the modeled outputs decreases.

6.2 Conclusions

The following conclusions were drawn from this study:

1   In the application of H/WQ models, the assumption of the spatial homogeneity of the rainfall may not be valid. The rainfall spatial variation increases with an increase in the size of the watershed. If only one gauge is used to measure the rainfall, the gauge located at the center of the watershed is not always the best representative gauge, although a gauge located at or near the center of the watershed gives a relatively better representation of the area-weighted rainfall.

2   The radar-scanned rainfall may be in error by up to a factor of ten as compared to raingauge rainfall. These data should be calibrated using raingauge data before it is used in H/WQ models.

3   Rainfall data error produces two types of errors in the results. The first is the error in the estimation of an optimum set of parameters. The second type of error introduced is output error.

4   A large uncertainty in the estimated parameters results from the spatial variability of the rainfall. An input rainfall error results in an erroneous estimate of the model parameters.

5   The uncertainty in the estimated parameters using a single gauge, as measured by C.V. and relative error, exceeds the measurement uncertainty. Even in the case of

170

physically-based distributed parameter models, the rainfall uncertainty will result in parameter uncertainty.

6   Spatial variability of rainfall introduces uncertainty into model outputs when rainfall measured at a single gauge is used. A larger range in the input rainfall values in a single event results in a larger range in model outputs.

7   Rainfall variability, when measured in terms of C.V. and relative error, results in larger output errors with a fixed set of parameters.

8   For individual events, a gauge located at the center of the watershed does not always result in the minimum output error.

9   Since the installation and maintenance of a dense network of raingauges may be cost prohibitive, a radar-scanned rainfall field calibrated with the raingauge data should be used to capture the true rainfall pattern for application in H/WQ models.

10   Spatial variability of rainfall should be captured and used in H/WQ models in order to accurately assess the release and transport of pollutants. Since rainfall is a driving force behind many kinds of pollutant release and subsequent transport and spread mechanisms, ignoring this property of rainfall in the application of H/WQ models will put a limit on the accuracy of the model results.

6.3 Recommendations for Future Research

The directions for recommended future research include:

1. The effect of rainfall spatial variability on model parameters/outputs was estimated using the data from the two subwatersheds from the Little Washita basin. Since the rainfall spatial variability increases with the size of the watershed, the data from the entire Little Washita basin should be used. Comparison with similar studies shows that the errors introduced in model parameters and outputs increase with the size of the watershed. The results of this study should be tested with larger watersheds.

2. Application of radar data to capture the rainfall variability is a problem if the radar data is not calibrated. Research should be done to see how many gauges are needed to calibrate the radar data before it can be applied to H/WQ models.

3. Rainfall spatial variability was captured using the Theissen polygon method. A study should be done to assess the effect of rainfall spatial variability on model parameters/outputs by using a better method like kriging or inverse distance method to interpolate the rainfall data at the grid level.

4. The only observed data available in this study was rainfall volume. The sediment and nutrient data were simulated using best estimate of parameters and were assumed as the observed outputs. Research should be conducted using data from a watershed where measured water quality data are available.

5. Only a few outputs and parameters were considered in this research. The effect of rainfall spatial variability on other parameters and outputs should be assessed.

REFERENCES

Agricultural Research Service (ARS). 1991. Hydrology of the Little Washita River Watershed, Oklahoma. USDA Agricultural Research Service Press.

Allred, B., and C.T. Haan. 1996. Small Watershed Monthly Hydrologic Modeling System. Users Manual. Biosystems and Agricultural Engineering Department, Oklahoma State University, Stillwater, OK.

Atlas, D. 1990. Radar in meteorology. American Meteorological Society, Lancaster Press, Lancaster, Pennsylvania.

Atlas, D., C.W. Ulbrich, and R. Meneghini. 1984. The multi-parameter remote measurement of rainfall. Radio Science 19:3-22.

Amorocho, J., and B. Wu. 1977. Mathematical models for the simulation of cyclonic storm sequences and precipitation fields. J. Hydrol. 32:329-345.

Amorocho, J., and A. Brandstetter. 1967. The representation of storm precipitation fields near ground level. J. Geophys. Res., 72:1145-1164.

Arnold, J.G., B.A. Engel, and R. Srinivasan. 1993. A continuous time, grid cell watershed model. Proceedings of the Application of Advanced Information Technologies: Effective Management of Natural Resources Conference. ASAE, St. Joseph, MI.

Battan, L.J. 1973. Radar observations of the atmosphere. Univ. of Chicago Press. Illinois.

Beasley, D.B., L.F. Huggins, and E.J. Monke. 1980. ANSWERS: A model for watershed planning. Trans. ASAE 23(4):938-944.

Bellon, A., and G.L. Austin. 1984. The accuracy of short-term radar rainfall forecasts. J. Hydrology 70: 35-49.

Berndtsson, R., and J. Niemczynowicz. 1988. Spatial and temporal scales in rainfall analysis - some aspects and future perspectives. J. Hydrology. 100:293-313.

Beven, K.J., and G.M. Hornberger. 1982. Assessing the effect of rainfall pattern of precipitation on modeling stream flow hydrographs. Water Resour. Bull., 18(5):823-829.

Brandes, E. 1975. Optimizing rainfall estimates with the aid of radar. J. Appl. Meteorol. 14:1339-1345.

Bras, R.L., and I. Rodriguez-Iturbe. 1976. Rainfall generation: A nonstationary time-varying multidimensional model. Water Resour. Res., 12(3):450-456.

Briggs, B.H., G.J. Phillips, and D.H. Shinn. 1950. The analysis of observations of spaced receivers of the fading of radio signals. Proc. Phys. Soc., London., B63:106-121.

Cain, D.E. and P.L. Smith Jr. 1976. Operational adjustment of radar estimated rainfall with rain gauge data: A statistical evaluation. Prep., Radar Meteorol. Conf. 17th. pp 533-538.

Cole, J.A., and J.D.F. Sheriff. 1972. Some single- and multi-site models of rainfall within discrete time increments. J. Hydrol., 17:97-113.

Collier, C.G. 1986. Accuracy of rainfall estimates by radar, Part II: Comparison with raingauge network.

Corradini, C., and V.P. Singh. 1985. Effect of spatial variability of effective rainfall on direct runoff by geomorphologic approach. J. Hydrol., 81:27-43.

Davis, L.V. 1955. Geology and groundwater resources of Grady and Northern Stephen counties, Oklahoma. Oklahoma Geological Survey Bull. 73, 184pp.

Dawdy, D.R., and J.M. Bergman. 1969. Effect of rainfall variability on stream flow simulation. Water Resour. Res., 5(5):958-969.

Doviak, R.J., and D.S. Zrnic. 1984. Doppler radar and weather observations. Academic Press, Inc.

Eagleson, P.S. 1978. Climate, soil, and vegetation, 2. The distribution of annual precipitation derived from observed storm sequences. Water Resources Res. 14:713-721.

Eagleson, P.S. 1984. The distribution of catchment coverage by stationary rainstorms. Water Resources Res. 20(5):581-590.

Faures, J., D.C. Goodrich, D.A. Woolhiser, and S. Sorooshian. 1995. Impact of small-scale spatial variability on runoff modeling. J. Hydrology 173:309-326.

Felgate, D.G., and D.G., Read. 1975. Correlation analysis of the cellular structure of storms observed by rain gauges. J. Hydrol. 24:191-200.

Filho, A.J.P. 1996. Mesoscale rainfall fields: Analysis and hydrometeorologic modeling. Ph.D. Dissertation. University of Oklahoma, Norman, OK.

Goddard, J.W.F. and S.M. Cherry. 1984. The ability of dual-polarization radar (copolar linear) to predict rainfall rate and microwave attenuation. Radio Science, 19:201-208.

Goodrich, D.C., J Faures, D.A. Woolhiser, L.J. Lane, and S. Sorooshian. 1995. Measurement and analysis of small-scale convective storm rainfall variability. J. Hydrology 173:283-308.

Grayman, W.M., and P.S. Eagleson. 1969. Stream flow record length for modeling catchment dynamics. Hydrodynamics Laboratory, M.I.T., Cambridge, Mass., Rep. No. 114.

Greene D.R., and M.D. Hudlow. 1992. Hydrometeorologic grid mapping procedure. AWRA International Symposium on Hydrometeorology. Dever, Colorado. June 13-17.

Grunwald S., and H. -G Freede. 1996. Using AGNPSm in German watersheds. Unpublished report. Dept. of Natural Resources Management. Div. of Soil and Water Protection, Senckenbergstr.3, D-35390. Giessen, Germany.

Haan, C.T. 1989. Parametric uncertainty in hydrologic modeling. Trans. ASAE 32(1):137-146.

Haan, C.T., B. Allred, D.E. Storm, G.J. Sabbagh, and S. Prabhu. 1995. Statistical procedure for evaluating hydrologic/water quality models. Trans. ASAE 38(3): 725-733.

Haan, C.T., B.J. Barfield, and J.C. Hayes. 1994. Design Hydrology and Sedimentology for Small Catchments. Academic Press, Inc., San Diego, California 92101.

Hamlin M.J. 1983. The significance of rainfall in the study of hydrological processes at basin scale. J. Hydrology. 65:73-94.

Hovind, Y.D. 1965. Estimating the errors for gauge measured precipitation in the United States. J. of Hydraulic Eng. 25:345-402.

Jia, Z. 1994. Real-time flood forecasting using automatic parameter optimization and rainfall projections. Ph.D. Dissertation. Biosystems and Agricultural Engineering Department, Oklahoma State University, Stillwater, Oklahoma.

Knisel, W.G. (ed). 1980. CREAMS: A field-scale model for chemicals, runoff, and erosion from agricultural management systems. Conservation Research Report No. 26. USDA-SEA. Washington, D.C. 643 p.

Krajewski, W.F., 1987. Cokriging of radar-rainfall and rain gauge data. J. Geophysical Res. 92(D8):9571-9580.

Krajewski, F.W., V. Lakshmi, K.P. Grorgakakos, and C.J. Subhas. 1991. A Monte Carlo study of rainfall sampling effect on a distributed catchment model. Water Resour. Res., 27(1):119-128.

Kruizinga, S., and G.J. Yperlaan. 1978. Spatial interpolation of daily totals of rainfall. J. Hydrology 36:65-73.

Lane, L.J., and M.A. Nearing (Eds.) 1989. USDA-Water erosion prediction project: Hillslope profile model documentation. USDA-ARS-NSERL Report No. 2.

Legates, D.R., and C.J. Willmott. 1990. A high resolution climatology of gauge-corrected, global precipitation. Int. J. Clim. 1:111-127.

Liu, C., and W.F. Krajewski. 1996. A comparison of methods for calculation of radar-rainfall hourly accumulations. Water Resources Bulletin 32(2):305-315.

Loukas, A., and M.C. Quick. 1996. Spatial and temporal distribution of storm precipitation in southwestern British Columbia. J. Hydrology 174:37-56.

Luzio, M. D. and M.A. Lenzi. 1995. The importance of proper rainfall inputs for the applicability of the AGNPS model integrated with geographic information system at watershed scale. *In* the proceedings of the International Symposium on Water Quality Modeling.

Ma, S. 1993. Integrating GIS and remote sensing approaches with NEXRAD to investigate the impacts of spatial scaling of hydrologic parameters on storm-runoff modeling. Ph.D. Dissertation. University of Oklahoma Library. Norman, OK.

Majkowski, J., J.M. Ridgeway, and D.R. Miller. 1981. Multiplicative sensitivity analysis and its role in development of simulation models. Ecological Modeling 12:191-208.

Marshall, J.S., W. Hitchfeld, and Gunn, K.L.S. 1955. Advances in radar weather. Adv. Geophysics 2:1-56.

Meadows, M.E., M.M. Kollitz, and J.R. Dickerson. 1994. Characterization and storm water management implications of spatially variable rainfall. Paper No. 942129. American Society of Agricultural Engineers, St. Joseph, MI.

Mejia, J.M., and I. Rodriguez-Iturbe. 1974. On the synthesis of random field sampling form the spectrum: An application to the generation of hydrologic spatial processes. Water Resour. Res., 10(4):705-711.

National Severe Storms Laboratory (NSSL), 1992. "Investigation of NEXRAD storm data with rain gauge data. Unpublished Research Report.

Obled, C., J. Wending, and K. Beven. 1994. The sensitivity of hydrological models to spatial rainfall patterns: an evaluation using observed data. J. Hydrol. 159:305-333.

Osmond, D.L., R.W. Gannon, J.A. Gale, D.E. Line, C.B. Knott, K.A. Phillips, M.H. Turner, M.A. Foster, D.E. Lehning, S.W. Coffey, and J. Spooner. 1997. WATERSHEDSS: A decision support system for watershed-scale nonpoint source water quality problems. J. American Water Resource Association 33(2):327-341.

O'Connell, P.E., and E. Todini. 1996. Modeling of rainfall, flow and mass transport in hydrological systems: an overview. J. Hydrology. 175:3-16.

Pereira, A.J., and K.C. Crawford. 1995. Integrating WSR-88D estimates and Oklahoma Mesonet measurements of rainfall accumulations: A statistical approach. Paper presented at 27th Conference on Radar Meteorology. Vail, Colorado. Oct 9-13.

Rhenals-Fegueredo, A.E., I. Rodriguez-Iturbe, and J. C. Schaake. 1974. Bidimensional spectral analysis of rainfall events. Rep. 193, R.M. Parsons Laboratory for Water Resources and Hydrodynamics, Massachusetts Institute of Technology, Cambridge, MA.

Rodriguez-Iturbe, I., V.K. Gupta, and E. Waymire, 1984. Scale consideration on the modeling of temporal rainfall. Water Resour. Res. 20(11):1611-1619.

Rodriguez-Iturbe, I., W. Qinliang, B.L. Jacobs, and P.S. Eagleson. 1987. Spatial Poisson models of stationary storm rainfall: theoretical development. Report No. 305. MIT Press, Cambridge, Mas. 02139.

Rudra, R.P., W.T. Dickinson, and E.L. Von Euw. 1993. The importance of precise rainfall inputs in nonpoint source pollution modeling. Am. Soc. Ag. Eng. 36(2): 445-450.

Sabbagh, G.J, D.E. Storm, M.D. Smolen, C.T. Haan, and M.S. Gregory. 1995. Illinois River Basin-Treatment Prioritization. Final Report. Department of Biosystems and Agricultural Engineering, Oklahoma State University, Stillwater, OK 74078.

Seed, A.W., and G.L. Austin. 1990. Sampling errors for raingauge-derived mean areal daily and monthly rainfall. J. Hydrology 118:163-173.

Seliga, T.A., G. Aron, K. Aydin, and E. White. 1992. Storm runoff simulation using radar rainfall rates and a unit hydrograph model (SYN-HYD) applied to GREVE watershed. *In:* Am. Meteor. Soc., 25th Int. Conf. on Radar Hydrology. pp. 587-590.

Seo, D.J., W.F. Krajewski, and D.S. Bowles. 1990. Stochastic interpolation of rainfall data from rain gages and radar using cokriging 1. Design of experiments. Water Resour. Res. 26(3):469-477.

Shah, S.M.S., P.E. O'Connell, and J.R.M. Hosking. 1996a. Modeling the effects of spatial variability in rainfall on catchment response. 1. Formulation and calibration of a stochastic rainfall field model. J. Hydrology 175: 67-88.

Smith, J.A., D.J. Seo, M.L. Baeck, and M.D. Hudlow. 1996. An intercomparison study of NEXRAD precipitation estimates. Water Resour. Res. 32(7):2035-2045.

Srinivasan, R. and B.A. Engel. 1994. A spatial decision support system for assessing agricultural nonpoint source pollution. Water Resources Bulletin 30:441-452.

Tabios III, G.Q., and J. Salas. 1985. A comparative analysis of techniques for spatial interpolation of precipitation. Water Resour. Bulletin 21(3): 365-380.

Troutman, B. 1983. Runoff predictions errors and bias in parameter estimation induced by spatial variability of precipitation. Water Resour. Res., 19(3):791-810.

USACERL, 1993. GRASS 4.1 user's reference manual. U.S. Army Corps of Engineers, Construction Engineering Research Laboratories, Champaign, Illinois.

USDA-ARS, 1991. Hydrology of the Little Washita River Watershed: data and analysis. National Agricultural Water Quality Laboratory. Durant, OK 74702.

Valdes, J.B., and I. Rodriguez-Iturbe. 1985. Approximations of temporal rainfall from a multidimensional model. Water Resour. Res. 21(8):1259-1270.

Waymire, E., 1985. Scaling limits and self-similarity in precipitation fields. Water Resour. Res. 21(8):1271-1281.

Waymire, E., and V.K. Gupta. 1981 a. The mathematical structure of rainfall representation, 1, A review of the stochastic rainfall models. Water Resour. Res., 17(5):1261-1272..

Waymire, E., and V.K. Gupta, 1981 b. The mathematical structure of rainfall representation, 3, Some applications of the point process theory to rainfall processes. Water Resour. Res. 17(5):1286-1294.

Waymire, E., V.K. Gupta, and I. Rodriguez-Iturbe. 1984. A spectral theory of rainfall at the meso-B scale. Water Resour. Res. 20(10):1453-1465.

Williams, J.R., C.A. Jones, and P.T. Dyke. 1984. A modeling approach to determining the relationship between erosion and soil productivity. Trans. ASAE. 27(1):129-144.

Wilson, J.W. 1970. Integration of radar and gage data for improved rainfall measurement. J. Appl. Meteorol. 9:489-497.

Wilson, J.W., and E.A. Brandes. 1979. Radar measurement of rainfall - A summary. Bull. Am. Meteorol. Soc., 60:1048-1058.

Wilson, C.B., J.B. Valdes, and I. Rodriguez-Iturbe. 1979. On the influence of the spatial distribution of rainfall on storm runoff. Water Resour. Res., 15(2):321-328.

Woodley, W.L., A.R. Olsen, A. Herndon, and V. Wiggert. 1975. Comparison of gage radar methods of convective rain measurements. J. Appl. Meteorol. 14: 909-928.

Young, R.A., R.S. Allesi, and S.E. Needham. 1992. Application of a distributed parameter model for watershed assessment. In: Managing Water Resources During Global Change. American Water Resources Association, 107-115.

Young, R.A., C.A. Onstad, D.D. Bosch, and W.P. Anderson. 1987. AGNPS, Agricultural non-point-source pollution model: A watershed analysis tool. U.S. Department of Agriculture. Conservation research report 35, 80 p.

Young, R.A., C.A. Onstad, D.D. Bosch, and W.P. Anderson. 1989. AGNPS: A nonpoint-source pollution model for evaluating agricultural watersheds. J. of Soil and Water Conser. 44(2):168-173.

APPENDIX - 1

Rainfall observed by Micronet stations for the rainfall dates analyzed

Table A1.1 Rainfall observed by micronet stations for the rainfall dates analyzed

STID	3/27/96	3/28/96	Event total (mm)	4/21/96	4/22/96	Event total (mm)
110	16.36	7.05	23.41	5.83	21.51	27.34
111	30.01	-33.87	-3.86	-0.25	31.28	31.03
121	17.78	5.84	23.62	2.68	36.81	39.49
122	0.76	0.2	0.96	6.24	17.62	23.86
123	28.65	7.15	35.8	4.47	19.99	24.46
124	28	7.77	35.77	4.62	12.96	17.58
125	23.91	9.68	33.59	4.03	28.45	32.48
130	**31.92**	**8.89**	**40.81**	**14.49**	**13.31**	**27.8**
131	**27.75**	**7.25**	**35**	**11.58**	**8.39**	**19.97**
132	**9.91**	**8.65**	**18.56**	**6.2**	**10.57**	**16.77**
133	**24.74**	**11.03**	**35.77**	**5.98**	**15.65**	**21.63**
134	**26.87**	**-27.2**	**-0.33**	**-0.37**	**22.54**	**22.17**
135	29.53	-33.53	-4	4.37	13.89	18.26
136	3.62	4.92	8.54	2.72	25.31	28.03
137	12.91	5.93	18.84	2.34	34.97	37.31
144	38.24	-39.96	-1.72	2.18	42.67	44.85
145	29.27	-26.9	2.37	-0.21	27.85	27.64
146	30.09	-31.95	-1.86	3.2	23.81	27.01
147	**33.42**	**-34.15**	**-0.73**	**9.57**	**15.53**	**25.1**
148	**28.34**	**9.78**	**38.12**	**8.43**	**18.55**	**26.98**
149	**23.87**	**8.24**	**32.11**	**7.97**	**11.52**	**19.49**
150	**24.96**	**6.59**	**31.55**	**11.05**	**5.8**	**16.85**
151	**10.56**	**7.37**	**17.93**	**5.58**	**11.7**	**17.28**
152	**10.99**	**7.56**	**18.55**	**11.85**	**8.66**	**20.51**
153	**29.14**	**10.09**	**39.23**	**13.01**	**21.71**	**34.72**
154	**23.49**	**9.3**	**32.79**	**3.01**	**21.78**	**24.79**
155	**23.04**	**-23.39**	**-0.35**	**-0.45**	**32.27**	**31.82**
156	24.79	-24.72	0.07	4.8	36.48	41.28
157	23.67	-23.43	0.24	10.92	42.8	53.72
158	38.88	-39.37	-0.49	8	33.83	41.83
159	32.51	-33.34	-0.83	2.85	27.26	30.11
160	34.76	-34.32	0.44	6.02	47.68	53.7
161	**-998**	**-998**	**-1996**	**-998**	**-998**	**-1996**
162	**31.95**	**7.82**	**39.77**	**9.59**	**27.05**	**36.64**
163	**26.57**	**8.81**	**35.38**	**15.62**	**34.78**	**50.4**
164	26.06	6.61	32.67	11.55	18.41	29.96
165	23.24	-23.6	-0.36	4.64	45.57	50.21
166	32.54	-32.81	-0.27	9.94	47.63	57.57
167	33.68	-34.12	-0.44	8.72	24.61	33.33
168	15.42	-15.45	-0.03	7.49	17.35	24.84
181	2.32	8.56	10.88	-0.19	0.7	0.51
182	23.67	-23.51	0.16	5.48	26.86	32.34

Numbers in the bold represent the gauges used in this study.
Negative numbers represent an erroneous rainfall.

181

Table A1.1 Cont.

STID	5/31/96	6/1/96	Event total (mm)	7/9/96	7/10/96	Event total (mm)
110	11.64	56.14	67.78	48.34	49.22	97.56
111	13.2	54.48	67.68	52.28	55.7	107.98
121	15.23	53.38	68.61	76.05	28.48	104.53
122	12.53	49.48	62.01	55.38	39.64	95.02
123	19.49	49.93	69.42	41.22	52.91	94.13
124	18.13	57.12	75.25	32.57	49.76	82.33
125	19.27	61.8	81.07	32.82	34.71	67.53
130	**31.84**	**44.61**	**76.45**	**44.71**	**57.22**	**101.93**
131	**28.39**	**50.88**	**79.27**	**82.45**	**54.57**	**137.02**
132	**24.47**	**64.96**	**89.43**	**43.04**	**30.77**	**73.81**
133	**20.59**	**60.56**	**81.15**	**36.13**	**42.07**	**78.2**
134	**22.18**	**46.28**	**68.46**	**37.57**	**49.24**	**86.81**
135	19.58	53.24	72.82	50.23	37.26	87.49
136	13.9	50.31	64.21	77.38	36.76	114.14
137	16.2	47.49	63.69	80.26	35.32	115.58
144	34.6	58.49	93.09	56.34	14.15	70.49
145	12.77	48.04	60.81	49.32	18.68	68
146	25.63	41.24	66.87	48.6	15.96	64.56
147	**29.08**	**52.31**	**81.39**	**35.29**	**45.14**	**80.43**
148	**35.12**	**44.63**	**79.75**	**26.46**	**41.34**	**67.8**
149	**39.87**	**54.72**	**94.59**	**19.1**	**27.59**	**46.69**
150	**37.75**	**40.65**	**78.4**	**50.41**	**47.83**	**98.24**
151	**38.52**	**40.5**	**79.02**	**57.22**	**68.94**	**126.16**
152	**34.61**	**46.65**	**81.26**	**12.4**	**35.28**	**47.68**
153	**36.29**	**49.85**	**86.14**	**6.89**	**35.6**	**42.49**
154	**27.05**	**53.54**	**80.59**	**4.71**	**30.82**	**35.53**
155	**17.85**	**45.45**	**63.3**	**27.43**	**13.7**	**41.13**
156	44.62	58.67	103.29	25.97	13.36	39.33
157	25.4	66.18	91.58	32.46	14.28	46.74
158	15.14	60.36	75.5	27.59	7.44	35.03
159	21.98	68.17	90.15	14.77	11.95	26.72
160	24.38	60.8	85.18	20.24	10.11	30.35
161	**18.62**	**38.47**	**57.09**	**15.42**	**15.38**	**30.8**
162	**19.34**	**49.62**	**68.96**	**23.02**	**17.52**	**40.54**
163	**23.05**	**54.44**	**77.49**	**3.64**	**36.85**	**40.49**
164	16.29	45.37	61.66	10.61	36.81	47.42
165	0.26	0.03	0.29	5.66	20.76	26.42
166	17.54	55.53	73.07	7.13	7.56	14.69
167	19.86	54.44	74.3	15.25	6.09	21.34
168	12.53	67.93	80.46	23.15	5.15	28.3
181	13.36	47.51	60.87	17.1	58.93	76.03
182	31.86	46.54	78.4	18.91	22.53	41.44

Table A1.1 Cont.

STID	8/1/96	8/3/96	Event total (mm)	10/27/96 (mm)	11/6/96 (mm)
110	4.26	33.66	37.92	14.34	9.04
111	8.51	27.3	35.81	24.52	14.53
121	14.84	33.15	47.99	8.14	11.19
122	15.44	38.11	53.55	27.43	13.21
123	17.56	41.24	58.8	8.86	6.19
124	20.84	39	59.84	11.74	11.09
125	-39.78	37.77	-2.01	40.76	14.67
130	**-12.87**	**21.62**	**8.75**	**9.56**	**21.72**
131	**-19.12**	**30.5**	**11.38**	**14.39**	**14.27**
132	**-33.33**	**30.22**	**-3.11**	**26.7**	**6.96**
133	**19.91**	**31.85**	**51.76**	**44.51**	**9**
134	**22**	**30.06**	**52.06**	**11.25**	**7.31**
135	10.75	23.55	34.3	10.6	-6.21
136	18.2	25.52	43.72	30.57	4.62
137	10.06	36.6	46.66	16.02	5.6
144	15.93	29.88	45.81	6.01	34.28
145	11.14	20.19	31.33	11.17	29.88
146	11.12	15.98	27.1	7.86	-2.1
147	**15.95**	**34.57**	**50.52**	**13.72**	**-6.23**
148	**19.07**	**15.17**	**34.24**	**30.39**	**7.9**
149	**21.4**	**18.4**	**39.8**	**28.11**	**8.5**
150	**-12.89**	**12.65**	**-0.24**	**12.8**	**8.28**
151	**29.33**	**13.42**	**42.75**	**10.47**	**16.55**
152	**-21.5**	**7.99**	**-13.51**	**17.28**	**8.94**
153	**-19.58**	**5.24**	**-14.34**	**38.25**	**1.14**
154	**13.1**	**8.66**	**21.76**	**20.21**	**-0.65**
155	**0.16**	**11.57**	**11.73**	**-0.61**	**28.8**
156	23.33	28.83	52.16	9.99	44.72
157	11.82	27.32	39.14	10.69	24.08
158	-37.17	13.36	-23.81	7.23	18.62
159	10.74	8.17	18.91	12.65	43.46
160	-33.15	12.34	-20.81	17.89	42.28
161	**-26.15**	**10.21**	**-15.94**	**-0.21**	**18.8**
162	**10.39**	**7.5**	**17.89**	**15.81**	**7.68**
163	**-24.43**	**8.03**	**-16.4**	**20.13**	**2.98**
164	-19.66	-0.12	-19.78	18.31	5.93
165	-32.95	0.02	-32.93	10.43	4.35
166	-36.66	0.13	-36.53	9.13	39.32
167	-24.12	2.09	-22.03	16.39	30.37
168	-21.1	2.4	-18.7	9.28	17.5
181	-3.09	-0.05	-3.14	3.06	-0.11
182	8.35	11.11	19.46	7.08	-1.66

APPENDIX - 2

Optimum parameter estimates for the rainfall events analyzed

Table A2.1 Optimum parameter estimates for the rainfall event on 3/27/96
using the individual gauge rainfall values for the Cyril watershed

Gauge #	Rainfall (mm)	Slope (%)	CN	S parameter (mm)	K factor
130	40.9	0.93	52	234	0.34
131	35.1	1.16	56	200	0.32
132	18.5	2.53	71	104	0.58
149	32.0	1.33	58	184	0.32
150	31.5	1.33	60	169	0.34
151	18.0	2.75	71	104	0.51
152	18.5	2.53	71	104	0.58
153	39.1	0.97	54	216	0.32
Base	31.0	1.6	58	184	0.34

Table A2.2 Optimum parameter estimates for the rainfall event on 5/31/96
using the individual gauge rainfall values for the Cyril watershed

Gauge #	Rainfall (mm)	Slope (%)	CN	S parameter (mm)	K factor
130	76.5	1.87	38	414	0.3
131	79.2	1.65	37	432	0.32
132	89.4	1.2	34	493	0.31
149	94.5	1.24	32	540	0.29
150	78.5	1.65	37	432	0.34
151	79.0	1.65	37	432	0.32
152	81.3	1.4	36	452	0.36
153	86.1	1.3	34	493	0.36
Base	78.5	1.6	37	432	0.34

Table A2.3 Optimum parameter estimates for the rainfall event on 7/9/96
using the individual gauge rainfall values for the Cyril watershed

Gauge #	Rainfall (mm)	Slope (%)	CN	S parameter (mm)	K
130	102	1.65	36	452	0.41
131	137	1	32	540	0.28
132	73.7	2.7	46	298	0.48
149	46.7	3.7	61	162	0.72
150	98.0	2.15	37	432	0.34
151	126	1.1	32	540	0.33
152	47.8	3.8	59	177	0.67
153	42.4	4.05	62	156	0.79
base	112	1.6	33	516	0.34

Table A2.4 Optimum parameter estimates for the rainfall event on 8/1/96
using the individual gauge rainfall values for the Cyril watershed

Gauge #	Rainfall (mm)	Slope (%)	CN	S parameter (mm)	K
130	21.6	2.7	78	71.6	0.38
131	30.5	0.4	74	89.2	0.09
132	30.5	0.4	74	89.2	0.09
149	39.6	2.2	65	137	0.09
150	14.2	1.6	85	44.8	0.43
151	68.1	1.6	46	298	0.15
152	7.87	8.2	90	28.2	0.87
153	5.33				
Base	26.4	1.6	71	104	0.34

Table A2.5 Optimum parameter estimates for the rainfall event on 11/6/96
using the individual gauge rainfall values for the Cyril watershed

Gauge #	Rainfall (mm)	Slope (%)	CN	S parameter (mm)	K
130	9.65	1.8	77	75.9	0.38
131	14.5	0.77	72	98.8	0.17
132	26.7	0.55	62	156	0.05
149	28.2	1.2	59	177	0.26
150	12.7	1.69	74	89.2	0.48
151	10.4	1.74	77	75.9	0.28
152	17.3	0.8	69	114	0.33
153	38.4	0.55	52	234	0.05
Base	12.4	1.6	74	89.2	0.34

Table A2.6 Optimum parameter estimates for the rainfall event on 11/6/96
using the individual gauge rainfall values for the Cyril watershed

Gauge #	Rainfall (mm)	Slope (%)	CN	S parameter (mm)	K
130	21.8	1.6	66	131	0.38
131	14.2	1.44	74	89.2	0.23
132	6.86	1.6	82	55.8	0.2
149	8.38	1.58	82	55.8	0.19
150	8.38	1.58	82	55.8	0.19
151	16.5	1.44	74	89.2	0.19
152	8.89	1.55	82	55.8	0.23
153	1.27				
Base	12.1	1.6	75	84.7	0.34

Table A2.7 Optimum parameter estimates for the rainfall event on 3/27/96
using the individual gauge rainfall values for the Cement watershed

Gauge #	Rainfall (mm)	Slope (%)	CN	S parameter (mm)	K
151	18.0	5.24	70	109	0.55
132	18.5	5.21	69	114	0.58
152	18.5	5.21	69	114	0.58
150	31.5	3.9	58	184	0.32
149	32.0	3.69	58	184	0.32
154	32.8	3.69	57	192	0.33
131	35.1	3.63	55	208	0.31
163	35.3	3.61	55	208	0.3
133	35.8	3.57	55	208	0.27
148	38.1	3.11	54	216	0.28
153	39.1	3.60	52	234	0.26
162	39.9	3.43	52	234	0.24
130	40.9	3.57	51	244	0.23
Base	32.5	3.71	56	200	0.33

Table A2.8 Optimum parameter estimates for the rainfall event on 4/21/96
using the individual gauge rainfall values for the Cement watershed

Gauge #	Rainfall (mm)	Slope (%)	CN	S parameter (mm)	K
132	16.8	6.79	72	98.8	0.68
151	17.3	6.78	72	98.8	0.59
149	19.6	6.11	70	109	0.56
131	20.1	6.11	69	114	0.56
152	20.6	6.05	69	114	0.5
133	21.8	5.94	68	120	0.46
134	22.1	5.89	68	120	0.44
154	24.6	5.67	65	137	0.39
147	25.1	5.78	65	137	0.36
148	26.9	5.37	63	149	0.38
130	27.7	5.36	63	149	0.34
155	31.8	5.31	59	177	0.28
153	34.8	5.0	57	192	0.25
162	36.6	4.7	56	200	0.25
163	50.3	3.33	47	286	0.25
150	16.8	6.79	72	98.8	0.68
Base	24.6	3.71	63	149	0.33

Table A2.9 Optimum parameter estimates for the rainfall event on 5/31/96
using the individual gauge rainfall values for the Cement watershed

Gauge #	Rainfall (mm)	Slope (%)	CN	S parameter (mm)	K
161	57.2	5.14	52	234	0.38
134	68.6	4.32	47	286	0.35
162	68.8	4.26	46	298	0.36
130	76.5	4.17	43	337	0.3
163	77.5	4.02	43	337	0.3
150	78.5	3.91	42	351	0.32
151	79.0	3.91	42	351	0.31
131	79.2	3.83	42	351	0.31
148	79.8	3.82	42	351	0.31
154	80.5	3.80	41	366	0.32
133	81.3	3.79	41	366	0.31
153	86.1	3.55	39	397	0.31
132	89.4	3.48	38	414	0.29
149	94.5	3.32	36	452	0.28
147	81.3	3.79	41	366	0.31
152	81.3	3.79	41	366	0.31
Base	83.3	3.71	39	397	0.33

Table A2.10 Optimum parameter estimates for the rainfall event on 7/9/96
using the individual gauge rainfall values for the Cement watershed

Gauge #	Rainfall (mm)	Slope (%)	CN	S parameter (mm)	K
161	30.7	6.22	64	143	0.87
154	35.6	6	60	169	0.7
163	40.4	5.02	57	192	0.74
162	40.6	5.02	56	200	0.77
155	41.1	4.94	56	200	0.76
153	42.4	4.94	55	208	0.71
149	46.7	4.66	52	234	0.66
152	47.8	4.61	51	244	0.66
148	67.8	3.97	41	366	0.4
132	73.9	3.88	39	397	0.33
133	78.2	3.67	37	432	0.33
147	80.5	3.61	36	452	0.32
134	86.9	3.33	34	493	0.31
150	98.3	2.98	30	593	0.3
130	102	2.76	29	622	0.31
151	126	2.31	24	804	0.27
131	137	2.07	23	850	0.28
Base	64.3	3.71	33	516	0.33

Table A2.11 Optimum parameter estimates for the rainfall event on 10/27/96
using the individual gauge rainfall values for the Cement watershed

Gauge #	Rainfall (mm)	Slope (%)	CN	S parameter (mm)	K
130	9.65	5.54	76	80.2	0.59
131	14.5	3.94	72	98.8	0.37
132	26.7	3.01	60	169	0.2
133	44.5	2.1	47	286	0.14
134	11.2	4.47	75	84.7	0.52
148	30.5	2.54	57	192	0.2
149	28.2	2.71	59	177	0.19
150	12.7	4.36	73	93.9	0.59
151	10.4	4.45	76	80.2	0.52
152	17.3	3.7	69	114	0.32
153	38.4	2.15	51	244	0.18
154	20.3	3.44	66	131	0.25
162	15.7	3.91	70	109	0.46
163	20.1	3.57	66	131	0.25
147	11.9	4.41	74	89.2	0.56
Base	23.4	3.71	55	208	0.33

Table A2.12 Optimum parameter estimates for the rainfall event on 7/9/96 using the
individual gauge rainfall values from calibrated rainfall for the Cement watershed

Gauge #	Rainfall (mm)	Slope (%)	CN	S parameter (mm)	K
130	102	7.45	64	143	0.86
131	137	2.96	22	901	0.22
132	73.9	4.06	39	397	0.43
133	78.0	4.06	37	432	0.39
134	86.9	3.5	34	493	0.4
147	80.5	3.64	36	452	0.45
148	67.8	4.49	41	366	0.45
149	46.7	6.22	53	225	0.5
150	98.3	3.32	30	593	0.35
151	126	3.02	24	804	0.25
152	47.8	5.96	52	234	0.53
153	42.4	6.3	55	208	0.63
154	35.6	6.86	60	169	0.76
155	41.1	6.7	56	200	0.59
161	30.7	7.45	64	143	0.86
162	40.6	6.61	57	192	0.59
163	40.4	6.68	57	192	0.59
Base	64.5	3.71	30	593	0.33

APPENDIX - 3

AGNPS outputs obtained using optimum parameters and rainfall observed at each gauge

location one at a time

Table A3.1 Model outputs estimated for the rainfall event on 3/27/96 using the individual
gauge rainfall and optimum parameter values for the Cyril watershed

Gauge #	Rainfall (mm)	Runoff volume (mm)	Total Sediment (Mg)	Sediment-N (kg/ha)	Sediment-P (kg/ha)
151	18.0	0.003	0.01	0	0
132	18.5	0.003	0.01	0	0
152	18.5	0.003	0.01	0	0
150	31.5	0.185	9.87	0.02	0.01
149	32.0	0.340	15.8	0.02	0.01
131	35.1	0.554	24.4	0.03	0.02
153	39.1	0.831	35.4	0.06	0.03
130	40.9	1.17	44.2	0.07	0.03
Base	31.0	0.330	13.9	0.02	0.01

Table A3.2 Model outputs estimated for the rainfall event on 5/31/96 using the individual
gauge rainfall and optimum parameter values for the Cyril watershed

Gauge #	Rainfall (mm)	Runoff volume (mm)	Total Sediment (Mg)	Sediment-N (kg/ha)	Sediment-P (kg/ha)
130	76.5	0.60	110	0.12	0.06
150	78.5	0.76	129	0.15	0.07
151	79.0	0.76	131	0.15	0.07
131	79.2	0.76	132	0.15	0.07
152	81.3	0.96	153	0.17	0.08
153	86.1	1.43	198	0.20	0.10
132	89.4	1.71	224	0.22	0.11
149	94.5	2.34	271	0.26	0.13
Base	78.5	0.76	128	0.15	0.07

Table A3.3 Model outputs estimated for the rainfall event on 7/9/96 using the individual
gauge rainfall and optimum parameter values for the Cyril watershed

Gauge #	Rainfall (mm)	Runoff volume (mm)	Total Sediment (Mg)	Sediment-N (kg/ha)	Sediment-P (kg/ha)
153	42.4	0	0	0	0
149	46.7	0	0.01	0	0
152	47.8	0	0.01	0	0
132	73.7	0.11	13.6	0.02	0.01
150	98.0	1.43	256	0.25	0.13
130	102	1.68	290	0.28	0.14
151	126	5.36	577	0.48	0.24
131	137	7.38	732	0.58	0.29
Base	112	3.05	401	0.36	0.18

Table A3.4 Model outputs estimated for the rainfall event on 8/1/96 using the individual
gauge rainfall and optimum parameter values for the Cyril watershed

Gauge #	Rainfall (mm)	Runoff volume (mm)	Total Sediment (Mg)	Sediment-N (kg/ha)	Sediment-P (kg/ha)
152	7.87	0	0.02	0	0
150	14.2	0.12	4.38	0.01	0.00
130	21.6	0.97	26.17	0.04	0.02
131	30.5	2.74	59.83	0.08	0.04
132	30.5	2.74	59.83	0.08	0.04
149	39.6	6.18	114	0.13	0.07
151	68.1	19.8	317	0.30	0.15
153	5.33	0	0	0	0
Base	26.4	4.06	67.1	0.09	0.04

Table A3.5 Model outputs estimated for the rainfall event on 10/27/96 using the individual
gauge rainfall and optimum parameter values for the Cyril watershed

Gauge #	Rainfall (mm)	Runoff volume (mm)	Total Sediment (Mg)	Sediment-N (kg/ha)	Sediment-P (kg/ha)
130	9.65	0.05	1.80	0	0.00
151	10.4	0.05	1.80	0	0.00
150	12.7	0.13	4.74	0.01	0.01
131	14.5	0.33	10.74	0.02	0.01
152	17.3	0.66	18.89	0.03	0.02
132	26.7	2.36	52.35	0.07	0.04
149	28.2	3.14	64.97	0.08	0.04
153	38.4	7.01	124	0.15	0.07
Base	12.4	0.14	4.94	0.01	0.01

Table A3.6 Model outputs estimated for the rainfall event on 11/6/96 using the individual
gauge rainfall and optimum parameter values for the Cyril watershed

Gauge #	Rainfall (mm)	Runoff volume (mm)	Total Sediment (Mg)	Sediment-N (kg/ha)	Sediment-P (kg/ha)
149	8.38	0.03	0.79	0	0
150	8.38	0.03	0.79	0	0
152	8.89	0.03	0.79	0	0
131	14.2	0.44	13.6	0.02	0.01
151	16.5	0.44	13.8	0.02	0.01
130	21.8	1.99	44.8	0.07	0.03
132	6.86	0.03	0.78	0	0
153	1.27	0	0	0	0
Base	12.1	0.30	10.5	0.02	0.01

Table A3.7 Model outputs estimated for the rainfall event on 3/27/96 using the individual
gauge rainfall and optimum parameter values for the Cement watershed

Gauge #	Rainfall (mm)	Runoff volume (mm)	Total Sediment (Mg)	Sediment-N (kg/ha)	Sediment-P (kg/ha)
151	18.0	0.01	1.12	0	0
132	18.5	0.01	1.47	0	0
152	18.5	0.01	1.47	0	0
150	31.5	0.36	153	0.04	0.02
149	32.0	0.39	174	0.04	0.02
154	32.8	0.45	205	0.06	0.03
131	35.1	0.64	306	0.08	0.04
163	35.3	0.67	319	0.08	0.04
133	35.8	0.72	343	0.09	0.04
148	38.1	0.98	461	0.11	0.05
153	39.1	1.10	517	0.11	0.06
162	39.9	1.20	561	0.12	0.06
130	40.9	1.34	622	0.13	0.07
Base	32.5	0.56	242	0.07	0.03

Table A3.8 Model outputs estimated for the rainfall event on 4/21/96 using the individual
gauge rainfall and optimum parameter values for the Cement watershed

Gauge #	Rainfall (mm)	Runoff volume (mm)	Total Sediment (Mg)	Sediment-N (kg/ha)	Sediment-P (kg/ha)
132	16.8	0.06	8.71	0	0
151	17.3	0.07	10.6	0	0
149	19.6	0.14	31.6	0.01	0.01
131	20.1	0.17	37.8	0.01	0.01
152	20.6	0.19	44.9	0.01	0.01
133	21.8	0.26	65.8	0.02	0.01
134	22.1	0.28	70.6	0.02	0.01
154	24.6	0.48	136	0.04	0.02
147	25.1	0.53	152	0.04	0.02
148	26.9	0.72	212	0.06	0.03
130	27.7	0.82	240	0.07	0.03
155	31.8	1.42	411	0.10	0.05
153	34.8	1.98	563	0.12	0.06
162	36.6	2.35	659	0.15	0.07
163	50.3	6.03	1611	0.29	0.15
150	16.8	0.06	8.71	0	0
Base	24.6	0.78	443	0.10	0.05

Table A3.9 Model outputs estimated for the rainfall event on 5/31/96 using the individual
gauge rainfall and optimum parameter values for the Cement watershed

Gauge #	Rainfall (mm)	Runoff volume (mm)	Total Sediment (Mg)	Sediment-N (kg/ha)	Sediment-P (kg/ha)
161	57.2	0.29	398	0.10	0.05
134	68.6	0.96	1509	0.28	0.14
162	68.8	0.98	1539	0.28	0.14
130	76.5	1.74	2493	0.41	0.21
163	77.5	1.86	2629	0.44	0.22
150	78.5	1.99	2766	0.45	0.22
151	79.0	2.05	2836	0.46	0.23
131	79.2	2.08	2871	0.46	0.23
148	79.8	2.15	2941	0.47	0.24
154	80.5	2.25	3052	0.48	0.24
133	81.3	2.35	3165	0.50	0.25
153	86.1	3.04	3887	0.59	0.30
132	89.4	3.56	4403	0.65	0.33
149	94.5	4.43	5240	0.75	0.37
147	81.3	2.35	3165	0.50	0.25
152	81.3	2.35	3165	0.50	0.25
155	63.2	0.58	898	0.18	0.09
Base	83.3	3.13	3395	0.53	0.27

Table A3.10 Model outputs estimated for the rainfall event on 7/9/96 using the individual
gauge rainfall and optimum parameter values for the Cement watershed

Gauge #	Rainfall (mm)	Runoff volume (mm)	Total Sediment (Mg)	Sediment-N (kg/ha)	Sediment-P (kg/ha)
161	30.7	0	0.13	0	0
154	35.6	0	0.54	0	0
163	40.4	0	1.18	0	0
162	40.6	0	1.22	0	0
155	41.1	0	1.31	0	0
153	42.4	0	1.55	0	0
149	46.7	0.01	3.07	0	0
152	47.8	0.01	3.93	0	0
148	67.8	0.21	402	0.10	0.05
132	73.9	0.41	924	0.19	0.09
133	78.2	0.61	1388	0.26	0.13
147	80.5	0.73	1728	0.31	0.15
134	86.9	1.18	2769	0.45	0.23
150	98.3	2.32	4735	0.70	0.35
130	102	2.76	5395	0.76	0.38
151	126	6.74	10727	1.33	0.67
131	137	9.02	13585	1.60	0.80
Base	64.3	1.41	2367	0.39	0.20

Table A3.11 Model outputs estimated for the rainfall event on 10/27/96 using the individual gauge rainfall and optimum parameter values for the Cement watershed

Gauge #	Rainfall (mm)	Runoff volume (mm)	Total Sediment (Mg)	Sediment-N (kg/ha)	Sediment-P (kg/ha)
130	9.65	0	0.02	0	0
131	14.5	0	0.24	0	0
132	26.7	0.09	26.35	0.01	0.01
133	44.5	1.65	802	0.17	0.08
134	11.2	0	0.06	0	0.00
148	30.5	0.23	95.4	0.03	0.02
149	28.2	0.14	48.2	0.02	0.01
150	12.7	0	0.14	0	0
151	10.4	0	0.04	0	0
152	17.3	0	0.51	0	0
153	38.4	0.84	429	0.10	0.05
154	20.3	0.02	2.24	0	0
162	15.7	0	0.34	0	0
163	20.1	0.02	2.00	0	0
147	11.9	0	0.10	0	0
Base	23.4	0.37	68.3	0.02	0.01

Table A3.12 Model outputs estimated for the rainfall event on 7/9/96 using the individual
calibrated radar rainfall and optimum parameter values for the Cement watershed

	Rainfall (mm)	Runoff volume (mm)	Total Sediment (Mg)	Sediment-N (kg/ha)	Sediment-P (kg/ha)
	21.3	0	0	0	0
	22.6	0	0	0	0
	30.0	0	0	0	0
	30.2	0	0	0	0
	30.7	0	0	0	0
	31.0	0	0	0	0
	31.8	0	0	0	0
	32.5	0	0	0	0
	33.8	0	0.10	0	0
	36.1	0	0.27	0	0
	37.1	0	0.36	0	0
	38.9	0	0.56	0	0
	41.4	0	0.89	0	0
	42.7	0	1.07	0	0
	43.2	0	1.15	0	0
	44.7	0	1.41	0	0
	46.0	0	1.64	0	0
	47.0	0	1.86	0	0
	49.5	0	2.51	0	0
	51.6	0.01	3.29	0	0
	55.4	0.01	7.57	0	0
	56.9	0.02	10.6	0	0
	57.7	0.02	12.5	0.01	0
	59.9	0.03	19.5	0.01	0
	61.5	0.04	25.4	0.01	0.01
	62.5	0.05	30.1	0.01	0.01
	66.8	0.08	59.8	0.02	0.01
	67.1	0.09	62.2	0.02	0.01
	69.6	0.11	88.7	0.03	0.01
	71.1	0.13	139	0.04	0.02
	94.5	1.06	3100	0.49	0.25
	98.0	1.32	3777	0.57	0.29
	102	1.67	4566	0.67	0.34
	107	2.18	5587	0.78	0.39
	112	2.66	6491	0.89	0.45
	112	2.69	6546	0.90	0.45
	122	4.04	8859	1.14	0.57
	126	4.66	9855	1.24	0.62
	137	6.50	12695	1.52	0.76
	142	7.41	14047	1.65	0.83
	167	13.0	22367	2.40	1.20
	171	14.1	24002	2.53	1.27
	189	18.7	31226	3.13	1.56
Base	64.5	1.43	3337	0.53	0.26

APPENDIX - 4

Computer program to estimate the AGNPS parameters

```
/* ****************************************************************

This program is used to estimate the parameter uncertainty induced in the AGNPS parameters
due to spatial variability of rainfall. It is also used to estimate the output   uncertainty due to
rainfall spatial variability. This program estimates the parameters
using the following steps


   1. Read the rainfall depth and observed output values from a data file "rainfall.dat".
   2. Calculate the slope, K and CN for the specified step size.
    3. Update the AGNPS input file for each permutation of slope and K, and CN for the
       number of increments specified. It runs the modified AGNPS using the updated input
       information for each events.
   4. Record the predicted output values and then calculate the relative error for each output.

   5. This method is known as the "brute force" method and is described by Allred and Haan
      (1994).


      User of this program is expected to be familiar with the AGNPS input file format
          and description.
                              Indrajeet Chaubey


   ******************************************************************** */


/* ***************************************************
*                    List of Variables
*        ncell = Number of cells in the watershed
*        N = Number of rainfall values used to estimate parameters
*        deltaS = Slope increment (fraction)
*        deltaCN = CN increment
*        deltaK = USLE K factor increment (fraction)
*        S_incr = Number of slope increments used
*        CN_incr = Number of CN increment used
*        K_incr = Number of K factor increments used
*        amc = Antecedent moisture condition
*        slength = Slope length
*        sed = Observed sediment transport at the watershed outlet
*        runoff = Observed runoff volume at the watershed outlet
*        sedmntN = Observed sediment-attached N at the watershed outlet (kg)
*        sedmntP = Observed sediment-attached P at the watershed outlet (kg)
*        tot_sol_N = Observed total soluble N at the watershed outlet (kg)
*        tot_sol_P = Observed total soluble  P at the watershed outlet (kg)
*        energy = Energy intensity value for the rainfall
*        cfact = USLE C factor
*        kfact = USLE K factor
```

```
*        pfact = USLE P factor
*        scc = Surface conditioning constant
*        n = Manning's roughness constant
*        eng = Energy intensity value calculated by AGNPS
*        duration = Rainfall duration
*        rainfall = Total event rainfall volume (inches)
*        nitro = N concentration in rainfall (ppm)
*        rv = Runoff volume predicted by ANPS at the watershed outlet (inches)
*        area = Area of the watershed (acres)
*        areac = Area of each cell (acres)
*        ropk = Runoff rate at the outlet cell (cfs)
*        tss = Total sediment yield at the watershed outlet (tons)
*        sederr = Relative error in total sediment prediction
*        rverr = Relative error in runoff volume prediction
*        sedNerr = Relative error in sediment-N prediction
*        sedPerr = Relative error in sediment-P prediciton
*        TSNerr = Relative error in soluble N prediction
*        TSPerr = Relative error in soluble P prediction
*        sumerr = Total relative errors in outputs considered
*        CellRain = Grid-based rainfall value for each AGNPS cell (inches)
*
* ************************************************************ */


#include <stdio.h>
#include <stdlib.h>
#include <process.h>
#include <math.h>
#include <io.h>
#include <string.h>

/* This is total number of cells in the watershed. It should be changed to
    a watershed-specific number from AGNPS before the program is run. */
#define ncell 4027
#define N 3
#define deltaS 1.0
#define deltaCN 1
#define deltaK 1.0

#define S_incr 1
#define CN_incr 1
#define K_incr 1
```

```c
int main ()
{
        int i, j, k, m, curve,check;
        int amc[N],CN, OM, COD;
        int slength;
        float rain[N], sed[N], runoff[N];
        float sedmntN[N], sedmntP[N], tot_sol_N[N], tot_sol_P[N];
        float energy[N];

        float cfact, kfact, pfact, scc, n;
        char soil[10];
        float BaseN, BaseP, poreN, poreP;
        float runoffN, runoffP, leachN, leachP;
        float sedN, TSN, sedP, TSP;

        float eng, duration, rainfall, nitro;
        float rv, area, areac;
        float ropk, tss;
        float sederr, rverr, sumerr;
        float sedNerr, sedPerr, TSNerr, TSPerr;
        char type[3], string[81], string1[81];
        int a, b, c, d, f, g;
        int a1, a2, a3, a4, a5, a6, a7;
        float CellRain, e;
        char temp1[80], *p1, *p4;
        int p0, p2, p3, p5, p6, x, x1;
        int pr1, pr2, pr3;                      /* used to increment K, C, and P factors */

        long sumCN, avgCN;
        float sum_slope, avg_slope;
        float sum_kfact, avg_kfact;

        FILE *ifp;
        FILE *temp, *ofp;

        /* "rainfall.txt" file contains observed raifall and outputs */
        if( (ifp = fopen("rainfall.txt", "r")) == NULL)
        {
                printf("\n Error: Cannot open rainfall.txt file");
                exit (1);
        }
```

```c
/*  Initiate all arrays to zero  */

for(i=0; i<N; i++)
        {
                amc[i]=0;
                rain[i]=0.0;
                sed[i]=0.0;
                runoff[i]=0.0;
                energy[i]=0.0;
                sedmntN[i]=0.0;
                sedmntP[i]=0.0;
                tot_sol_N[i]=0.0;
                tot_sol_P[i]=0.0;
        }

        /* Initiate all error values to zero */
                sederr=0.0;
                rverr=0.0;
                sedNerr = 0.0;
                sedPerr = 0.0;
                TSNerr = 0.0;
                TSPerr = 0.0;
                sumerr=0.0;

        for(i=0;i<N;i++)
        {
                fscanf(ifp, "%d %f %f %f %f %f %f %f",
                        &amc[i],&rain[i],&runoff[i],&sed[i],   &sedmntN[i],
                &sedmntP[i], &tot_sol_N[i], &tot_sol_P[i] );
                fgets(string1,80,ifp);

                /* ------------------------------------------------------
                Calculate the rainfall energy for each rainfall
                --------------------------------------------------- */
                energy[i] = 17.90 * pow(rain[i], 2.0619);
                energy[i] = energy[i] / pow(24.0, 0.4134);
        }

fclose(ifp);
```

```
/* -----------------------------------------------------------------------------
The following part of the program updates the data file for AGNPS (input.dat)
 for every rainfall value. It runs the AGNPS model for every possible combination
of slope, K factor, and CN and records sediment yield and runoff volume loading
for each run
-------------------------------------------------------------------------------- */


ofp = fopen("cnslp.txt", "wt");
fprintf(ofp, " Slope  CN  K  rain  RV  TSS  SedN  TSN  SedP  TSP  rverr  Sederr
SedNerr  SedPerr  TSNerr  TSPerr  Sumerr\n\n");
fclose(ofp);

for(k=0; k<N; k++)
{
for(i=0; i<S_incr; i++)
{
for(pr1=0; pr1<K_incr; pr1++)
{
for(j=0; j<CN_incr; j++)
{
 sumCN = 0;
 avgCN = 0;
 sum_kfact = 0.0;
 avg_kfact = 0.0;
 sum_slope = 0.0;
 avg_slope = 0.0;

/* "input.dat" is the input file for AGNPS. "temp.dat" is the "input.dat" file
    modified by this program.  This file is used by this program to run the AGNPS
*/
   ifp = fopen("input.dat", "r");
   temp = fopen("temp.dat", "w");

      for(m=0; m<5; m++)
      {
              fgets(string, 80, ifp);
              fputs(string, temp);
      }

/* update the file input.dat */
        fscanf(ifp, "%s%f%f%f%f\n", type, &eng, &duration, &rainfall, &nitro);
```

```
/* update energy value and rainfall value */

        fprintf(temp, "%16s%8.2f%8.1f%8.2f%8.2f\n",
                    type,energy[k],duration,rain[k],nitro);


    for(m = 0; m < ncell; m++)
        {

            fscanf(ifp,    "%d    %d    %d    %d    %d    %d    %f    %d",
                &a,&f,&b,&g,&c,&CN,&e,&d);

/* The following one line is used to get to the grid point of optimum CN.
    It must be commented out when estimating the parameter */

    /*        CN = CN - 40;          */

/* Change the CN by the specified step size          */
                CN = CN + j*deltaCN;
                if(CN >= 100)
                    CN = 100;
/* I think it is a bug in the AGNPS program. If the curve number
    for any of the cells is zero, the program terminates with an
    error message that 'floating point error detected and could
    not be handled.' I have put this condition to make CN a non
    zero positive number.        -Indrajeet                          */

            if(CN <= 0)
                CN = 5;


/* The following one line is used only to get the starting
values for the parameter estimation. It should be commented
out when actually estimating the parameters. */

/*              e = e * 1.0;                */

        e += e*i*deltaS;
        if(e <= 0.0)
            e = 0.0;

            fprintf(temp,"%8d%8d%8d%8d%8d%8d%8.2f%8d\n",
                        a,f,b,g,c,CN,e,d);
            sumCN +=CN;
```

```c
            sum_slope += e;

            /* The following lines reads the grid rainfall value and
                    modifies it from the input rainfall file    */
        fgets(string, 65, ifp);
            /* USLE Parameter are extracted here */
                fscanf(ifp, "%d %f %f %f %f %f %d", &slength, &n, &kfact,
                &cfact, &pfact, &scc, &COD);

    /* The following one line is used to get the starting point for K */
            /*      kfact = kfact * 1.0;              */

                kfact += kfact*pr1*deltaK;
    /* Check for the boundary conditions (0≤ K ≤ 1.0)
                if(kfact >= 1.0)
                    kfact = 1.0;
                if(kfact <= 0.0)
                    kfact = 0.0;

                sum_kfact += kfact;

                fprintf(temp, "%16d %8.3f %8.3f %8.4f %8.2f %8.2f %8d\n",
                slength, n, kfact, cfact, pfact, scc, COD);

                fscanf(ifp, "%d%d%d%d%d%d%d%f",
                    &a1,&a2,&a3,&a4,&a5,&a6,&a7,&CellRain);
                fprintf(temp, "%16d%8d%8d%8d%8d%8d%8d%8.2f\n",
                a1,a2,a3,a4,a5,a6,a7,rain[k]);    /* change to rain[k] */

    /* 2 lines of soil information is read here */
                fscanf(ifp, "%s %f %f %f %f",
                    soil, &BaseN, &BaseP, &poreN, &poreP);
                fprintf(temp, "%4s %8.4f %8.4f %8.2f %8.2f\n",
                    soil, BaseN, BaseP, poreN, poreP);
                fscanf(ifp, "%f %f %f %f %d",
                    &runoffN, &runoffP, &leachN, &leachP, &OM);
                fprintf(temp, "%16.3f %8.3f %8.3f %8.3f %8d\n",
                    runoffN, runoffP, leachN, leachP, OM);

                fgets(string, 80, ifp);

                fgets(string, 80, ifp);
                strcpy(temp1, string);
```

```c
        p1 = strtok(temp1, " ");

        p0 = strcmp(p1, "Fert:");
        p2 = strcmp(p1, "Pest:");
        p3 = strcmp(p1, "Channel:");

        if(p0 == 0)
          {
             fputs(string, temp);
             fgets(string, 80, ifp);
             strcpy(temp1, string);
             p4 = strtok(temp1, " ");
             p5 = strcmp(p4, "Pest:");
             p6 = strcmp(p4, "Channel:");

             if(p5==0)
               {
                   fputs(string, temp);
                   for(x1=0; x1<7; x1++)
                     {
                           fgets(string, 80, ifp);
                           fputs(string, temp);
                     }
               }
             if(p6==0)
               {
                   fputs(string, temp);
                   for(x1=0; x1<3; x1++)
                     {
                       fgets(string, 80, ifp);
                       fputs(string, temp);
                     }
               }
          }

        if(p2==0)
          {
            fputs(string, temp);
            for(x1=0; x1<7; x1++)
              {
                   fgets(string, 80, ifp);
                   fputs(string, temp);
              }
```

```
                          }

                    if((p2!=0) && (p3==0))
                       {
                              fputs(string, temp);
                              for(x1=0; x1<3; x1++)
                                 {
                                    fgets(string, 80, ifp);
                                    fputs(string, temp);
                                 }
                       }

              }
              fclose(ifp);
              fclose(temp);


/* AGNPS is run here using the input file "temp.dat" */
/* Note that the agrain is the modified AGNPS that uses grid-based rainfall and
   energy intensity values   */
              check=system("agrain temp.dat 0 0 0");
              printf("%d\n",check);


/* Get the relevent results from the outputfile
          and write it to the CNSLP.OUT file        */

       ifp = fopen("temp.nps", "r");

       for(m = 0; m<4; m++)
       {
              fgets(string, 80, ifp);
       }

       fscanf(ifp, "%f%f%f%f%d%s%f%f%f", &area, &areac, &rainfall, &eng,
                                     &a, &g, &rv, &ropk, &tss);
       fscanf(ifp, "%f %f %*f %f %f %*f %*f %*f",
              &sedN, &TSN, &sedP, &TSP);


/* Absolute relative errors for each output is calculated here */
/* Here the residual is defined as
          "Measured value - simulated value "    */

       sederr = fabs((sed[k] - tss)/sed[k]);
```

206

```c
      rverr = fabs((runoff[k] - rv)/runoff[k]);
      if(sedmntN[k] != 0.0)
        sedNerr = fabs((sedmntN[k] - sedN)/sedmntN[k]);
      if(sedmntN[k] == 0.0)
        sedNerr = 0.0;
      if(sedmntP[k] != 0.0)
        sedPerr = fabs((sedmntP[k] - sedP)/sedmntP[k]);
      if(sedmntP[k] == 0.0)
        sedPerr = 0.0;
      if(tot_sol_N[k] != 0)
        TSNerr = fabs((tot_sol_N[k] - TSN)/tot_sol_N[k]);
      if(tot_sol_N[k] == 0.0)
        TSNerr = 0.0;
      if(tot_sol_P[k] != 0.0)
        TSPerr = fabs((tot_sol_P[k] - TSP)/tot_sol_P[k]);
      if(tot_sol_P[k] == 0.0)
        TSPerr = 0.0;
      sumerr = sederr+rverr+sedNerr+sedPerr+TSNerr+TSPerr;

      fclose(ifp);

      /* Here the average parameter estimates for the watershed is calculated */
      avgCN = (long) sumCN/ncell;
      avg_slope = sum_slope/ncell;
      avg_kfact = sum_kfact/ncell;

      /* The error statistics and the output and parameter estimates are written
         in the "cnslp.txt" file for each permutation of slope, K, and CN. */
      ofp = fopen("cnslp.txt", "at");

      fprintf(ofp,"%4.2f %4ld %4.2f %4.2f %5.4f %5.2f %5.2f %7.4f %7.4f %7.4f
%5.4f %5.4f %5.4f %5.4f %5.4f %5.4f %5.4f\n",
              avg_slope, avgCN, avg_kfact, rain[k], rv, tss, sedN, TSN, sedP, TSP,
              rverr, sederr, sedNerr, sedPerr, TSNerr, TSPerr, sumerr);

      fclose(ofp);

    }
   }
  }
 }
 return 0;
}
```

APPENDIX - 5

Computer program to process DPA rainfall data

```
/* **************************************************************************
         This program is used to read the NEXRAD rainfall file stored in DPA format.
         It reads the binary rainfall data, converts that to the hourly total rainfall (mm) and
         stores that to another file that can be imported into a GIS as an ascii file.
                                    Indrajeet Chaubey
   ************************************************************************* */


#include <stdio.h>
#include <math.h>

#define min_value -6
#define increment 0.125

main(int argc, char *argv[] )
{
         int precip_array[131][131];
         char buffer[146];
   unsigned char row[1024];
    short num_bytes;
    short value;
    short num_cells;
         char file_name[1024];
         int i, j, k;
    int row_total;
    float exp1, value1;
    int value_mm;
         FILE *ip, *fp;


         ip = fopen(argv[1], "rb");
         if(!ip)
   {
       printf("\nCannot open the file");
       exit(1);
   }
   fp = fopen(argv[2],"w");

   /* This is the header file to display the rainfall data into ARC/INFO or ARC/VIEW.
       To display it into another GIS package, the header information must be changed
         accordingly. */
   fprintf(fp, "ncols 131\n");
   fprintf(fp, "nrows 131\n");
   fprintf(fp, "xllcorner 396507.61933\n");
```

```c
        fprintf(fp, "yllcorner 3651134.3594\n");

        fprintf(fp, "cellsize 4000\n");
        /* End of the header information. */

        /*  Read the header of the DPA file and ignore it. */
        fread(buffer, sizeof(char), 146, ip);
        for(i=0;i<131;i++)
        {
            row_total = 0;
            fread(&num_bytes, sizeof(short),1,ip);
            printf("\nNum_bytes = %d", num_bytes);
            fread(row, sizeof(char),num_bytes,ip);
            for(j=0; j< num_bytes/2; j++)
            {
              num_cells = row[2*j];
              value = row[2*j+1];
              printf("\nvalue = %d", value);
              if( value ==0 )
                   value_mm = 0;
              else if((value ==255) || (value == -1) )
                   value_mm = 999;
              else
                {
                    exp1 = (value * increment + min_value)/10.0;
                    value1 = pow(10.0, exp1);
                    value_mm = (int) (value1+0.5);
                }
              for(k=0; k<num_cells;k++)
                {
                    precip_array[i][(row_total - 1) +k] = value_mm;
                    fprintf(fp, "%d ",value_mm);
                }
              row_total += num_cells;
              printf(" Row total = %d", row_total);
            }
          fprintf(fp,"\n");
          printf("\nColumn total = %d", i);
        }
        fclose(ip);
        fclose(fp);
}
```

VITA

Indrajeet Chaubey

Candidate for the Degree of

Doctor of Philosophy

Dissertation: EFFECT OF SPATIAL VARIABILITY OF RAINFALL ON MODELING HYDROLOGIC/WATER QUALITY PROCESSES

Major Field: Biosystems Engineering

Biographical:

Personal Data: Born in Ballia, India, on January 8, 1969, the son of Parmatma Nand Chaubey and Rajrani Chaubey.

Education: Graduated from Government Intermediate College, Allahabad in June,1986; received Bachelor of Technology degree in Agricultural Engineering from University of Allahabad, Allahabad, India in June 1991; received Masters of Science degree in Biological and Agricultural engineering from University of Arkansas, Fayetteville, Arkansas, U.S.A. in May 1994. Completed the requirements for the degree of Doctor of Philosophy in Biosystems and Agricultural Engineering at Oklahoma State University, Stillwater, Oklahoma, U.S.A. in December 1997.

Experience: Graduate Research Assistant, Department of Biosystems and Agricultural Engineering, Oklahoma State University, Stillwater, Oklahoma (August 1994 to present); Teaching Assistant, Department of Biosystems and Agricultural Engineering, Oklahoma State University, Stillwater, Oklahoma (August 1995 to December 1995); Graduate Assistant, Department of Biological and Agricultural Engineering, University of Arkansas, Fayetteville, Arkansas (January 1992 to July 1994).

Professional Memberships: ASAE - The Society for Engineering in Agriculture, Food, and Biological Systems; American Water Resources Association; Alpha Epsilon, Gamma Sigma Delta.